Investigations into the role of *Sugaryenhancer1* in maize endosperm development and the effects of long-term divergent selection in a sweet corn population

By

Carl. A. Branch

A dissertation submitted in partial fulfillment of the requirements for the degree of

Doctor of Philosophy

(Plant Breeding and Genetics)

at the

University of Wisconsin-Madison

2024

Date of Final Oral Examination: 2024-05-30

The dissertation is approved by the following members of the Final Oral Committee

William F. Tracy, Professor, Plant and Agroecosystem Sciences

Shawn Kaeppler, Professor, Plant and Agroecosystem Sciences

Ane, Jean-Michel, Professor, Plant and Agroecosystem Sciences

Simon, Philip, Professor, Plant and Agroecosystem Sciences

Acknowledgements

First and foremost, I would like to thank Dr. Bill Tracy, for instilling in me a love of classical plant breeding, an admiration for the “breeder’s eye”, and an appreciation for good sweet corn. I hope that, as I continue in the world of plant breeding, future colleagues and collaborators recognize Bill’s influence—my goal is to join the ranks of alumni of the UW-Madison Sweet Corn Breeding and Genetics Program in taking the lessons I learned with Bill and applying them to new challenges. I would also like to thank my committee members, Drs. Shawn Kaeppler, Phil Simon, and Jean-Michel Ane for broadening my horizons during my time here at UW-Madison. Being able to learn at an institution represented by an accomplished group of faculty exposed me to the variety of ideas and viewpoints that are the cornerstone of higher education.

Not only am I fortunate and honored to have been a part of Team Sweet, I’m lucky to have been mentored on the grittier points of managing a field breeding program by the unparalleled Pat Flannery, program manager. Don’t believe his claims to be “just a guy”. Throughout my graduate student career, I’ve also been surrounded by skilled and passionate colleagues. Thank you to alumni Lily Hislop, Lexie Wilson, and Cat McCluskey for being inspiring examples with whom I could learn from and collaborate. Thank you also to the current Team Sweet graduate students for putting up with me as I wrapped up my degree, and to the undergraduates who helped collect field data during long summer days.

Thank you to the UW-Madison Nordic Ski Club, and to the fish fry guys, for providing spaces that weren’t corn-focused.

I’d also like to thank my family, for putting me on this path from an early age. My parents, for giving high standards for good vegetables, a love of science, and the optimism that are all necessary to become a plant breeder. Eric, for being a participant in my uncontrolled twin study and for being part of a competitive environment that I hope also drives you to succeed. And thank you, Sarah, for your unwavering love and confidence in me.

Table of Contents

Abstract

Sweet corn has a long history of economic and cultural significance and an equally long history of working its way through the institutions of plant breeding. Sweet corn breeders, in addition to improving the agronomic traits desired for row and commodity crops, must also improve traits such as nutritional value, appearance, and eating quality that promote consumer appeal. This dichotomy means that, despite the extensive public and private interest in sweet corn breeding, opportunities remain for furthering understanding of how current sweet corn germplasm can be used to improve desired traits. This work promotes these goals by studying the interactions and associations between the *Sugaryenhancer1* (*Se1*) gene and the levels of nutritionally relevant vitamin A- and vitamin E-related traits, by leveraging transcriptomics and metabolomics to investigate specific effects of the *Se1* gene, and by using a divergently selected sweet corn population to explore the limits of selection and variation.

The first chapter is a literature review to introduce the topics of sweet corn, maize starch synthesis, and endosperm development. The second chapter focuses on the relationship between the presence of the *Se1* and the levels of carotenoid and tocochromanol traits. As vitamins and antioxidants, these compounds are of increasing interest to both sweet corn breeders and consumers. This research used a diverse panel of sugary1 sweet corn lines both with and without a functional *Se1* gene to compare the amounts of secondary metabolites. Here, even in the presence of effects from population structure and kinship, the *Se1* locus was found to contribute to significant variation in the levels of certain carotenoids and certain tocochromanols. Notably, the levels of lutein, zeaxanthin, and tocotrienols were decreased in lines homozygous for the recessive *se1* allele, but levels of the lutein intermediate zeinoxanthin were increased.

The third chapter is a continuation of the work with *sugaryenhancer1,* and, given the associations with sugars, carotenoids, and tocochromanols, investigate the relevant metabolic pathways. A set of near-isogenic lines with and without *Se1* were screened for differentially expressed genes (DEGs) and differentially accumulated metabolites. Results showed that *se1* affected sugar and starch metabolism at both the transcript and metabolite level, and expression of the cytochrome P450 gene that converts zeinoxanthin to lutein was reduced. Both the gene expression analysis and the widely-targeted metabolomics analysis highlighted differences in genes and compounds associated with the phytohormone regulation of the developing endosperm. This adds to the body of evidence that, instead of a direct role in starch metabolism, *Se1* has a regulatory role upstream of the production of starch, carotenoids, and tocochromanols, warranting additional studies into the role of phytohormones in affecting sweet corn quality.

The final chapter used a divergently selected *sugary1* sweet corn population to observe the effects of long-term selection on the timing of vegetative phase change, and on a suite of traits related to plant growth and disease resistance. Using the last leaf with juvenile wax as a metric, divergent selection resulted in plants with an extremely accelerated or extremely delayed vegetative phase change compared to the source population. Later vegetative phase change resulted in increases in susceptibility to common rust infection and greater plant height, and earlier vegetative phase change affected ear length and ear width. Beyond relevance for disease management, this study presents a case of the effects of divergent selection and the ability for plant breeders to continue to exploit genetic variation through many cycles of selection.

1 Chapter One: Literature Review

1.1 Importance of maize and starch

Through a sequence of both natural and artificial selection, the wild grass teosinte (*Zea mays* ssp. *parviglumis*) was domesticated into maize (*Zea mays* ssp. *mays*), which in 2022 was grown over 200 million hectares globally and had an agricultural value of $324 billion dollars (Food and Agricultural Organization of the United Nations, 2022). The vast majority of this value is driven by the plant's ability to fix carbon from CO_2 into glucose, and store it in kernels as starch, a stable polymer of linked glucose molecules (Martin & Smith, 1995). For that reason, the production of starch in maize endosperm, or reduction in the amount of starch in sweet corn, is essential to maize as food, feed, or fuel. Many of the major steps of starch synthesis and the evolution of causal genes important in maize kernel development have been described (L. C. Hannah, 2005; James & Myers, 2009). However, the regulation of starch synthesis is still only partially elucidated even after decades of maize being a plant model for quantitative genetics, biochemistry, and molecular biology. From a plant breeding perspective, understanding the regulation of starch synthesis during kernel development would identify new breeding targets and allow for the development of maize for new uses and markets (Tracy, Shuler, & Dodson-Swenson, 2019).

Of the types of maize that predominate the US market, the form of carbohydrates stored in kernels draws a contrast between the two most widely-grown types. Dent corn is the high-starch maize that makes up the majority of corn grown in the US. The starch synthesis pathway in dent corn has fully-functional enzymes at all major steps, resulting in a kernel that is near 70% starch, with the ratio of amylose to amylopectin being about 25:75 (Darrah, McMullen, & Zuber,

2018; L. C. Hannah, 2005; James & Myers, 2009). In comparison, most sweet corn kernels contain between 15% and 35% starch (Creech & McArdle, 1966). Modern dent corn is derived from a combination of 'Northern Flint' and 'Southern Dent' landraces, with most of the contribution coming from Southern Dent (Van Heerwaarden, Hufford, & Ross-Ibarra, 2012). In comparison, sweet corn originated as the result of mutations in the starch synthesis gene *Su1*. In developing sweet corn types, indigenous people observed and fixed a recessive *su1* allele; this occurred in five independent events (Tracy, Whitt, & Buckler, 2006). However, there are dozens of other alleles at the *su1* locus that have been observed and studied. Many *su1* mutations reduce starch levels and increase sucrose and phytoglycogen, giving dry kernels a wrinkled, glassy appearance.

1.2 Domestication of maize from teosinte

Emergence of maize from teosinte involved an increase of starch and a reduction of protein relative to overall kernel mass; starch granules in maize kernels are both larger and more abundant than in teosinte grains (Holst, Moreno, & Piperno, 2007). Genes in the starch synthesis pathway have been implicated as being under selection during domestication and diversification of maize (Whitt, Wilson, Tenaillon, Gaut, & Buckler IV, 2002), including starch and sucrose synthases and starch branching and debranching enzymes (Tracy, Whitt, & Buckler, 2006; Whitt et al., 2002). Since these genes affect the amount and composition of endosperm starch, selection for or against recessive mutations resulted in large changes in kernel phenotype important for culinary properties, further increasing the food value of ancient maize.

The derivation of ancient maize from the teosinte *Zea mays* ssp. *parviglumis* is a classic example of domestication syndrome, or the collection of traits that are commonly changed in the development of a cultivated crop from a wild relative. Compared to the wild relative, a

domesticated plant will tend to have larger or more numerous seeds per seed head, altered seed composition, reduced seed dormancy, and reduced lateral growth (Moyers, Morrell, & Mckay, 2018; Piperno, Ranere, Holst, Iriarte, & Dickau, 2009). Domestication of teosinte began in the Balsas River drainage of southwest Mexico around 9000 years before present. *Zea mays* ssp. *parviglumis* is a highly branched grass, with each branch bearing a terminal staminate inflorescence (Doebley, 2004). Teosinte produces a large number of "ears"—lacking central cob and open glume structures—each bearing up to 12 fruitcases, each with a single kernel, in contrast to the several hundred kernels produced in an ear of modern maize (Doebley, Stec, Wendelt, & Edwardst, 1990; C. J. Yang et al., 2019). Despite similar grain weight per plant, 114 grams for teosinte and 122 grams for maize landraces, teosinte has much greater fecundity, with over 4,300 seeds per plant compared to 350 in landraces (C. J. Yang et al., 2019). Teosinte fruitcases are composed of hardened glumes and cupules, which were an obstacle to using teosinte as a food source (Stitzer & Ross-Ibarra, 2018; Swarts et al., 2017). A handful of large-effect genes regulate much of the plant architecture differences that separate teosinte and maize. *Teosinte branched1 (Tb1)* is a major driver of domestication traits in maize, controlling the apical dominance traits that result in the differences in lateral branching between teosinte and maize (Doebley, 2004). Another gene, *teosinte glume architecture1* (*tga1)*, has even more profound effects on the domestication phenotype in maize; this locus controls the presence of the teosinte fruitcase which is absent in the naked kernels of modern maize. Regulatory networks built in and around these major domestication genes also contribute the modern maize phenotype (Doebley, 2004; Guan et al., 2023). Maize populations genetically and morphologically close to modern maize were emerging 4,400 years ago; at this point, maize was beginning to diversify into the types and market classes recognized today (Swarts et al., 2017).

1.3 Maize kernel development

The development of maize kernels begins with the double fertilization found in flowering plants. Pollen lands on the silk, the stigma of the female flower, and a pollen tube grows toward the ovule via the silk, at rate near 1 cm per hour (Barnabas & Fidvalsky, 1984; Vollbrecht & Evans, 2017). The pollen tube releases two sperm cells into the ovule; one sperm cell fertilizes the haploid egg, resulting in a diploid zygote. The other fertilizes the central cell containing two nuclei, creating the triploid endosperm (Faure et al., 2003; Olsen, 2020). After double fertilization, there are three stages of endosperm development: early development, up until 7 days after pollination (DAP), endosperm differentiation, lasting until 12 to 13 DAP, and the grain-filling stage which continues until the kernel is fully developed (Dai, Ma, & Song, 2021; Olsen, 2020; Sabelli & Larkins, 2009b). Early endosperm development consists of rapid mitotic divisions followed by cell wall growth (Dai et al., 2021; Sabelli & Larkins, 2009a). Endosperm differentiation results in distinct regions by 12-13 DAP. The aleurone layer is the outermost endosperm region. Aleurone cells function in metabolism of nutrient storage molecules in seed germination (Hoecker, Vasil, & McCarty, 1995; H. Wu, Becraft, & Dannenhoffer, 2022). The starchy endosperm occupies most of the endosperm space and contains starch and protein bodies. Starch granules are produced and stored in amyloplasts. Zein bodies account for 60% of kernel protein mass (H. Wu et al., 2022). Endosperm starch will eventually form 70% of kernel dry weight (L. C. Hannah, 2005; James & Myers, 2009). The basal endosperm transfer layer (BETL), the region where nutrients enter the endosperm from the pedicel, has a role in movement of compounds necessary for production of starch and other storage molecules. Sugar transport through the BETL will affect the rate of starch synthesis. (Olsen, 2020). The embryo

surrounding region (ESR), basal intermediate zone, conduction zone, and subaleurone region also develop during endosperm differentiation (Sabelli & Larkins, 2009b; H. Wu et al., 2022).

The next stage of endosperm development is the maturation stage, when endosperm cells increase in size and deposition of starch and other storage molecules, including lipids and proteins occurs (Ingle, Beitz, & Hageman, 1965). The central endosperm region is most active until around 8-12 DAP, with high rates of mitosis and endoreduplication, when genome content and cell size increase (Sabelli & Larkins, 2009a). At around 16 DAP, programmed cell death begins and kernel dry weight increases rapidly. Programmed cell death and accumulation of storage compounds continues through the end of kernel maturation, which ends in seed dormancy and kernel desiccation. After desiccation, a mature maize kernel will be at 15% percent moisture or less and can maintain viability during storage under good conditions, (Capelle et al., 2010).

1.4 Regulation of maize kernel development via phytohormones

Plant hormones have a part in dictating almost every aspect of plant development, and can be grouped into eleven major classes; abscisic acid (ABA), auxin, brassinosteroids, cytokinins, ethylene, gibberellins (GA), jasmonic acid, polyamines, salicylic acid, nitric oxide, and strigolactone (R. Jones, Ougham, Thomas, & Waaland, 2013). Different hormones dominate at different stages of kernel development, and control seed germination and maintain dormancy. Major hormones regulating kernel and endosperm development include auxin, ABA, GA, and cytokinin. The biosynthesis and degradation of these hormones, and the interactions between them, help regulate starch synthesis, seed dormancy, germination, stress tolerance, and seed longevity (Hoecker et al., 1995; R. J. Jones & Setter, 2000; Locascio, Roig-Villanova, Bernardi, & Varotto, 2014).

Auxins are amino acid-derived phytohormones that contain an indole ring. Indole-3-acetic acid (IAA) is the most abundant auxin. Early in endosperm development, around 4 DAP, auxin responses are detected (Doll, Depège-Fargeix, Rogowsky, & Widiez, 2017). Auxin levels increase rapidly at 10-15 DAP promoting endoreduplication and cell differentiation, and shift the kernel metabolism towards accumulation of storage molecules (R. J. Jones & Setter, 2000). The production of auxin is partly controlled by the level of sugars in developing kernels. This interaction regulates the movement of sugars through the BETL, when auxin levels are high (Doll et al., 2017; Leclere, Schmelz, & Chourey, 2010). At later stages, auxin will regulate seed dormancy through interactions with the ABA signaling pathway (Hussain et al., 2020; Liu et al., 2013).

ABA is another key hormone regulating maize development, even though it is often considered a stress-response hormone (R. J. Jones & Setter, 2000). In developing kernels under normal environmental conditions, ABA is required to maintain dormancy and prevent precocious germination; it will also affect grain fill. When applied at the early endosperm development stage, ABA decreases kernel fill; ABA applied later will increase kernel size (R. J. Jones & Brenner, 1987; Yue, Lingling, Xie, Coulter, & Luo, 2021). Part of this temporally-dependent effect is thought to be due to the interaction between sucrose and ABA as a part of the regulation of starch synthesis (Huang et al., 2016). In the presence of heat or drought stress, ABA accumulation will increase more rapidly at later developmental stages, and result in an earlier cessation of starch synthesis and grain fill (Z. Wang, Mambelli, & Setter, 2002). The stress-induced ABA mechanism aid the kernel in adapting to abiotic stress via activating responses to reactive oxygen species and altering solute movement (Rajasheker et al., 2019; J. Zhang, Jia, Yang, & Ismail, 2006).

The ratio and antagonism between ABA and GA regulates the dormancy-inducing functions of ABA, balancing the germination pathways that are positively regulated by GA (White & Rivin, 2000). During germination, the aleurone layer releases amylases and proteases that break down starchy endosperm and allow use of the nutrient reserves initiating plant growth (Sabelli, 2012; Sabelli & Larkins, 2009b). ABA can inhibit production of these hydrolytic enzymes; GA will stimulate production of these enzymes to allow germination (Harvey & Oaks, 1974). If a mutation results in in a deficiency of ABA, or elevates GA production, precocious germination occurs rather than seed dormancy (Hoecker et al., 1995). The interaction between these hormones has practical applications in the production of maize seed; even in the absence of environmental stress, a genetic inclination towards this "pre-germ" can result in non-viable seed and losses in yield.

Similar to how ABA and GA antagonistically regulate plant processes, auxin and cytokinin also function in tandem balancing various aspects of growth and development, best illustrated by the auxin/cytokinin ratios needed in tissue culture to generate roots and stems from callus tissue (R. Jones et al., 2013). In maize endosperm development, cytokinins promote cell division, and levels increase early in endosperm development, and decline during starch accumulation as auxin levels increase (R. J. Jones & Setter, 2000; Sabelli, 2012). Cytokinins contribute to heat tolerance and supplementation will help maintain kernel set and yield (Cheikh & Jones, 1994).

1.5 The starch synthesis pathway

Maize, like all plants, relies on starch for both short and long-term energy storage. For short-term storage in leaves, starch is produced during the daytime and degraded at night to support metabolic function in the absence of photosynthesis. For long-term storage, as in maize

kernels, endosperm starch provides an energy source for germinating embryos (Lloyd & Kossmann, 2015). Production of starch in the endosperm, in addition to resulting in sufficient germination and seed quality, is the primary driver of maize economic and nutritional value (Sabelli & Larkins, 2009b).

Endosperm starch synthesis begins in leaf tissue with sucrose synthesized from the photosynthesis product glyceraldehyde-3-phosphate (L. C. Hannah, 2005; L. Curtis Hannah, Shaw, Clancy, Georgelis, & Boehlein, 2017). Sucrose is transported via phloem and enters the developing seed through the pedicel (Boehlein, Shaw, Boehlein, Boehlein, & Hannah, 2018). Sucrose synthases then produce uridine diphosphate glucose (UDP-glucose) and fructose from sucrose and UDP. Through a series of transferases both UDP-glucose and a portion of the fructose are separately converted to glucose-1-phosphate, which is the substrate for the primary dedicated reaction of starch synthesis (L. C. Hannah & Nelson, 1976). UDP-glucose pyrophosphorylase produces glucose-1-phosphate. Next, glucose-1-phosphate is combined with a single ATP molecule to produce adenosine diphosphate (ADP) glucose and a pyrophosphate byproduct. ADP-glucose is then moved into the amyloplast, where the majority of starch synthesis occurs relevant to endosperm development (James & Myers, 2009).

In the amyloplast, starch synthesis is initiated by adding glucose monomers, from ADP-glucose, onto malto-oligosaccharides; these are short chains of three or more maltose molecules connected by alpha-(1-4)-glycosidic linkages (Cao, James, & Myers, 2000). These chains are extended and modified by starch synthases and starch branching and debranching enzymes. Starch synthases add monomers to the end of the chain with additional alpha-(1-4) linkages; starch branching enzymes cause branching of starch chains using alpha-{1-6) linkages (Gao, Wanat, Stinard, James, & Myers, 1998; Hennen-Bierwagen et al., 2008). Different classes of

starch synthases affect starch composition. Granule-bound starch synthase (GBSS) elongate glucan chains linearly only, resulting in the production of amylose (Lloyd & Kossmann, 2015; Macdonald & Preiss, 1983). Other starch synthases, classified as SSI – SSIV, including starch synthases IIa and IIb, elongate amylopectin molecules, also through alpha-(1,4) glycosidic bonds (Hennen-Bierwagen et al., 2008). Removing GBSS from the system will result in endosperm deficient in amylose, while altering the other starch synthases will affect the chain lengths and overall physical qualities of amylopectin (Darrah et al., 2018). Starch branching enzymes SBEI, SBEIIa, and SBEIIb support production of amylopectin by breaking alpha-(1-4) linkages and creating alpha-(1-6) linkages. By cleaving the alpha-(1,6) bonds in amylopectin, starch debranching enzymes (DBE) are thought to allow for the proper crystallization of the starch molecules in the amyloplast (Lin et al., 2013). The isoamylases *Su1 (Isa1), Isa2,* and *Isa3*, as well as pullulanase, all trim growing starch molecules and produce shorter glucan chains (Lin et al., 2013). Isoamylase1 cleaves glycosidic bonds within phytoglycogen, and mutating *Su1* results in an endosperm very high in water-soluble phytoglycogen (Li, Ilarslan, James, Myers, & Wurtele, 2007; Lin et al., 2013). *Isa2* protein is thought to physically interact with isoamylase1 as an heterodimer protein complex, though the *isa2* mutation has little or no effect on endosperm starch production (Lin et al., 2013). Pullulanase degrades starch and short-chain malto-oligosaccharides to produce maltose and panose (Hii, Tan, Ling, & Ariff, 2012; Shi, Sweedman, & Shi, 2018; C. Wu, Colleoni, Myers, & James, 2002). As endosperm development continues, semi-crystalline starch granules accumulate in the amyloplast for long-term energy storage (Sabelli & Larkins, 2009b).

Degradation is the fate of much of the endosperm starch, either during endosperm development or during germination (Kowles & Phillips, 1988; Lloyd & Kossmann, 2015). After

reaching physiological maturity, maize kernels can remain stable for decades; after planting and imbibition, alpha- and beta- amylase enyzmes are activated to break down starch polymers, either internally, for alpha-amylase, or from the non-reducing end, for beta-amylase. The products of degradation, maltose and glucose fuel cellular processes in early seedling development (Struk, 2018; Xue et al., 2021).

1.6 Regulation and Disruption of Starch Synthesis

Regulation of endosperm starch synthesis is required by the plant to ensure seed quality and a next generation; disruptions in this pathway are required in pursuit of breeding high quality sweet corn (Tracy et al., 2019, 2006). A regulatory balance between starch for seed quality and sugar for eating quality is found in sweet corn, where endosperm starch synthesis is influenced by many plant processes at different levels of regulation (Huang et al., 2016; Sun et al., 2021). Regulation of starch synthesis includes direct effects, as in the case of single protein-coding genes where a knockout has clear and discernable impacts, and more indirect regulatory conditions, such as heat stress causing a reduction in grain fill, where starch synthesis is reduced even though all genes directly in the pathway are functional (L. Curtis Hannah et al., 2017; X. Wang et al., 2019). The S*hrunken2* gene, encoding the large subunit of adenosine diphosphate pyrophosphorylase, is an example of direct regulation. On the opposite side of the spectrum, abiotic factors such as heat stress can indirectly depress starch synthesis. Excessive heat, over 95 degrees, has been shown to reduce starch accumulation by reducing enzyme function at major points in the starch synthesis pathway, including AGPases, starch synthases, and debranching enzymes (Cheikh & Jones, 1994; H. Yang, Gu, Ding, Lu, & Lu, 2018). Outside of the direct endosperm starch synthesis pathway, introducing heat-stable forms of key enzymes that work in the pentose-phosphate pathway to move glucose into the endosperm starch synthesis pathway

can prevent some of the heat-induced loss in kernel starch (Han et al., 2020; Ribeiro, Hennen-Bierwagen, Myers, Cline, & Settles, 2020).

1.7 Sweet Corn Breeding

Effective control of the regulation and disruption of starch synthesis leads to a sweet corn with a suite of favorable traits that allows for both agronomic utility and consumer desirability (Revilla, Anibas, & Tracy, 2021; Tracy et al., 2019). In terms of agronomic utility, the ideal sweet corn plant has kernels with enough starch for good germination and vigor in a range of growing conditions. In terms of consumer desirability, the ideal sweet corn plant has ears with kernels high in sugar and low in starch (Tracy, 1996). Too little sugar and too much starch leads to a kernel that is tough and inedible, but too little starch results in kernels with weak germination in the field (Revilla et al., 2021). While not the only considerations of plant breeders, managing the tradeoffs between starch and sugar is a defining feature of sweet corn breeding (Creech & McArdle, 1966; Dodson-Swenson & Tracy, 2015).

Early sweet corn breeding used material largely derived from two populations, ‘Stowell’s Evergreen’ and ‘Golden Bantam’, and these two groups form distinct groups within maize phylogeny. Compared to field corn, sweet corn clades are closer to teosinte progenitors (Y. Hu et al., 2021). All early sweet corn possessed *su1* alleles (Tracy et al., 2006). As sweet corn breeding was commercialized and hybrid use became the norm, *su1-reference,* also known as the *su1-ne* allele became the dominant sweet corn allele. This particular allele makes a non-catalytic isoamylase1/starch debranching enzyme. The wild type allele would normally trim glycan chains to allow for starch granule formation (Lin et al., 2013). The high levels of water-soluble polysaccharides instead of starch granules in *su1* sweet corn are responsible for the desirable

creamy mouthfeel in commercial *su1* hybrids; this endosperm type has kernels consisting of 15.6% sugars, 22.8% water-soluble polysaccharides, and 28% starch (Creech, 1965). The relatively high starch content in *su1* hybrids provides for good germination (Dodson-Swenson & Tracy, 2015; Tracy et al., 2006).

In the 1940s and 1950s, work developed describing a new type of sweet corn, driven by a mutation distinct from *su1*. This shriveled-kernel mutation was named *shrunken2* (*sh2, sh2-ref*) (Tracy, 1996). It was later shown to be a gene encoding the large subunit of AGPase, the rate-limiting step in starch synthesis. Professor John Laughnan at the University of Illinois proposed the utility of the *sh2* gene as a new sweet corn allele and he released the first *sh2* hybrid. As a result of the high levels of sugar, *sh2* has overtaken *su1* types in the marketplace; contributing to this is the fact that most *sh2* sweet corn has enough natural sugar to replace sugar that was generally added in processing. The low rate of sugar to starch conversion in *sh2* kernels results in a longer shelf life of fresh ears than other sweet corn types. However, due to differences in polysaccharide levels, *su1* hybrids outperform *sh2* hybrids in cold-soil germination, so *su1* sweet corn is used by processing companies for early harvests, despite the lower sugar levels. The *sh2* allele results in a non-functional large subunit of the cytoplasmic AGPase, and starch levels are reduced compared to the wild-type levels (L. C. Hannah & Nelson, 1976; Tracy, 1996). However, an intermediate mutation, *sh2-i,* does not completely eliminate AGPase function, (Dodson-Swenson & Tracy, 2015). Both of these mutations are used in commercial sweet corn, despite a trade-off between seed quality in the mature kernels and sugar content in immature kernels (Dodson-Swenson & Tracy, 2015; Tracy et al., 2019).

Besides *su1* and *sh2,* another gene used in sweet corn breeding is *sugary enhancer1* (*se1*) and is only used with homozygous *su1*. The name implies its function of "enhancing" the effect

of *su1* on sugar levels in sweet corn kernels (Ferguson, Rhodes, & Dickinson, 1978; La Bonte & Juvik, 1990). Sweet corn homozygous for both *se1* and *su1* alleles possesses high sucrose levels, closer to that of *sh2* hybrids, but levels of water-soluble polysaccharides close to that of *su1* (Finegan et al., 2022; La Bonte & Juvik, 1990; X. Zhang et al., 2019). At fresh eating stage, *su1se1* sweet corn is tender and generally sweet, yet maintains the creamy texture of *su1* corn (Ferguson et al., 1978). However, *su1se1* types convert sugar to starch rapidly after harvest, and lack the longer shelf-life of *sh2* hybrids.

Unlike the other major sweet corn genes, the *Se1* locus does not encode a gene with a confirmed place in the starch synthesis pathway. The *se1* allele was initially identified in the inbred IL677a, the product of a three-way cross between Bolivia 1035 and IL44b, and IL442a (Ferguson et al., 1978). Bolivia 1035 is a floury-type South American corn. RA Brink named the gene due to its effect on sweet corn quality (Brink, 1978). The *se1* allele from IL677a was rapidly incorporated into public and private breeding programs, including those of the University of Illinois and the University of Wisconsin from which each developed a large number of homozygous *se1* sweet corn inbreds. Since the release of IL677a, these two programs have released the majority of publicly available *se1* germplasm (Gerdes, Behr, Coors, & Tracy, 1993). Later work showed that the original source of *se1* in sweet corn was inbred IL44b, which was derived from a Stowell's Evergreen open pollinated cultivar.

1.8 Nutritional Value of Sweet Corn

Sweet corn possesses desirable qualities as a vegetable in that it is high in vitamins and antioxidants, and certain minerals; due to fresh consumption of sweet corn, many of these compounds have greater bioavailability compared to field corn (Revilla et al., 2021; Rouf Shah,

Prasad, & Kumar, 2016). Other secondary metabolites also affect the nutritional quality of sweet corn, including phenolic acids, flavonoids, and anthocyanins. Compared to field corn, sweet corn is higher in vitamin C and folate (Siyuan, Tong, & Liu, 2018). Rates of nutrient accumulation changes with kernel maturity, meaning that any genetic manipulation of vitamin or antioxidant levels must take into account the process of endosperm development (X. Hu et al., 2021; Špoljarić Marković et al., 2020). Interest in vitamins and antioxidants in sweet corn has resulted in recent breeding objectives that have included both increasing nutrient levels and the screening and characterization of nutrients in existing germplasm (Ibrahim & Juvik, 2009; Siyuan et al., 2018). In sweet corn, recent association studies have attempted to tease apart beneficial alleles and differences between endosperm types with regards to nutritional quality. Sweet corn with the *shrunken2* endosperm type has been found to have greater levels of carotenoids--including provitamin A compounds and vitamin E than other types (Baseggio et al., 2020, 2019; Hershberger et al., 2022). Significant genetic variation has also been found for mineral components in sweet corn, including iron and zinc (Baseggio et al., 2021). This work suggests that loci exist that can be exploited using marker-based or genomic selection, but also that natural variation exists to lend itself to more traditional plant breeding methods.

1.9 Research Objectives

This dissertation seeks to build on existing knowledge of maize endosperm development, with particular emphasis on the regulation of the starch synthesis pathway in sweet corn, and with regards to the role of *sugaryenhancer1*. Furthermore, as sweet corn breeders seek to improve their germplasm by focusing on previously undervalued traits, such as vitamin or antioxidant content, and understanding of the effects of *Se1* on maize kernel secondary metabolism is necessary. To achieve these ends, the research presented here includes an analysis

from a sweet corn diversity panel, including lines with and without a functional *Se1* allele, focusing on carotenoids and tocochromanols. Using a pair of near-isogenic lines that differ only at the *Se1* locus, additional analysis was done to assess the gene expression and metabolite accumulation with and without *Se1*. Analysis of the metabolic pathways involved in the transcriptomic or metabolic changes will help to further elucidate the functions of *Se1* in the starch synthesis pathway and in other parts of kernel development.

1.10 Chapter One References

Barnabas, B., & Fidvalsky, L. (1984). Adhesion and germination of differently treated maize pollen grains on the stigma. *Acta Botanica Hungarica*, *30*, 329–332.

Baseggio, M., Murray, M., Magallanes-Lundback, M., Kaczmar, N., Chamness, J., Buckler, E. S., … Gore, M. A. (2020). Natural variation for carotenoids in fresh kernels is controlled by uncommon variants in sweet corn. *Plant Genome*, *13*(1), 1–19. https://doi.org/10.1002/tpg2.20008

Baseggio, M., Murray, M., Magallanes-Lundback, M., Kaczmar, N., Chamness, J., Buckler, E. S., … Gore, M. A. (2019). Genome-Wide Association and Genomic Prediction Models of Tocochromanols in Fresh Sweet Corn Kernels. *The Plant Genome*, *12*(1), 180038. https://doi.org/10.3835/plantgenome2018.06.0038

Baseggio, M., Murray, M., Wu, D., Ziegler, G., Kaczmar, N., Chamness, J., … Gore, M. A. (2021). Genome-wide association study suggests an independent genetic basis of zinc and cadmium concentrations in fresh sweet corn kernels. *G3: Genes, Genomes, Genetics*, *11*(8). https://doi.org/10.1093/g3journal/jkab186

Boehlein, S. K., Shaw, J. R., Boehlein, T. J., Boehlein, E. C., & Hannah, L. C. (2018). Fundamental differences in starch synthesis in the maize leaf, embryo, ovary and endosperm. *Plant Journal*, *96*(3), 595–606. https://doi.org/10.1111/tpj.14053

Brink, R. A. (1978). Identity and sources of a sugar enhancer gene significant for sweet corn quality. *Maize Genetics Cooperation News Letter, 52*, 110–112.

Cao, H., James, M. G., & Myers, A. M. (2000). Purification and characterization of soluble starch synthases from maize endosperm. *Archives of Biochemistry and Biophysics*, *373*(1), 135–146. https://doi.org/10.1006/abbi.1999.1547

Capelle, V., Remoué, C., Moreau, L., Reyss, A., Mahé, A., Massonneau, A., … Prioul, J. L. (2010). QTLs and candidate genes for desiccation and abscisic acid content in maize kernels. *BMC Plant Biology*, *10*. https://doi.org/10.1186/1471-2229-10-2

Cheikh, N., & Jones, R. J. (1994). Disruption of maize kernel growth and development by heat stress: Role of cytokinin/abscisic acid balance. *Plant Physiology*, *106*(1), 45–51. https://doi.org/10.1104/pp.106.1.45

Creech, R. G., & McArdle, F. J. (1966). Gene Interaction for Quantitative Changes in Carbohydrates in Maize Kernels. *Crop Science*, *6*(2), 192–194. https://doi.org/10.2135/cropsci1966.0011183x000600020026x

Dai, D., Ma, Z., & Song, R. (2021). Maize endosperm development. *Journal of Integrative Plant Biology*, *63*(4), 613–627. https://doi.org/10.1111/jipb.13069

Darrah, L. L., McMullen, M. D., & Zuber, M. S. (2018). Breeding, Genetics and Seed Corn Production. In *Corn: Chemistry and Technology, Third Edition* (3rd ed., pp. 19–41). https://doi.org/10.1016/B978-0-12-811971-6.00002-4

Dodson-Swenson, H. G., & Tracy, W. F. (2015). Endosperm carbohydrate composition and kernel characteristics of shrunken2-intermediate (Sh2-i/ sh2-i su1/su1) and shrunken2-intermediate–sugary1- reference (sh2-i/sh2-i su1-r/su1-r) in sweet corn. *Crop Science*, *55*(6), 2647–2656. https://doi.org/10.2135/cropsci2015.03.0188

Doebley, J. (2004). The genetics of maize evolution. *Annual Review of Genetics*, *38*, 37–59. https://doi.org/10.1146/annurev.genet.38.072902.092425

Doebley, J., Stec, A., Wendelt, J., & Edwardst, M. (1990). Genetic and morphological analysis of a maize-teosinte F2 population: Implications for the origin of maize (molecular markers/evolution/Zea/restriction fragment length polymorphism/quantitative genetics). *Proc. Natl. Acad. Sci. USA*, *87*(December), 9888–9892.

Doll, N. M., Depège-Fargeix, N., Rogowsky, P. M., & Widiez, T. (2017). Signaling in Early Maize Kernel Development. *Molecular Plant*, *10*(3), 375–388. https://doi.org/10.1016/j.molp.2017.01.008

Faure, J. E., Rusche, M. L., Thomas, A., Keim, P., Dumas, C., Mogensen, H. L., … Chaboud, A. (2003). Double fertilization in maize: The two male gametes from a pollen grain have the ability to fuse with egg cells. *Plant Journal*, *33*(6), 1051–1062. https://doi.org/10.1046/j.1365-313X.2003.01692.x

Ferguson, J. E., Rhodes, A. M., & Dickinson, D. B. (1978). The genetics of suary enhancer (se), an independent modifier of sweet corn (su). *Journal of Heredity*, *69*(6), 377–380. https://doi.org/10.1093/oxfordjournals.jhered.a108976

Finegan, C., Boehlein, S. K., Leach, K. A., Madrid, G., Hannah, L. C., Koch, K. E., … Resende, M. F. R. (2022). Genetic Perturbation of the Starch Biosynthesis in Maize Endosperm Reveals Sugar-Responsive Gene Networks. *Frontiers in Plant Science*, *12*(February), 1–16. https://doi.org/10.3389/fpls.2021.800326

Food and Agricultural Organization of the United Nations. (2022). Value of Agricultural Production.

Gao, M., Wanat, J., Stinard, P. S., James, M. G., & Myers, A. M. (1998). Characterization of dull1, a maize gene coding for a novel starch synthase. *Plant Cell*, *10*(3), 399–412. https://doi.org/10.1105/tpc.10.3.399

Gerdes, J. T., Behr, C. F., Coors, H. G., & Tracy, W. F. (1993). Sweet Corn. In *Compilation of North American Maize Breeding Germplasm*.

Guan, J. C., Li, C., Flint-Garcia, S., Suzuki, M., Wu, S., Saunders, J. W., … Koch, K. E. (2023). Maize domestication phenotypes reveal strigolactone networks coordinating grain size evolution with kernel-bearing cupule architecture. *Plant Cell*, *35*(3), 1013–1037. https://doi.org/10.1093/plcell/koac370

Han, Z., Wang, B., Tian, L., Wang, S., Zhang, J., Guo, S. L., … Chen, Y. (2020). Comprehensive dynamic transcriptome analysis at two seed germination stages in maize (Zea mays L.). *Physiologia Plantarum*, *168*(1), 205–217. https://doi.org/10.1111/ppl.12944

Hannah, L. C. (2005). Starch synthesis in the maize endosperm. *Maydica*, *50*(3–4), 497–506.

Hannah, L. C., & Nelson, O. E. (1976). Characterization of ADP-glucose pyrophosphorylase from shrunken-2 and brittle-2 mutants of maize. *Biochemical Genetics*, *14*(7–8), 547–560. https://doi.org/10.1007/BF00485834

Hannah, L. Curtis, Shaw, J. R., Clancy, M. A., Georgelis, N., & Boehlein, S. K. (2017). A brittle-2 transgene increases maize yield by acting in maternal tissues to increase seed number . *Plant Direct*, *1*(6), 1–9. https://doi.org/10.1002/pld3.29

Harvey, B. M., & Oaks, A. (1974). The role of gibberellic acid in the hydrolysis of endosperm reserves in Zea mays. *Planta*, *121*(1), 67–74. https://doi.org/10.1007/BF00384007

Hennen-Bierwagen, T. A., Liu, F., Marsh, R. S., Kim, S., Gan, Q., Tetlow, I. J., … Myers, A. M. (2008). Starch biosynthetic enzymes from developing maize endosperm associate in multisubunit complexes. *Plant Physiology*, *146*(4), 1892–1908. https://doi.org/10.1104/pp.108.116285

Hershberger, J., Tanaka, R., Wood, J. C., Kaczmar, N., Wu, D., Hamilton, J. P., … Gore, M. A. (2022). Transcriptome-wide association and prediction for carotenoids and tocochromanols in fresh sweet corn kernels. *Plant Genome*, *15*(2), 1–16. https://doi.org/10.1002/tpg2.20197

Hii, S. L., Tan, J. S., Ling, T. C., & Ariff, A. Bin. (2012). Pullulanase: Role in starch hydrolysis and potential industrial applications. *Enzyme Research*, *2012*. https://doi.org/10.1155/2012/921362

Hoecker, U., Vasil, I. K., & McCarty, D. R. (1995). Integrated control of seed maturation and germination programs by activator and repressor functions of viviparous-1 of maize. *Genes and Development*, *9*(20), 2459–2469. https://doi.org/10.1101/gad.9.20.2459

Holst, I., Moreno, J. E., & Piperno, D. R. (2007). Identification of teosinte, maize, and Tripsacum in Mesoamerica by using pollen, starch grains, and phytoliths. *Proceedings of the National Academy of Sciences of the United States of America*, *104*(45), 17608–17613. https://doi.org/10.1073/pnas.0708736104

Hu, X., Liu, H., Yu, Y., Li, G., Qi, X., Li, Y., … Liu, R. H. (2021). Accumulation of phenolics, antioxidant and antiproliferative activity of sweet corn (Zea mays L.) during kernel maturation. *International Journal of Food Science and Technology*, *56*(5), 2462–2470. https://doi.org/10.1111/ijfs.14879

Hu, Y., Colantonio, V., Müller, B. S. F., Leach, K. A., Nanni, A., Finegan, C., … Resende, M. F. R. (2021). Genome assembly and population genomic analysis provide insights into the evolution of modern sweet corn. *Nature Communications*, *12*(1), 1227. https://doi.org/10.1038/s41467-021-21380-4

Huang, H., Xie, S., Xiao, Q., Wei, B., Zheng, L., Wang, Y., … Huang, Y. (2016). Sucrose and ABA regulate starch biosynthesis in maize through a novel transcription factor, ZmEREB156. *Scientific Reports*, *6*(February), 1–12. https://doi.org/10.1038/srep27590

Hussain, S., Kim, S. H., Bahk, S., Ali, A., Nguyen, X. C., Yun, D. J., & Chung, W. S. (2020). The Auxin Signaling Repressor IAA8 Promotes Seed Germination Through Down-Regulation of ABI3 Transcription in Arabidopsis. *Frontiers in Plant Science*, *11*(February), 1–11. https://doi.org/10.3389/fpls.2020.00111

Ibrahim, K. E., & Juvik, J. A. (2009). Feasibility for improving phytonutrient content in vegetable crops using conventional breeding strategies; case study with carotenoids and tocopherols in sweet corn and broccoli. *Journal of Agricultural and Food Chemistry*, *57*(11), 4636–4644. https://doi.org/10.1021/jf900260d

Ingle, J., Beitz, D., & Hageman, R. H. (1965). Changes in Composition during Development and Maturation of Maize Seeds. *Plant Physiology*, *40*(5), 835–839. https://doi.org/10.1104/pp.40.5.835

James, M., & Myers, A. (2009). Seed Starch Synthesis. In J. L. Bennetzen & S. C. Hake (Eds.), *Handbook of Maize: Its Biology* (pp. 439–456). https://doi.org/10.1007/978-0-387-79418-1_22

Jones, R. J., & Brenner, M. L. (1987). Distribution of Abscisic Acid in Maize Kernel during Grain Filling. *Plant Physiology*, *83*(4), 905–909. https://doi.org/10.1104/pp.83.4.905

Jones, R. J., & Setter, T. L. (2000). Hormonal regulation of early kernel development. *Physiology and Modeling Kernel Set in Maize*, (29), 25–42. https://doi.org/10.2135/cssaspecpub29.c3

Jones, R., Ougham, H., Thomas, H., & Waaland, S. (2013). Hormones and other signals. In *The Molecular Life of Plants* (1st ed., pp. 329–370). Hoboken, NJ: John Wiley & Sons, Ltd.

Kowles, R. V., & Phillips, R. L. (1988). Endosperm Development in Maize. *International Review of Cytology*, *112*(C), 97–136. https://doi.org/10.1016/S0074-7696(08)62007-0

La Bonte, D. R., & Juvik, J. A. (1990). Characterization of sugary-1 (su-1) sugary enhancer (se) Kernels in Segregating Sweet Corn Populations. *Journal of the American Society for Horticultural Science*, *115*(1), 153–157. https://doi.org/10.21273/jashs.115.1.153

Leclere, S., Schmelz, E. A., & Chourey, P. S. (2010). Sugar levels regulate tryptophan-dependent auxin biosynthesis in developing maize kernels. *Plant Physiology*, *153*(1), 306–318. https://doi.org/10.1104/pp.110.155226

Li, L., Ilarslan, H., James, M. G., Myers, A. M., & Wurtele, E. S. (2007). Genome wide co-expression among the starch debranching enzyme genes AtISA1, AtISA2, and AtISA3 in Arabidopsis thaliana. *Journal of Experimental Botany*, *58*(12), 3323–3342. https://doi.org/10.1093/jxb/erm180

Lin, Q., Facon, M., Putaux, J. L., Dinges, J. R., Wattebled, F., D'Hulst, C., … Myers, A. M. (2013). Function of isoamylase-type starch debranching enzymes ISA1 and ISA2 in the Zea mays leaf. *New Phytologist*, *200*(4), 1009–1021. https://doi.org/10.1111/nph.12446

Liu, X., Zhang, H., Zhao, Y., Feng, Z., Li, Q., Yang, H. Q., … He, Z. H. (2013). Auxin controls seed dormancy through stimulation of abscisic acid signaling by inducing ARF-mediated ABI3 activation in Arabidopsis. *Proceedings of the National Academy of Sciences of the United States of America*, *110*(38), 15485–15490. https://doi.org/10.1073/pnas.1304651110

Lloyd, J. R., & Kossmann, J. (2015). Transitory and storage starch metabolism: Two sides of the same coin? *Current Opinion in Biotechnology*, *32*, 143–148. https://doi.org/10.1016/j.copbio.2014.11.026

Locascio, A., Roig-Villanova, I., Bernardi, J., & Varotto, S. (2014). Current perspectives on the hormonal control of seed development in Arabidopsis and maize: A focus on auxin. *Frontiers in Plant Science*, *5*(AUG), 1–22. https://doi.org/10.3389/fpls.2014.00412

Macdonald, F. D., & Preiss, J. (1983). Solubilization of the Starch-Granule-Bound Starch Synthase of Normal Maize Kernels. *Plant Physiology*, *73*(1), 175–178. https://doi.org/10.1104/pp.73.1.175

Martin, C., & Smith, A. M. (1995). Starch Biosynthesis. *The Plant Cell*, *7*(7), 971–985.

Moyers, B. T., Morrell, P. L., & Mckay, J. K. (2018). Genetic Costs of Domestication and Improvement. *Journal of Heredity*, (August 2017), 103–116. https://doi.org/10.1093/jhered/esx069

Olsen, O. A. (2020). The Modular Control of Cereal Endosperm Development. *Trends in Plant Science*, *25*(3), 279–290. https://doi.org/10.1016/j.tplants.2019.12.003

Piperno, D. R., Ranere, A. J., Holst, I., Iriarte, J., & Dickau, R. (2009). Starch grain and phytolith evidence for early ninth millennium B.P. maize from the Central Balsas River Valley, Mexico. *Proceedings of the National Academy of Sciences of the United States of America*, *106*(13), 5019–5024. https://doi.org/10.1073/pnas.0812525106

Rajasheker, G., Jawahar, G., Jalaja, N., Kumar, S. A., Kumari, P. H., Punita, D. L., … Kishor, P. B. K. (2019). Role and regulation of osmolytes and ABA interaction in salt and drought stress tolerance. In *Plant Signaling Molecules: Role and Regulation under Stressful Environments*. https://doi.org/10.1016/B978-0-12-816451-8.00026-5

Revilla, P., Anibas, C. M., & Tracy, W. F. (2021). Sweet corn research around the world 2015–2020. *Agronomy*, *11*(3), 1–49. https://doi.org/10.3390/agronomy11030534

Ribeiro, C., Hennen-Bierwagen, T. A., Myers, A. M., Cline, K., & Settles, A. M. (2020). Engineering 6-phosphogluconate dehydrogenase improves grain yield in heat-stressed maize. *Proceedings of the National Academy of Sciences of the United States of America*, *117*(52), 33177–33185. https://doi.org/10.1073/PNAS.2010179117

Rouf Shah, T., Prasad, K., & Kumar, P. (2016). Maize—A potential source of human nutrition and health: A review. *Cogent Food and Agriculture*, *2*(1). https://doi.org/10.1080/23311932.2016.1166995

Sabelli, P. A. (2012). Replicate and die for your own good: Endoreduplication and cell death in the cereal endosperm. *Journal of Cereal Science*, *56*(1), 9–20. https://doi.org/10.1016/j.jcs.2011.09.006

Sabelli, P. A., & Larkins, B. A. (2009a). The contribution of cell cycle regulation to endosperm development. *Sexual Plant Reproduction*, *22*(4), 207–219. https://doi.org/10.1007/s00497-009-0105-4

Sabelli, P. A., & Larkins, B. A. (2009b). The development of endosperm in grasses. *Plant Physiology*, *149*(1), 14–26. https://doi.org/10.1104/pp.108.129437

Shi, J., Sweedman, M. C., & Shi, Y. C. (2018). Structural changes and digestibility of waxy maize starch debranched by different levels of pullulanase. *Carbohydrate Polymers*, *194*(January), 350–356. https://doi.org/10.1016/j.carbpol.2018.04.053

Siyuan, S., Tong, L., & Liu, R. H. (2018). Corn phytochemicals and their health benefits. *Food Science and Human Wellness*, *7*(3), 185–195. https://doi.org/10.1016/j.fshw.2018.09.003

Špoljarić Marković, S., Ledenčan, T., Viljevac Vuletić, M., Galić, V., Jambrović, A., Zdunić, Z., … Svečnjak, Z. (2020). Chemical components of kernel quality in sh2 sweet corn genotypes (Zea mays l. saccharata sturt.) as affected by harvest date. *Journal of Central European Agriculture*, *21*(3), 577–588. https://doi.org/10.5513/JCEA01/21.3.2677

Stitzer, M. C., & Ross-Ibarra, J. (2018). Maize domestication and gene interaction. *New Phytologist*, *220*(2), 395–408. https://doi.org/10.1111/nph.15350

Struk, S. (2018). *Elucidation of the protein-protein interaction network at play during strigolactone and karrikin signaling*. Retrieved from https://biblio.ugent.be/publication/8584183/file/8584184.pdf

Sun, H., Xu, H., Li, B., Shang, Y., Wei, M., Zhang, S., … Wu, Y. (2021). The brassinosteroid biosynthesis gene, ZmD11, increases seed size and quality in rice and maize. *Plant Physiology and Biochemistry*, *160*(January), 281–293. https://doi.org/10.1016/j.plaphy.2021.01.031

Swarts, K., Gutaker, R. M., Benz, B., Blake, M., Bukowski, R., Holland, J., … Burbano, H. A. (2017). Genomic estimation of complex traits reveals ancient maize adaptation to temperate North America. *Science*. https://doi.org/10.1126/science.aam9425

Tracy, W. F. (1996). History, Genetics, and Breeding of Supersweet (shrunken2) Sweet Corn. In *Plant Breeding Reviews* (Vol. 00, pp. 189–236). https://doi.org/https://doi.org/10.1002/9780470650073.ch7

Tracy, W. F., Shuler, S. L., & Dodson-Swenson, H. (2019). The use of endosperm genes for sweet corn improvement: A review of developments in endosperm genes in sweet corn since the seminal publication in plant breeding reviews, volume 1, by Charles Boyer and Jack Shannon (1984). *Plant Breeding Reviews*, *43*, 215–241. https://doi.org/10.1002/9781119616801.ch6

Tracy, W. F., Whitt, S. R., & Buckler, E. S. (2006). Recurrent mutation and genome evolution: Example of Sugary 1 and the origin of sweet maize. *Crop Science*. https://doi.org/10.2135/cropsci2006-03-0149tpg

Van Heerwaarden, J., Hufford, M. B., & Ross-Ibarra, J. (2012). Historical genomics of North American maize. *Proceedings of the National Academy of Sciences of the United States of America*, *109*(31), 12420–12425. https://doi.org/10.1073/pnas.1209275109

Vollbrecht, E., & Evans, M. M. S. S. (2017). Gametophyte interactions establishing maize kernel development. In *Maize kernel development* (pp. 16–27). https://doi.org/10.1079/9781786391216.0016

Wang, X., Zenda, T., Liu, S., Liu, G., Jin, H., Dai, L., … Duan, H. (2019). Comparative proteomics and physiological analyses reveal important maize filling-kernel drought-responsive genes and metabolic pathways. *International Journal of Molecular Sciences*, *20*(15). https://doi.org/10.3390/ijms20153743

Wang, Z., Mambelli, S., & Setter, T. L. (2002). Abscisic acid catabolism in maize kernels in response to water deficit at early endosperm development. *Annals of Botany*, *90*(5), 623–630. https://doi.org/10.1093/aob/mcf239

White, C. N., & Rivin, C. J. (2000). Gibberellins and seed development in maize. II. Gibberellin synthesis inhibition enhances abscisic acid signaling in cultured embryos. *Plant Physiology*, *122*(4), 1089–1097. https://doi.org/10.1104/pp.122.4.1089

Whitt, S. R., Wilson, L. M., Tenaillon, M. I., Gaut, B. S., & Buckler IV, E. S. (2002). Genetic diversity and selection in the maize starch pathway. *Proceedings of the National Academy of Sciences of the United States of America*, *99*(20), 12959–12962. https://doi.org/10.1073/pnas.202476999

Wu, C., Colleoni, C., Myers, A. M., & James, M. G. (2002). Enzymatic properties and regulation of ZPU1, the maize pullulanase-type starch debranching enzyme. *Archives of Biochemistry and Biophysics*, *406*(1), 21–32. https://doi.org/10.1016/S0003-9861(02)00412-5

Wu, H., Becraft, P. W., & Dannenhoffer, J. M. (2022). Maize Endosperm Development: Tissues, Cells, Molecular Regulation and Grain Quality Improvement. *Frontiers in Plant Science*, *13*(March). https://doi.org/10.3389/fpls.2022.852082

Xue, X., Du, S., Jiao, F., Xi, M., Wang, A., Xu, H., … Wang, M. (2021). The regulatory network behind maize seed germination: Effects of temperature, water, phytohormones, and nutrients. *Crop Journal*, *9*(4), 718–724. https://doi.org/10.1016/j.cj.2020.11.005

Yang, C. J., Samayoa, L. F., Bradbury, P. J., Olukolu, B. A., Xue, W., York, A. M., … Doebley, J. F. (2019). The genetic architecture of teosinte catalyzed and constrained maize domestication. *Proceedings of the National Academy of Sciences of the United States of America*, *116*(12), 5643–5652. https://doi.org/10.1073/pnas.1820997116

Yang, H., Gu, X., Ding, M., Lu, W., & Lu, D. (2018). Heat stress during grain filling affects activities of enzymes involved in grain protein and starch synthesis in waxy maize. *Scientific Reports*, *8*(1), 1–9. https://doi.org/10.1038/s41598-018-33644-z

Yue, K., Lingling, L., Xie, J., Coulter, J. A., & Luo, Z. (2021). Synthesis and regulation of auxin and abscisic acid in maize. *Plant Signaling and Behavior*, *16*(7). https://doi.org/10.1080/15592324.2021.1891756

Zhang, J., Jia, W., Yang, J., & Ismail, A. M. (2006). Role of ABA in integrating plant responses to drought and salt stresses. *Field Crops Research*, *97*(1 SPEC. ISS.), 111–119. https://doi.org/10.1016/j.fcr.2005.08.018

Zhang, X., Haro von Mogel, K. J., Lor, V. S., Hirsch, C. N., de Vries, B., Kaeppler, H. F., … Kaeppler, S. M. (2019). Maize sugary enhancer1 (se1) is a gene affecting endosperm starch metabolism. *Proceedings of the National Academy of Sciences of the United States of America*, *116*(41), 20776–20785. https://doi.org/10.1073/pnas.1902747116

2 Chapter Two: The Sugary enhancer1 (*se1*) Allele is Associated with Significant Decreases in Carotenoids and Tocotrienols in Yellow (*Y1*) sugary1 (*su1*) Sweet Corn

Carl Branch[1], Matheus Baseggio[2], Marcio Resende[3], William F. Tracy[1]

[1]Department of Plant and Agroecosystem Sciences, College of Agricultural and Life Sciences, University of Wisconsin- Madison, Madison, WI 53706, USA

[2]Seneca Foods, Le Sueur, MN 56058, USA

[3]Department of Horticultural Sciences, University of Florida, Gainesville, FL 32611, USA

Submitted to Journal of the American Society for Horticultural Science on April 5, 2024. Conditionally accepted and returned for revision April 24, 2024. Presented below as revised and returned for review.

2.1 Abstract

A distinctive phenotype of homozygous *sugary enhancer1 (se1)* sweet corn inbreds and hybrids is a light-yellow color in mature kernels. Carotenoid pigments contribute to yellow endosperm color in maize and are of nutritional importance in the human diet along with the related tocochromanols, the E vitamins. Tocochromanols, including both tocopherols and tocotrienols, are antioxidants important in human nutrition and cardiovascular health. Effects of the presence of *sugary enhancer1* allele on carotenoid and tocochromanol levels in

homozygous *su1, Y1* endosperm were evaluated in the Wisconsin Sweet Corn Diversity Panel. While population structure was present in the panel, the majority of variation in carotenoid levels was explained by genotype at the *se1* locus. *se1* was associated with significant decreases in the amount of lutein (34%) and zeaxanthin (36%) and decreases of tocotrienols by 12-65%. There were no significant differences in β-carotene and tocopherol levels between the two groups. Given that the biosynthesis pathways for carotenoids and tocochromanols are well-defined, these differences in carotenoids and tocotrienols between *su1Se1* and *su1se1* inbreds point to a broader role of *Se1* alleles in metabolic pathways beyond endosperm starch production.

2.2 Introduction

Sweet corn breeding has traditionally been shaped by the manipulation of a small number of key genes in the starch synthesis pathway, resulting in an increase in sugar accumulation in the developing maize endosperm at the cost of decreased starch production (Whitt et al. 2002). The *sugary1* (*su1*) mutation, a defect in the isoamylase1 starch-debranching enzyme, has the longest history of use in commercial breeding (Tracy et al. 2006). The majority of commercial sweet corns currently in use are supersweet "shrunken" types. The *shrunken2* (*sh2*) mutation is a null mutation in the AGPase large subunit (Preiss et al. 1990; Tracy et al. 2019). The *sugary enhancer1* (*se1)* mutation is a recessive modifier of *su1*, and can result in elevated sugar levels compared to sugary types (Tracy et al. 2019). Along with increases in sucrose and maltose, *se1* confers a light yellow endosperm phenotype when compared to a homozygous *Se1su1* sweet corn (Figure 2.1). While the exact mechanism through which *se1* affects kernel phenotype is unknown, it is likely to have regulatory role in starch synthesis and accumulation (Zhang et al. 2019). The taste and texture traits resulting from presence, absence, or combinations of these endosperm mutations have been the main targets of sweet corn breeding in the last half-century

(Tracy et al. 2019; Hu et al. 2021). However, as biofortified crops—plants where traditional breeding and/or gene editing have been used to specifically increase a food's nutritional value—have become a focus of plant breeders, sweet corn emerges as a viable candidate for biofortification.

Figure 2.1. Phenotypes of sugary-enhancer sweet corn kernels differing at the s*e1* locus. Both ears are from the same homozygous *se1 su1* inbred. The ear on the left was pollinated by a homozygous recessive *se1 su1* near isogenic inbred. The ear on the right was pollinated by a homozygous dominant *Se1 su1* isogenic inbred.

Biofortification approaches have been implemented with particular zeal in manipulating the levels of various vitamins and antioxidants, including but not limited to vitamin A and

vitamin E compounds, as a way to reduce both severe nutrient deficiency in developing countries and prevent the more subtle subclinical micronutrient deficiencies that occur in developed regions (Wurtzel et al. 2012; HarvestPlus; Food and Agricultural Organization of the United Nations (FAO) 2019). Successful biofortification programs rely on a combination of 1) known metabolic pathways for the trait of interest; 2) a target species with existing variation for the trait of interest; 3) nutrient stability in the final biofortified product. Without a target species that allows for clear and achievable goals, these points will slow the development and release of biofortified cultivars and increase costs for breeders, growers, and consumers; the result is an inefficient and ineffective biofortification program. Sweet corn, as currently consumed globally, possesses all three of the qualities necessary for effective biofortification. First, since maize is a model species for the plant genetics community, the biosynthesis pathways have been at least partially characterized for a number of compounds relevant to human nutrition, including the carotenoids and tocochromanols that provide biologically active vitamin A and vitamin E (Azmach et al. 2018; Bao et al. 2020; Diepenbrock et al. 2021). Furthermore, in both sweet corn and maize as a whole, there is extensive variation for these compounds that can be mined as the foundation for traditional breeding pipelines (Baseggio et al. 2019; Baseggio et al. 2020). Carotenoids, as a component of kernel color in sweet corn, are already under direct and indirect selection pressure as breeders optimize kernel color for consumer tastes (Ibrahim and Juvik 2009). Finally, in contrast to dried staple food products such grain corn or rice, sweet corn is eaten fresh, leaving less time for breakdown of any beneficial nutrients. Current forecasts suggest that sweet corn consumption in the United States will decline to 10 pounds per person, a 50% drop from previous peak consumption (Davis and Lucier 2021). Increasing the nutritional

value of sweet corn would have an added benefit of promoting consumer appeal in the face of declining fresh, frozen, and canned sweet corn sales.

Perhaps the most attractive biofortification targets in maize are high levels of provitamin A compounds and other carotenoids, and the tocochromanols, or vitamin E; these compounds fit into the framework for successful biofortification. Carotenoids, including but not limited to compounds with vitamin A activity, are naturally occurring pigments that function in light-harvesting and control reactive oxygen species in plants; they function as antioxidants in humans and are obtained through dietary intake. The carotenoids α-carotene, β-carotene, and β-cryptoxanthin are required for healthy vision, regular child development, and strong immune system function (Lima et al. 2016; Bird et al. 2017). Consumed from plant sources, these provitamin A carotenoids are cleaved to produce the biologically active vitamin A, or retinol. β-carotene can produce two units of retinol, while α-carotene and β-cryptoxanthin each yield one unit. Other carotenoids with significant human health implications are the macular pigments lutein and zeaxanthin, which help to absorb blue light in the foveola of the eye (Lima et al. 2016).

Recent work has been done to understand the biosynthesis pathways controlling both carotenoid and tocochromanol production in sweet corn, as well as measure the levels of these compounds in existing breeding material (Diepenbrock et al. 2017; Baseggio et al. 2019; Baseggio et al. 2020; Diepenbrock et al. 2021). In maize, synthesis of carotenoids and the tocotrienol class of tocochromanols takes place in the endosperm. Carotenoid synthesis begins with the production of isoprenoid precursors in the amyloplast. Through the methylerythritol (MEP) pathway, glyceraldehyde-3-phosphate and pyruvate are converted to isopentenyl pyrophosphate (IPP). Geranylgeranyl pyrophosphate synthase joins two units of IPP into

geranylgeranyl pyrophosphate (GGPP). Carotenoid synthesis enzymes will convert GGPP into first phytoene and then lycopene. Lycopene-cyclase enzymes add cyclohexyl rings to both ends of the lycopene molecule; at this point, the pathway splits into α-branch carotenes and β-branch carotenes, depending on which form of lycopene-cyclase catalyzed the initial reaction (Cuttriss et al. 2011; Wurtzel et al. 2012). In both branches, the cytochrome 450 β-ring hydroxylase (LUT1) and the β-carotene hydroxylase (CRTRB) catalyze the reaction converting the α- and β-carotene to zeinoxanthin and its isomer β-cryptoxanthin, respectively (Figure 2.2). The cytochrome 450 sigma-ring hydroxylase (LUT5) produces lutein from zeinoxanthin, and CRTRB produces zeaxanthin from lutein. As the accumulation products at the ends of the α- and β-branches of the pathway, lutein and zeaxanthin are the most abundant carotenoids in maize endosperm (Wurtzel et al. 2012). For this reason, increasing lutein and zeaxanthin production and storage is a logical place to begin carotenoid biofortification in sweet corn.

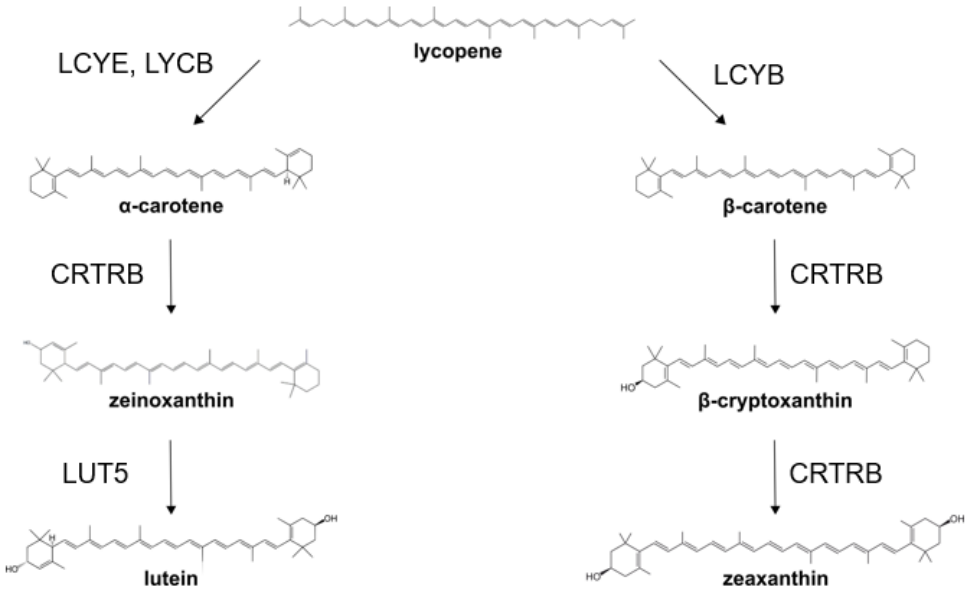

Figure 2.2. Carotenoid synthesis pathway showing the relationship and divergence between the compounds and enzymes in α-branch and β-branch carotenoids, starting from lycopene.

Tocochromanols can be synthesized in either the endosperm or the embryo, depending on what form is being produced (Diepenbrock et al. 2017; Bao et al. 2020). Similar to carotenoid synthesis, production of tocochromanol compounds also starts in the endosperm with GGPP through the MEP pathway; the production of tocopherols begins with phytyl-pyrophosphate instead and occurs in the embryo. Phytyl-pryophospate and homogentisate are combined by homogentisate phytyltransferase to form tocopherols, and GGPP and homogentisate are catalyzed by homogentisate geranylgeranyltransferase to form tocotrienols (Sen et al. 2006). Given the similarity to carotenoids in the early biosynthesis steps, increasing levels of vitamin E in sweet corn can be undertaken in tandem with increasing vitamin A.

Since almost most of the existing sweet corn germplasm uses one or more of the three primary endosperm mutations, breeders must pay close attention to interactions or associations between endosperm type and any potential biofortification trait. Sugar signaling in maize controls a range of biological processes; the combination of sucrose and abscisic acid regulates parts of starch synthesis via regulation of transcription (Huang et al. 2016). Abscisic acid is a derivative of zeaxanthin, presenting an intersection of starch and sugar synthesis and carotenoid accumulation. Understanding the carotenoid and tocochromanol traits in relation to the primary sweet corn endosperm types and their relative sugar levels is a foundation for future biofortification programs.

Previous work has been done using a diversity panel constructed to represent most of the genetic variation present in modern temperate sweet corn. A genome-wide association study (GWAS) identified a collection of key genes that were associated with elevated carotenoid levels, particularly within *sh2* inbreds (Baseggio et al., 2020). The same research group performed a similar GWAS using tocochromanol phenotype data, and found that variation in major genes and

differences between endosperm types were present in vitamin E-related traits as well (Baseggio et al. 2019). Included in both of these studies was the pair of near-isogenic lines (NILS) that was used to characterize *se1,* W822GSe and W822Gse, which are homozygous for the dominant and recessive *se1* alleles, respectively, but are homozygous recessive at the *sugary1* locus (Zhang et al. 2019). However, a limitation of these projects was that all inbreds in both studies, including the W822G NILS, were classified as either *su1, sh2,* or *su1sh2* mutants; sugary-enhancer inbreds were not analyzed as a separate group. Given that *se1* inbreds tend to have a lighter-colored kernel compared to their dominant-*Se1* counterparts, the diversity panel datasets present an opportunity to test the hypothesis on a population level that *se1* has less carotenoids than *su1* inbreds. Since any significant differences between endosperm types in the original analysis may have been confounded by including *se1* inbreds with *su1* inbreds, reanalyzing the carotenoid and tocopherol phenotypic data with the inclusion of *se1* genotype information serves two purposes: 1) to determine levels of carotenoids and tocochromanols in *se1* inbreds relative to sugary and shrunken inbreds, and 2) to identify any associations between *se1* and amounts of intermediates or products of the carotenoid and tocochromanol pathways.

2.3 Methods

2.3.1 Plant Materials and Metabolite Analysis

Data from the Wisconsin Sweet Corn Diversity Panel was used in this study, and was originally collected for publication in (Baseggio et al. 2019) and (Baseggio et al. 2020). Sweet corn lines and checks were grown in Aurora, NY, in the 2014 and 2015 growing seasons, with the full panel consisting of 411 lines common to each year. The panel was grown as an augmented incomplete block design, with blocks grouped based on plant height and inbreds randomized within blocks. Each incomplete block contained 20 experimental entries. Field

placement of entries within blocks and of sets of blocks within the field was randomized. Typical practices for sweet corn cultivation were used. Harvest maturity was determined to be 400 growing degree days, corresponding to approximately 21 days after pollination, when sweet corn is at the milk stage ideal for vegetable consumption. Before metabolite analysis, two self-pollinated ears were harvested from each plot, flash frozen in liquid nitrogen, and kernels from the two ears pooled and stored at -80 C. Then, 20 to 30 kernels from each plot were ground in liquid nitrogen for extraction and quantification of either carotenoids or tocopherols. Metabolite analysis was done on ground samples at Michigan State University (East Lansing, MI) using high-performance liquid chromatography (HPLC). Full HPCL conditions are described in Baseggio et. al. 2019 and Baseggio et. al. 2020.

After filtering for HPLC outliers and data normalization using Box-Cox transformation, HPLC data for the remaining samples were used to generate best linear unbiased predictors (BLUPs) using a mixed linear model in ASReml-r (Gilmour et al. 2009; Baseggio et al. 2019; Baseggio et al. 2020). In the full diversity panel, there were 308 lines with carotenoid phenotype data and 384 lines with tocochromanol phenotype data due to low-carotenoid, white-endosperm outliers being excluded from the carotenoid set (Baseggio et al. 2020). Endosperm mutations included in the full panel were *su1, su1se1, sh2, su1 sh2-i, brittle2 (bt2),* and ADX *amylose-extender (ae1), dull1 (du1) waxy1 (wx1).* In this experiment, only data from *su1/su1 Se1/Se1* and *su1/su1 se1/se1* lines were used.

2.3.2 Sugary-enhancer genotyping

To determine differences in carotenoid and tocopherol levels between *se1su1* and *Se1su1* lines, a subset of the *su1* lines from the BLUP dataset was selected for genotyping. This subset was selected as representative of publicly available genetic diversity within *su1* sweet corn

germplasm. Using PCR methods described in Zhang et. al. (2019), 115 *su1/su1* lines from the diversity panel were genotyped at the *se1* locus. Results were compared with genotype-by-sequencing data provided by Marcio Resende; lines with disagreement between PCR and GBS methods were removed from the data. This resulted in a dataset consisting of 30 *se1su1* and 58 *Se1su1* lines with carotenoid data, and 40 *se1su1* and 68 *Se1su1* lines with tocopherol data. All lines with carotenoid data had corresponding tocochromanol data, but 20 lines with tocopherol data did not have corresponding carotenoid data.

2.3.3 Statistical Analysis

First, 174,996 high-confidence single nucleotide polymorphisms (SNPs) were used to analyze population structure within TASSEL (Bradbury et al. 2007). These high-quality SNPs had a call rate above 70%, a minor allele frequency greater than 5%, and heterozygosity below 10%. The PCA function within TASSEL, using a covariance matrix, was used to obtain principal coordinates for the 108 lines with tocochromanol data, which included all lines with carotenoid data.

In order to detect statistically significant associations between endosperm type and levels of carotenoids or tocochromanols, a linear mixed model was constructed using the *mmer* function within the *sommer* package in R, using the BLUP datasets for phenotypic inputs (Covarrubias-Pazaran 2016). To control effects of different sample size and variance between the *se1Su1* and *su1su1* lines, sample weights, derived from the sample size over sample variance, were included. Population structure was controlled for by including the first four principal components and the kinship matrix from the TASSEL output. Wald tests within *sommer* were used to determine if there was a significant effect of genotype between *se1su1* and *Se1su1* lines on carotenoid or tocochromanol abundances (Covarrubias-Pazaran 2016). Pearson's correlations

between all combinations of carotenoid and tocochromanol traits were calculated separately for *se1* and *Se1* lines.

2.4 Results

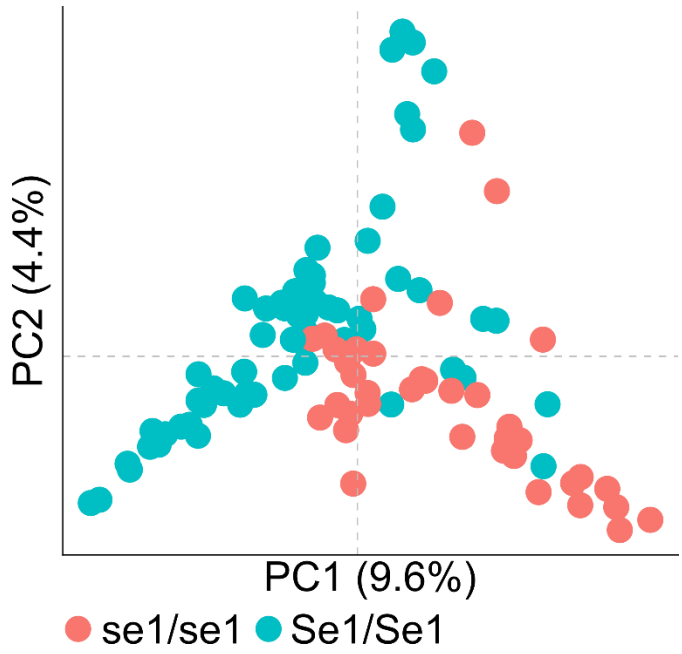

Figure. 2.3. Population structure by genotype at *sugary-enhancer1* locus. The majority of variation in carotenoid and tocochromanol traits was not due to relatedness among the Wisconsin Sweet Corn Diversity Panel subset used for analysis.

The first two principal coordinates explained 9.6 and 4.4 percent of the overall genetic variation in the dataset for this study (Fig. 2.3). Population structure is present in this dataset and does contribute significant variation for the majority of carotenoid and tocochromanol traits. However, the genotype at the *se1* locus explains additional trait variation not accounted for due to population structure. The magnitude of the *se1* effect varies by trait but is present to some degree in traits with significant differences. The majority of widely-used sugary-enhancer sweet corn inbreds have either been developed at public breeding programs at the University of Wisconsin-Madison and the University of Illinois or were derived from those lines, so some

structural effects are to be expected. Effects of population structure come from both public breeding programs each having a relatively small number of lines that can be found in pedigrees of much of their germplasm. Population structure and kinship cannot be ruled out as a factor driving differences in carotenoids and tocochromanols between *Se1su1* and *se1su1* lines, especially given the narrow genetic base in sweet corn compared to other types of corn (Hu et al. 2021). Among single-metabolite phenotypes, kinship effects were statistically significant for β-carotene ($p < 0.05$). In the case of lutein, PC1 significantly contributed to variation, but kinship did not (Supplementary Table S2.1).

Confirming the results of previous studies of carotenoid levels in sweet corn, lutein and zeaxanthin were the most abundant carotenoids in sugary-enhancer inbreds as well as the *Se1su1* inbreds (Figure. 2.4, Table 2.1). However, there was significantly more lutein and zeaxanthin in the *Se1su1* inbreds. There were differences with small effects between genotypes in the pathway intermediates β-cryptoxanthin and zeinoxanthin. Of the five carotenoid compounds with significant differences, zeinoxanthin was the only one enriched in the *se1su1* lines; β-cryptoxanthin, zeaxanthin, lutein, and antheraxanthin all had higher abundances in *Se1* lines. The patterns of composite carotenoid traits primarily reflected changes in lutein, zeaxanthin, and zeinoxanthin between genotypes. Overall, the relative abundances and rankings of each carotenoid compound were not significantly different between the *se1su1 group* and the *Se1su1*

groups, with the exception of zeinoxanthin increasing in abundance and no difference in the amount of lutein and zeaxanthin in the *se1su1* lines.

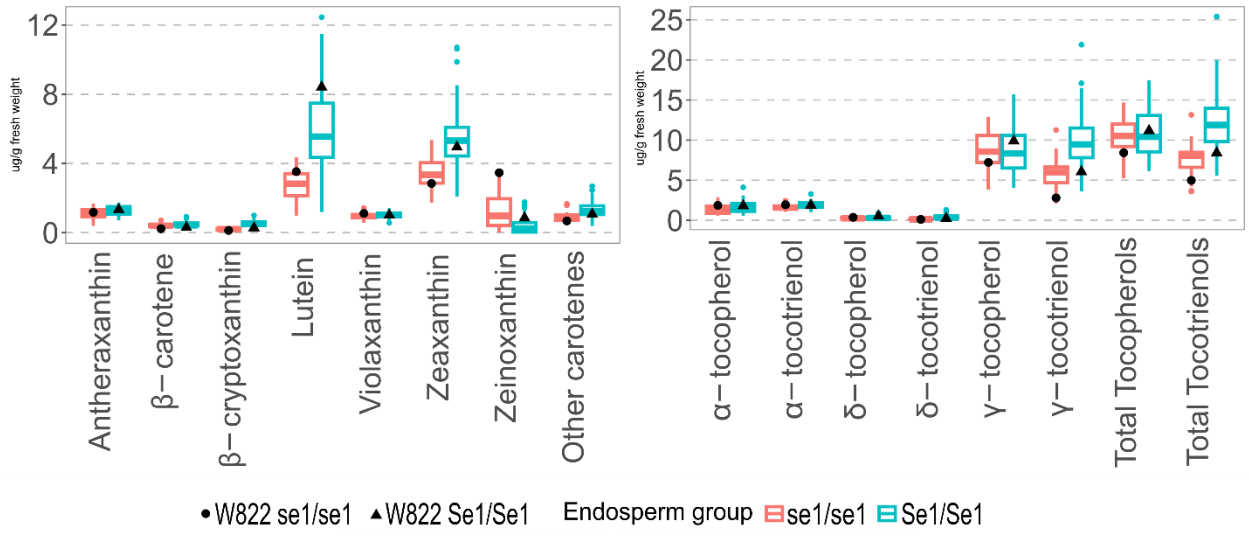

Figure 2.4. Variation in carotenoid and tocochromanol traits for *Se1/Se1* and *se1/se1* sweet corn lines. Boxplots for Se1/Se1 lines are shown in blue, se1/se1 lines are shown in red. Black points indicate trait values for the W822Gse (circle) and W822GSe (triangle) NILs as developed in Zhang et. al. (2019). All lines shown are homozygous for *su1*.

Table 2.1. Change in means between *se1su1* and *Se1su1* inbreds for single and composite carotenoid and tocochromanol traits.

Trait	*se1su1*	*Se1su1*	Difference[i]
	mean (µg g^{-1})		
β-Cryptoxanthin	0.205	0.534	-0.328***
Zeaxanthin	3.404	5.480	-2.076***
Zeinoxanthin	1.385	0.372	1.013*
Lutein	3.570	5.450	-1.88***
Other carotenes	0.866	1.364	-0.498**
Antheraxanthin	1.028	1.320	-0.292*
Violaxanthin	0.918	1.023	-0.105NS
β-Carotene	0.442	0.489	-0.047NS
Total xanthophylls	5.040	7.334	-2.294**
Total carotenoids	11.302	17.124	-5.822***
α-Xanthophylls	1.736	3.588	-1.852NS
β-Xanthophylls	5.698	8.232	-2.534**
Total carotenes	1.392	1.932	-0.54**
β-carotene over β-cryptoxanthin	2.407	1.008	1.399***

β-Cryptoxanthin over zeaxanthin	0.061	0.089	-0.029***
Zeinoxanthin over lutein	0.104	0.253	-0.149**
β-Carotene over β-cryptoxanthin and zeaxanthin	0.161	0.090	0.07*
Total carotenes over total xanthophylls	0.169	0.129	0.039NS
γ-tocotrienol	6.026	9.693	-3.667***
δ-tocotrienol	0.186	0.416	-0.23***
α-tocotrienol	1.591	1.934	-0.343NS
γ -tocopherol	9.320	8.588	0.731NS
α-tocopherol	1.438	1.606	-0.167NS
δ-tocopherol	0.326	0.314	0.012NS
Total tocotrienols and tocopherols	18.387	22.319	-3.932NS
Total tocotrienols	7.754	12.158	-4.404***
Total tocopherols	10.177	9.529	0.648NS
Total tocopherols over total tocotrienols	1.453	0.802	0.651***
γ-tocotrienol over γ-tocotrienol plus α-tocotrienol	0.762	0.818	-0.056*
α-tocotrienol over γ-tocotrienol	0.324	0.224	0.1*
δ-tocotrienol over γ-tocotrienol plus α-tocotrienol	0.025	0.035	-0.01NS
δ-tocotrienol over α-tocotrienol	0.133	0.238	-0.105NS
δ-tocotrienol over γ-tocotrienol	0.033	0.042	-0.009NS
α-tocotrienol over γ-tocopherol	0.161	0.217	-0.056NS
γ-tocopherol over γ-tocopherol plus α-tocopherol	0.861	0.827	0.034NS
δ-tocopherol over α-tocopherol	0.283	0.230	0.053NS
δ-tocopherol over δ-tocopherol	0.039	0.041	-0.003NS
δ-tocopherol over δ-tocopherol and α-tocopherol	0.032	0.033	-0.001NS
[i]NS, *, **, *** non-significant or significant at P ≤ 0.05, 0.01, or 0.001, respectively			

For tocochromanol levels, ranks by abundance were also different between genotypes. γ-tocochromanols, including both tocopherols and tocotrienols, were the most abundant in both *se1su1 and Se1su1 lines.* For each of the α-, γ-, and δ-tocochromanols, the levels of the corresponding α-, γ-, or δ-tocotrienols were significantly lower in sugary-enhancer inbreds lines compared to *Se1su1* lines. Tocopherols were not significantly different between the two groups. Since tocotrienols, but not tocopherols, are synthesized in the endosperm, it follows that effects of the endosperm mutation *se1* on carotenoids may be mirrored by tocotrienols, but not tocopherols. Our study is the first to confirm the association of *se1* with specific tocochromanol effects and changes in abundance between different tocochromanol compounds.

These results support the hypothesis that the lighter-yellow pericarp associated with the *sugary-enhancer* endosperm mutant is at least partially due to changes in carotenoid biosynthesis. Using a larger range of genotypes and representing a broader section of the sweet corn breeding germplasm, this study confirms the findings of Juvik et. al. 2009 in that the *se1* endosperm mutation was associated with lower levels of lutein and zeaxanthin but had no effect on tocopherols.

Correlations between and within the carotenoid and tocochromanol traits were similar to results seen in other studies (Baseggio et al. 2019; Baseggio et al. 2020). Within the *se1* lines, lutein was negatively correlated with zeinoxanthin, which is an intermediate in lutein production (Figure. 2.5). Along with the increase in zeinoxanthin in *se1* lines, this could indicate a bottleneck in lutein production within the endosperm as a result of either the *se1* mutation

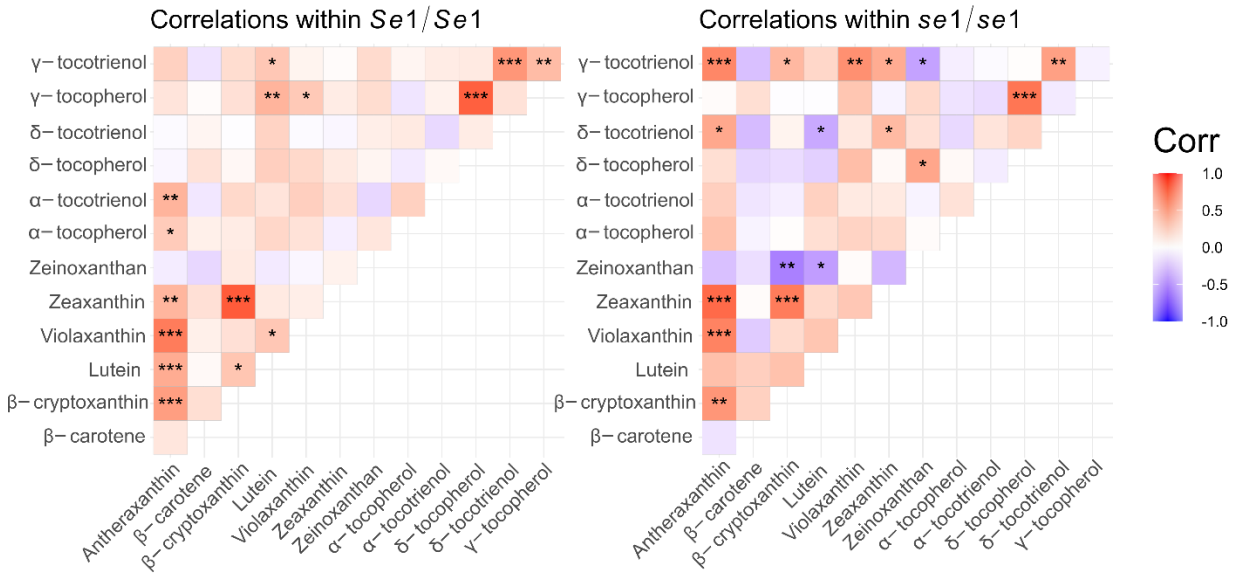

Figure 2.5. Correlations among *Se1/Se1* (left) and *se1/se1* lines (right) for individual carotenoid and tocochromanol traits. All lines are homozygous for *su1-ref.* *, **, *** significant at P ≤ 0.05, 0.01, or 0.001, respectively.

directly or as a result of the carbohydrate changes caused by *se1*. γ-tocochropherol and γ-

tocotrienol were the most abundant kernel tocochromanols; the two compounds are significantly correlated in *Se1su1* lines but not in *se1su1* lines.

2.5 Discussion

This study is informative for plant breeders interested in working with high-carotenoid or high-vitamin E sweet corn, especially those working in traditional breeding programs where gene editing, as has been done in other biofortified crops, faces cost or regulatory burdens. As traditional hybrid breeding revolves around both parent selection and population improvement, it's advantageous to use elite parents for producing new inbreds. In the case of carotenoids and tocochromanols in sweet corn, these results suggest that biofortification efforts should be focused on *sh2* and *su1* endosperm types rather than *se1* types. Since *se1* inbreds have reduced carotenoid and tocochromanol levels compared to their *Se1* counterparts, breeding with *se1* lines should be focused on markets where these nutrients are not a concern.

The results for each carotenoid or tocochromanol individual, sum or ratio trait can illuminate points in the biosynthesis pathways where *se1* may be interacting and identify *a priori* genes of interest for future expression studies. For example, a change in the ratio between compounds in adjacent steps in their biosynthesis pathway could be a result of altered function or expression of the enzyme that converts between the compounds. *se1su1* lines show an increase in zeinoxanthin but a decrease in β-cryptoxanthin. The carotenoid β-ring hydroxylase (CRTRB) is required for both steps from β-carotene to lutein, but a cytochrome P450 ε-ring hydroxylase (LUT1) is required to convert zeinoxanthin to lutein. Reduction in expression or activity of CRTRB would result in reduced conversion to zeaxanthin, and reduced expression of LUT1 would cause reduced production of lutein from zeinoxanthin. A similar inspection of the tocochromanol pathway and ratios of the compounds in this study shows that while tocotrienol

quantities are altered in *se1su1* lines, the ratios between tocochromanols traits and ratios between various tocotrienols are unchanged. This suggests that the key enzymes, tocopherol cyclase and tocopherol methyltransferase, which produce the α-, β-, and γ- tocochromanols, are not altered in expression or activity. A possible interaction between genes and substrates in the tocochromanol pathway and the *se1* locus occurs at or before the split between junction of tocotrienol synthesis and tocochromanol synthesis. Homogentisate geranylgeranyltransferase activity and the production of geranylgeranylpyrosphospate are points where tocotrienol synthesis differs from tocopherol synthesis and may be points of interaction with *se1*. While the data and discussion here are relevant to the biosynthesis pathways, future work is necessary to identify the effects of catabolic processes on these compounds and the effect degradation and conversion have on carotenoids and tocochromanols.

Carotenoids also serve as precursors to plant hormones, including abscisic acid (ABA); a change in carotenoid levels might shift ABA levels in the developing seed (Vallabhaneni and Wurtzel 2010). This may affect seed maturation and the balance between dormancy and germination processes, the latter of which also involves degradation of starch into simpler sugars (Huang et al. 2016). Taken together, the confluence of *se1* with carotenoid and tocochromanol synthesis suggests that *se1* may have systemic interactions beyond the starch synthesis pathway, possibly affecting CRTRB or LUT1, and shed light on possible roles of the dominant and recessive *alleles at the se1 locus*. Unlike the other primary sweet corn mutations *su1* and *sh2*, where the mutation contributes to a direct change in a functional enzyme, *se1* may have a more regulatory role in the starch synthesis pathway, where *se1* is able to interact with the synthesis of a number of secondary metabolites, including the pathways looked at here. However, more

research is necessary to identify specific places in the carotenoid and tocochromanol gene expression networks where starch synthesis pathways may be interacting.

2.6 Chapter Two References

Azmach G, Menkir A, Spillane C, Gedil M. 2018. Genetic loci controlling carotenoid biosynthesis in diverse tropical maize lines. G3 Genes, Genomes, Genet. 8(3):1049–1065. doi:10.1534/g3.117.300511.

Bao Y, Magallenes-Lundback M, Deason N, Dellapenna D. 2020. High throughput profiling of tocochromanols in leaves and seeds of Arabidopsis and Maize. Plant Methods. 16(1):1–14. doi:10.1186/s13007-020-00671-9. https://doi.org/10.1186/s13007-020-00671-9.

Baseggio M, Murray M, Magallanes-Lundback M, Kaczmar N, Chamness J, Buckler ES, Smith ME, DellaPenna D, Tracy WF, Gore MA. 2020. Natural variation for carotenoids in fresh kernels is controlled by uncommon variants in sweet corn. Plant Genome. 13(1):1–19. doi:10.1002/tpg2.20008.

Baseggio M, Murray M, Magallanes-Lundback M, Kaczmar N, Chamness J, Buckler ES, Smith ME, DellaPenna D, Tracy WF, Gore MA. 2019. Genome-Wide Association and Genomic Prediction Models of Tocochromanols in Fresh Sweet Corn Kernels. Plant Genome. 12(1):180038. doi:10.3835/plantgenome2018.06.0038.

Bird JK, Murphy RA, Ciappio ED, McBurney MI. 2017. Risk of deficiency in multiple concurrent micronutrients in children and adults in the United States. Nutrients. 9(7). doi:10.3390/nu9070655.

Bradbury PJ, Zhang Z, Kroon DE, Casstevens TM, Ramdoss Y, Buckler ES. 2007. TASSEL: Software for association mapping of complex traits in diverse samples. Bioinformatics. 23(19):2633–2635. doi:10.1093/bioinformatics/btm308.

Covarrubias-Pazaran G. 2016. Genome assisted prediction of quantitative traits using the R package sommer. :1–15.

Cuttriss AJ, Cazzonelli CI, Wurtzel ET, Pogson BJ. 2011. Carotenoids. In: Advances in Botanical Research. Vol. 58. p. 1–36.

Davis W, Lucier G. 2021. Vegetable and Pulses Outlook : April 2021 Per Capita Availability Up in 2020 Domestic Output Steady in 2020.

Diepenbrock CH, Ilut DC, Magallanes-Lundback M, Kandianis CB, Lipka AE, Bradbury PJ, Holland JB, Hamilton JP, Wooldridge E, Vaillancourt B, et al. 2021. Eleven biosynthetic genes explain the majority of natural variation in carotenoid levels in maize grain. Plant Cell. 33(4):882–900. doi:10.1093/plcell/koab032.

Diepenbrock CH, Kandianis CB, Lipka AE, Magallanes-Lundback M, Vaillancourt B, Góngora-Castillo E, Wallace JG, Cepela J, Mesberg A, Bradbury PJ, et al. 2017. Novel loci underlie

natural variation in vitamin E levels in maize grain. Plant Cell. 29(10):2374–2392. doi:10.1105/tpc.17.00475.

Gilmour AR, Gogel BJ, Cullis BR, Thompson R. 2009. ASREML USER GUIDE RELEASE 3.0. :1–310.

HarvestPlus; Food and Agricultural Organization of the United Nations (FAO). 2019. Biofortification: A food-systems solution to help end hidden hunger. Washington, DC.

Hu Y, Colantonio V, Müller BSF, Leach KA, Nanni A, Finegan C, Wang B, Baseggio M, Newton CJ, Juhl EM, et al. 2021. Genome assembly and population genomic analysis provide insights into the evolution of modern sweet corn. Nat Commun. 12(1):1227. doi:10.1038/s41467-021-21380-4. http://dx.doi.org/10.1038/s41467-021-21380-4.

Huang H, Xie S, Xiao Q, Wei B, Zheng L, Wang Y, Cao Y, Zhang X, Long T, Li Y, et al. 2016. Sucrose and ABA regulate starch biosynthesis in maize through a novel transcription factor, ZmEREB156. Sci Rep. 6(February):1–12. doi:10.1038/srep27590.

Ibrahim KE, Juvik JA. 2009. Feasibility for improving phytonutrient content in vegetable crops using conventional breeding strategies; case study with carotenoids and tocopherols in sweet corn and broccoli. J Agric Food Chem. 57(11):4636–4644. doi:10.1021/jf900260d.

Lima VC, Rosen RB, Farah M. 2016. Macular pigment in retinal health and disease. Int J Retin Vitr. 2(1):1–9. doi:10.1186/s40942-016-0044-9.

Preiss J, Danner S, Summers PS, Morell M, Barton CR, Yang L, Nieder M. 1990. Molecular characterization of the brittle-2 gene effect on maize endosperm ADPglucose pyrophosphorylase subunits. Plant Physiol. 92(4):881–885. doi:10.1104/pp.92.4.881.

Sen CK, Khanna S, Roy S. 2006. Tocotrienols: Vitamin E Beyond Tocopherols. Life Sci. 78(18):2088–2098.

Tracy WF, Shuler SL, Dodson-Swenson H. 2019. The use of endosperm genes for sweet corn improvement: A review of developments in endosperm genes in sweet corn since the seminal publication in plant breeding reviews, volume 1, by Charles Boyer and Jack Shannon (1984). Plant Breed Rev. 43:215–241. doi:10.1002/9781119616801.ch6.

Tracy WF, Whitt SR, Buckler ES. 2006. Recurrent mutation and genome evolution: Example of Sugary 1 and the origin of sweet maize. Crop Sci. doi:10.2135/cropsci2006-03-0149tpg.

Vallabhaneni R, Wurtzel ET. 2010. From epoxycarotenoids to ABA: The role of ABA 8′-hydroxylases in drought-stressed maize roots. Arch Biochem Biophys. 504(1):112–117. doi:10.1016/j.abb.2010.07.005. http://dx.doi.org/10.1016/j.abb.2010.07.005.

Whitt SR, Wilson LM, Tenaillon MI, Gaut BS, Buckler IV ES. 2002. Genetic diversity and selection in the maize starch pathway. Proc Natl Acad Sci U S A. 99(20):12959–12962. doi:10.1073/pnas.202476999.

Wurtzel ET, Cuttriss A, Vallabhaneni R. 2012. Maize provitamin A carotenoids, current resources, and future metabolic engineering challenges. Front Plant Sci. 3(FEB):1–12. doi:10.3389/fpls.2012.00029.

Zhang X, Haro von Mogel KJ, Lor VS, Hirsch CN, de Vries B, Kaeppler HF, Tracy WF, Kaeppler SM. 2019. Maize sugary enhancer1 (se1) is a gene affecting endosperm starch metabolism. Proc Natl Acad Sci U S A. 116(41):20776–20785. doi:10.1073/pnas.1902747116.

2.7 Chapter Two Supplementary Materials

Supplementary Table S2.1. Chi-square p-values indicating statistical significance of model terms for 38 carotenoid and tocochromanol individual, sum, or ratio traits. Genotype refers to the dosage at the *Se1* locus, and principal components PC1-PC4 were model covariates. Kinship refers to the significance of the kinship covariance matrix as a random effect. P-values are FDR-adjusted.

Trait	Genotype	PC1	PC2	PC3	PC4	Kinship
β-Cryptoxanthin	0.0000	0.2606	0.1632	0.8335	0.4410	1.0000
Zeaxanthin	0.0002	0.8593	0.6276	0.8610	0.7144	1.0000
Zeinoxanthin	0.0164	0.8750	0.7618	0.9804	0.6563	0.3752
Lutein	0.0000	0.0002	0.5409	0.5140	0.2617	0.8309
Other carotenes	0.0012	0.7263	0.8598	0.4831	0.6125	1.0000
Antheraxanthin	0.0323	0.9187	0.2249	0.7927	0.7453	0.2306
Violaxanthin	0.4831	0.9187	0.6549	0.8599	0.9187	0.1228
β-Carotene	0.6125	0.8732	0.2664	0.6125	0.9187	0.0239
Total xanthophylls	0.0012	0.0522	0.5815	0.5970	0.3279	0.4831
Total carotenoids	0.0001	0.0365	0.7818	0.5094	0.2874	0.7618
α-Xanthophylls	0.3946	0.0023	0.7623	0.5982	0.1228	0.5815
β-Xanthophylls	0.0016	0.8787	0.9187	0.5065	0.8622	0.3946
Total carotenes	0.0016	0.5752	0.8593	0.7618	0.6563	1.0000
β-carotene over β-cryptoxanthin	0.0000	0.9325	0.0006	0.0873	0.5499	0.5382
β-Cryptoxanthin over zeaxanthin	0.0000	0.4469	0.7467	0.8598	0.6838	0.9064
Zeinoxanthin over lutein	0.0097	0.8598	0.9187	0.8473	0.9187	0.0047
β-Carotene over β-cryptoxanthin and zeaxanthin	0.0149	0.9187	0.0327	0.2461	0.8841	0.8610
Total carotenes over total xanthophylls	0.5982	0.5970	0.9187	0.5815	0.9187	0.0089
γ-tocotrienol	0.0000	0.2760	0.1102	0.0220	0.7818	0.4831
δ-tocotrienol	0.0000	0.2041	0.6838	0.0073	0.2906	1.0000
α-tocotrienol	0.0970	0.9066	0.3988	0.9187	0.2934	0.2095
γ-tocopherol	0.3988	0.4831	0.8593	0.6563	0.5815	0.0864
α-tocopherol	0.6563	0.5065	0.4799	0.6270	0.7386	0.1526
δ-tocopherol	0.6270	0.6333	0.6270	0.9187	0.4386	0.1632
Total tocotrienols and tocopherols	0.0614	0.2167	0.2249	0.2249	0.6196	0.1190
Total tocotrienols	0.0000	0.2604	0.0572	0.0171	0.9187	0.5752
Total tocopherols	0.4654	0.3853	0.7724	0.7724	0.6270	0.1228
Total tocopherols over total tocotrienols	0.0000	0.7724	0.4799	0.5650	0.9203	0.1228
γ-tocotrienol over γ-tocotrienol plus α-tocotrienol	0.0365	0.9121	0.7618	0.2934	0.4718	0.0700
α-tocotrienol over γ-tocotrienol	0.0323	0.9187	0.6563	0.3097	0.3988	0.1228
δ-tocotrienol over γ-tocotrienol plus α-tocotrienol	0.4014	0.8610	0.6261	0.8593	0.4633	0.0000
δ-tocotrienol over α-tocotrienol	0.0001	0.5524	0.6270	0.0133	0.2436	1.0000
δ-tocotrienol over γ-tocotrienol	0.3725	0.9064	0.6125	0.9187	0.4344	0.0043
α-tocopherol over γ-tocopherol	0.4342	0.9421	0.8598	0.5065	0.5970	0.0097
γ-tocopherol over γ-tocopherol plus α-tocopherol	0.4344	0.9187	0.7927	0.5065	0.5970	0.0067

δ-tocopherol over α-tocopherol	0.3725	0.9187	0.1721	0.7649	0.4284	0.1722
δ-tocopherol over γ-tocopherol	0.2606	0.7818	0.3988	0.8787	0.5982	0.0323
δ-tocopherol over δ-tocopherol and α-tocopherol	0.2760	0.8523	0.4642	0.9187	0.5524	0.0221

3 Chapter Three: *sugaryenhancer1* Sweet Corn Exhibits Altered Stress-response and Phytohormone Metabolism

3.1 Abstract

Sweet corn breeding has pursued high eating quality through the manipulation of starch and sugar metabolism; of the major genes that define sweet corn endosperm types, the function

of *Sugaryenhancer1* (*Se1*) is still unknown, though it contains a FANTASTIC FOUR (FAF) protein domain that has been implicated in stress response and growth regulation in other species. While the absence of a functional *Se1* allele is associated with an increase in sugars and changes in carotenoids and tocochromanols, questions still remain as to the mechanisms through which these changes occur. Deeper knowledge of the effects of *Se1* in maize kernel development will help plant breeders make choices as to what germplasm to include in breeding programs and contribute to our understanding of maize starch synthesis. In this research, near-isogenic lines of the *sugary1* sweet corn W822, with genotypes *Se1/Se1* and *se1/se1*, were screened for changes in gene expression at 13, 16, 19, and 22 days after pollination; a widely-targeted metabolomics analysis was done on kernels sampled at 22 days after pollination. Differentially expressed genes were involved in starch and sucrose metabolism, and also genes involved in carotenoid synthesis, and in the production of the isoprenoid precursors that form the basis of carotenoids and tocotrienols. In particular, *lut5,* the enzyme converts zeinoxanthin to lutein, was downregulated, which would contribute to the reduction of lutein and increase in zeinoxanthin found in previous work. Confirming *Se1* as at least partially regulated starch and sugar metabolism, the metabolomic analysis found significant increases in malto-oligosaccharides and other starch degradation products. The combined metabolomics and transcriptomics also shed light on changes in phytohormone processes in *se1/se1* endosperm. Changes were observed in the pathways relating to the production, activation, or degradation of auxin, abscisic acid, gibberellin, cytokinin, brassinosteroids, and strigolactones. Changes in abiotic stress response pathways were also observed, mirroring the effects of FAF genes in other crops. Given the metabolomic shifts observed here, it's likely that *Se1* has a broad regulatory role in endosperm

development, with only one of many effects being the changes in sugars that make it useful to sweet corn breeding.

3.2 Introduction

While the vast majority of maize production is primarily grain corn meant for feed or fuel, sweet corn has economic and culinary importance in the United States, with domestic production centered in Washington, Florida, and the Upper Midwest (USDA-NASS, 2023). In addition to standard agronomic traits, sweet corn breeders have focused on manipulation of the endosperm starch pathways as the primary target of modern sweet corn breeding (Revilla, Anibas, & Tracy, 2021; William F. Tracy, Shuler, & Dodson-Swenson, 2019). Current breeding populations are increasingly dominated by the *shrunken2 (sh2,* Zm00001eb159060*)* endosperm mutation that provides the highest sugar levels and lowest starch at the fresh eating stage (Tracy et al., 2019). However, the rate of starch and sucrose accumulation in developing kernels is a highly polygenic trait, where levels of starch, sucrose, glucose, and fructose vary widely among genetic backgrounds, even in *sh2* homozygotes (Azanza, Tadmor, Klein, Rocheford, & Juvik, 1996; R. G. Creech & McArdle, 1966; Finegan et al., 2022; Soberalske & Andrew, 1978, 1980; T. Wang et al., 2015). Furthermore, simply introducing *sh2* into a non-sweet corn will not result in a sweet and tender high-quality sweet corn without further breeding.

Shrunken2 encodes the large subunit of adenosine-diphosphate pyrophosphorylase, which, as the enzyme responsible for creating the ADP-glucose required for starch synthesis, is the rate-limiting step in the pathway. When *sh2* is homozygous recessive, sucrose accumulates instead of starch (Hannah & Nelson, 1976; Hu et al., 2021). Other recessive alleles are used in sweet corn breeding, such as *sugary1* (*su1*, Zm00001eb174590), which is the classic sweet corn

gene found in the earliest sweet corn populations and is still widely used in commercial production (William F. Tracy, Whitt, & Buckler, 2006). *Su1* encodes a starch-debranching enzyme, isoamylase1. Recessive allele results in elevated sucrose levels and an increase in water-soluble polysaccharides. *Brittle1* (*bt1*, Zm00001eb235570) encodes the transmembrane protein that moves ADP-glucose into the amyloplast. *Brittle2* (*bt2*, Zm00001eb176800) is a gene encoding the AGPase small subunit and when recessive results in a kernel phenotype similar to *sh2* (Tracy et al., 2019). Neither of these mutations used in sweet corn as widely as *sh2,* though *bt2* is used in "triplesweets", which contain three or more recessive alleles (Tracy et al., 2019). The combination of mutant alleles *amylose extender1* (*ae1*, Zm00001eb242610), *dull endosperm1* (*du1*, Zm00001eb413290), and *waxy1* (*wx1,* Zm00001eb378140), which are noncatalytic alleles of starch branching enzme IIb (SBEIIb), starch synthase IIIa, and granule-bound starch synthase, respectively, has also been used in sweet corn, but have not had commercial impact. (Creech, 1965; Gao, Wanat, Stinard, James, & Myers, 1998; Revilla et al., 2021).

Sugaryenhancer1 (*se1*, Zm00001eb115450) is another gene that has been widely used in commercial germplasm, though not to the extent of *sh2* and *su1*. Originally described as a recessive modifier of *su1*, it has primarily been used in combination with *su1,* and occasionally with other sweet corn genes (La Bonte & Juvik, 1990; Tracy et al., 2019). Compared to *su1/su1* kernels with the dominant *Se1/Se1* genotype, *su1/su1 se1/se1* kernels have more sucrose and maltose and a pale yellow endosperm color (La Bonte & Juvik, 1990; X. Zhang et al., 2019). The *se1/se1* kernels are also reduced in reduced in carotenoids and tocotrienols (Branch, Baseggio, Resende, & Tracy, 2024). Sweet corn with *se1* will also be noticeably more tender, perhaps through a reduction in pericarp thickness (W. F. Tracy & Galinat, 1987). Germplasm from *se1*

inbreds has been used to improve tenderness in current *sh2* hybrids (A.M. Rhodes, personal communication to W.F. Tracy).

Unlike other major sweet corn genes, researchers have not been able to associate *se1* into a specific point in the starch synthesis pathway. Zhang et. al. (2019) provided a full characterization of the *se1* in regards to its sequence and structure, and through RNA interference-mediated transgenic maize experiments, proved definitively that *se1* was the cause of the distinctive high-maltose phenotype. The wild type *Se1* allele was found to be an endosperm-specific gene encoding a 184 amino acid protein of unknown function but including a FANTASTIC FOUR (FAF) protein domain (X. Zhang et al., 2019).

Fantastic four (FAF) genes were first identified as shoot meristem regulators in Arabidopsis, involving the CLV3-WUS feedback loop. In Arabidopsis, FAF genes act to repress WUSCHEL transcription factors, and are in turn repressed by CLAVATA proteins (Wahl, Brand, Guo, & Schmid, 2010). Also in Arabidopsis, *EAR1,* enhancer of ABA co-receptor1, contains the FAF protein domain; loss of EAR1 results in ABA hypersensitivity through interactions with protein phosphatases that negatively regulate ABA signaling (K. Wang et al., 2018). Other work has identified additional functions of additional FAF genes in *Capsicum annuum* and *Solanum lycopersicum.* In *Capsicum annuum,* FAF genes were identified with stress-tolerance functions. Drought and salt stress induced FAF expression; silencing of an FAF gene both enhanced drought tolerance and reduced tolerance to salt stress (Lim, Bae, & Lee, 2022). In *S. lycopersicum,* FAF genes contributed to regulatory control of flowering time (Shang et al., 2024; D. Zhang et al., 2024). While FAF genes have been demonstrated to have a range of functions in a variety of species, no definitive functions of FAF or FAF-like genes have been described in maize with the exception of *se1* as involved in carbohydrate metabolism.

While no direct interaction between the starch synthesis pathway and *se1* or its FAF domain could be inferred, gene expression patterns, including an upregulation of a pullulanase-type starch debranching enzyme (*zpu1*, Zm00001eb088740) suggested that *se1* may be regulating starch degradation to produce maltose (X. Zhang et al., 2019). Other research identified *Se1* as a central regulator of a gene expression network that included *Scarecrow-like1* (SCL1, Zm00001eb344400) and gibberellin and 26S proteasome-ubiquitin pathway genes, implicating *Se1* as having a role in GA signaling, possibly regulating germination-like processes that lead to starch degradation and maltose production (Finegan et al., 2022).

Despite uncertainty over the specific function of *Se1* in maize development, a hypothesis emerges where *Se1* has a broad regulatory function in kernel metabolism. Net biosynthesis of starch, carotenoids, and tocotrienols are suppressed in *se1/se1* endosperm, indicating changes in nutrient storage and antioxidant activity (Ibrahim & Juvik, 2009; X. Zhang et al., 2019). Higher-level control of these processes occurs through the balance of phytohormones present; the connection to GA signaling described in Finegan et. al. (2022) and the potential interactions of FAF-like genes with ABA regulatory and stress response pathways suggests that metabolic and transcriptomic profiling of *se1/se1* kernels would reveal more diverse transformations than expected in a starch-synthesis gene.

Here, transcriptomes of *Se1/Se1* and *se1/se1* isolines were analyzed for differential gene expression at multiple timepoints during kernel development to confirm the role of *Se1* as modulating carotenoid and tocotrienol synthesis. A widely-targeted metabolomics assay followed to identify compounds enriched in *se1/se1* genotype; the combined transcriptomic and metabolomic analyses point toward *Se1* as also causing variation in phytohormone synthesis and regulation. Efforts to understand the interactions between various phytohormones and the

accumulation of starch, sugar, or other nutritional components in sweet corn will allow plant breeders the to exploit variation in these pathways as a route to maintain genetic gain.

3.3 Methods and Materials

3.3.1 Plant material and sample collection

The *su1*/*su1* sweet corn inbred W822*Se1se1* was previously developed at the University of Wisconsin-Madison and used for sequencing and characterization of the *Se1* and *se1* alleles, (Zhang et. al. 2019). Briefly, the Wisconsin-developed supersweet (*sh2sh2*) inbred Wh8419 and 'Terminator', a *su1su1 Se1se1* hybrid, were crossed and offspring self-pollinated for 15 generations. Progeny segregating smooth-kernel and wrinkled-kernel phenotypes were selected each generation of self-pollination and maintained as the heterozygous inbred family W822*Se1se1*. Smooth kernels had the homozygous dominant *Se1/Se1* genotype, wrinkled kernels had the homozygous recessive *se1/se1* genotype. The different genotypes were planted in the 2021 growing season as single replicates in four-row plots 3.5 meters long with .76 meter row spacing, and thinned to 12 plants per row. All plant material was grown at the West Madison Agricultural Research Station in Madison, Wisconsin. Plants were hand pollinated, either self- or cross-pollinated to produce three endosperm genotype classes: *Se1/Se1/Se1, Se1/se1/se1*, and *se1/se1/se1*. Heterozygote endosperm types were created by pollinating *se1/se1* plants with pollen from *Se1/Se1* plants.

Pollinations were done on the same day, and all plants were hand pollinated to minimize cross contamination. Fresh corn sampling for analysis was done at 13,16, 19, and 22 days after pollination (DAP). Five ears, each a biological replicate, were harvested from each plot in the

morning at the set DAP. They were flash frozen in liquid nitrogen and stored at -80 C until RNA extraction.

3.3.2 RNA extraction

Bulk kernel extraction was done on developing endosperm from the frozen kernels, with kernels from each ear composing a biological replicate. While frozen, the pericarp and embryo were peeled away from the endosperm; endosperm from several kernels in a biological replicate were then pooled to obtain enough tissue for RNA extraction. Extraction was done using an acid phenol:chloroform method with a lithium-chloride precipitation step (Vennapusa, Somayanda, Doherty, & Jagadish, 2020). A modification to the published protocol was to homogenize tissue in reinforced microcentrifuge tubes in a bead mill with 1 mL of extraction buffer rather than use a mortar and pestle; this increased homogenization efficiency and preserved tissue integrity. To remove proteins, polysaccharides, and organic compounds, a second chloroform-only step was added. To further purify the sample after precipitation, an additional ethanol washing step was used.

3.3.3 RNA Quality and Sequencing

RNA quality was assessed using a Nanodrop spectrophotometer to assess RNA concentration and purity and then run on an Agilent Bioanalyzer to assess RNA integrity (RIN). RIN values ranged from 6.8 to 10, with an average value of 9.3, indicating extraction of high-quality RNA. RNA evaluation and Illumina Truseq Stranded library preparation was done according to the manufacturer's protocol by the University of Wisconsin Biotechnology Center, followed by sequencing to generate 150 bp paired-end reads on an Illumina NovaSeq X Plus. 46 samples passed all stages of quality checks and library preparation; sequencing yielded 1350.8 million total reads, with an average of 29.3 million reads per sample.

3.3.4 Sequence data processing and differential expression analysis

Reads were trimmed and filtered using Trimmomatic and then mapped to the B73v5 reference genome using the STAR aligner (Bolger, Lohse, & Usadel, 2014; Dobin et al., 2013; Hufford et al., 2021). Trimming and filtering provided paired reads and reads without a surviving mate; these orphan reads were aligned as single-end reads separately from the paired reads that had both mates remaining after trimming. Within the STAR command, the --quantMode flag was used to quantify reads per gene; raw count files from the paired and orphan reads for each sample were then merged and used for downstream analysis. The unique mapping rate ranged from 65.58 percent to 85.51 percent with an average mapping rate of 76.04 percent. All read processing was performed with computational resources provided by the UW-Madison Center For High Throughput Computing in the Department of Computer Sciences. Data from W822 *Se1/Se1* and W822 *se1/se1* were used for further analysis.

Raw count matrices from 18 W822 *Se1/Se1* samples and 14 W822 *se1/se1* samples were used to identify differentially expressed genes in DESeq2 in R, with each genotype/timepoint combination considered a separate treatment (Love, Huber, & Anders, 2014). Expression was normalized using the default options and low-expression genes filtered out to reduce noise, leaving only genes with at least ten reads in at least three samples. Principal component analysis was done using the PCAtools package in R (Blighe & Lun, 2021).

3.3.5 Coexpression Network Analysis

The same gene count matrices were used as input for identifying gene expression networks using the Weighted Correlation Network Analysis package in R (Langfelder & Horvath, 2008). A soft thresholding power of 18 was chosen using the sft() command to ensure a scale-free signed network and network modules were constructed with the blockwisemodules()

command. Module eigengene values, the value most representative of a gene expressions network's modules, were used to find module-genotype associations. Correlations between the module eigengene value and both DAP and *Se1* genotype were used to identify gene expression modules that were closely associated with the effects of the *se1/se1* genotype. Modules with significant correlations were used in further analysis.

3.3.6 Gene Ontology Enrichment Analysis

Using the gprofiler2 package in R, the endosperm-expressed genes in this experiment were assigned gene ontology terms (GO terms) and Kyoto Encyclopedia of Genes and Genomes (KEGG) pathway annotations from the Esembl Plants database (Kinsella et al., 2011; Raudvere et al., 2019). Differentially expressed genes within each timepoint and genes within each significant module were then search for enriched GO terms; significant GO terms or KEGG annotations were classifications that were impacted by genotype at the *Se1* locus. The enrichment analysis was performed against a background gene list containing all endosperm-expressed genes in this analysis and up- and downregulated genes were considered separately.

3.3.7 Metabolomics analysis

In order to identify metabolite differences between W822 *Se1/Se1* and W822 *se1/se1*, three samples of each genotype were selected from 22 DAP frozen kernels for widely-targeted metabolomics analysis. Sample extraction and ultra-performance liquid chromatography tandem mass spectrometry (UPLC-MS/MS) analysis was performed as described in supplementary materials by MetwareBio (Metware Biotechnology Co., Ltd., Wuhan, China). Briefly, samples were lyophilized before a methanol extraction and centrifugation and supernatant was used for UPLC-MS/MS. Metabolites were semi-quantitatively identified using MetwareBio databases and relative content for each metabolite data was used for principal component analysis and

downstream analysis. Orthogonal partial least-squares analysis was done using MetaboAnalystR to determine the variable important in projection (VIP), p-value, and fold-change for each metabolite (Chong & Xia, 2018). Differentially accumulated metabolites (DAMs) were identified between W822 *Se1/Se1* and W822 *se1/se1* and selected based on a VIP score greater than 1 and p-value less than 0.05. Similar to gene ontology enrichment, differential metabolites were matched to KEGG pathway annotations and analyzed to find pathways that were enriched in DAMs using the hypergeometric method provided by the FELLA package in R (Picart-Armada, Fernández-Albert, Vinaixa, Yanes, & Perera-Lluna, 2018).

3.4 Results

3.4.1 Structure and Expression of Se1 and se1 transcripts

The *se1* mutation is a deletion in the exon region of the gene; the promoter region, 5` UTR, and transcription start sites, as well as part of the 3` UTR, are still present as based on the B73v5 gene model. Putative non-coding transcripts were observed in lines with *se1*; all *se1* samples in this study showed reads mapping to the downstream region adjacent to *Se1*. These transcripts extend to the start of the Zm00001eb115470 promoter, a gene encoding a chloroplast glutathione synthetase. Previous studies have shown *Se1* expression peaks around 16 DAP (X. Zhang et al., 2019). Here, the largest difference in *Se1* expression occurred at 13 DAP and *Se1* transcripts were present throughout timepoints (Figure 3.1). Non-significant differences were observed in the expression of *Se1* vs. *se1* at 16 and 19 DAP. Visualization of reads mapped to the reference genome in samples homozygous for the *se1* allele all showed the *se1* deletion in Zm0001eb115450 that was previously characterized (X. Zhang et al., 2019). Regardless of the number of reads aligned to the locus during read mapping, the W822 *Se1/Se1* and W822 *se1/se1* lines in this experiment indeed differed at the Zm00001eb115450 locus (Figure 3.2).

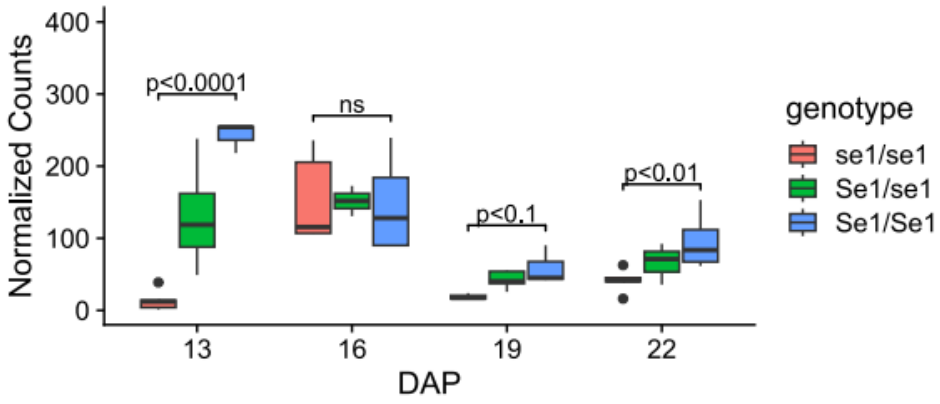

Figure 3.1. Gene Expression at Se1 Locus. Normalized reads per gene for Zm00001eb115450 at each time-point x genotype combination. Significance values are given for contrast between se1/se1 and Se1/Se1. FDR-adjusted p-values and normalized count values were calculated within DESeq2.

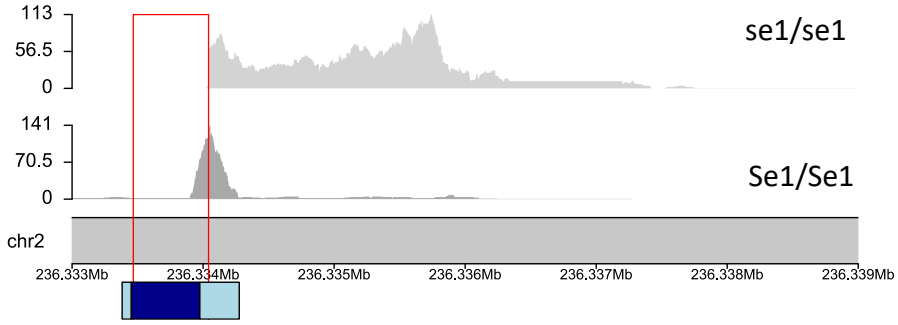

3.4.2 Principal component analysis

Principal component analysis showed clustering based on genotype (Figure 3.3). To determine which principal components contributed to variance for specific experimental variables, Pearson's correlation estimates were performed between the first ten principal

Figure 3.2. Gene expression at Se1 locus. BAM alignments are shown at Zm00001eb115450 gene model, with the exon in dark blue and UTRs in light blue. Alignments are representative of Se1/Se1 samples (lower) and se1/se1 samples (upper). The region of the se1 deletion as described in Zhang et. al. (2019) is shown in red.

Figure 3.3. Principal Component Analysis. Samples were segregating at the *Se1* locus; all genotypes are shown. DAP, days after pollination.

components and the variables sampling time (DAP) and genotype (Figure 3.4). PC1 and PC2 were most significantly correlated with DAP (r = 0.9 and r = 0.28, respectively).

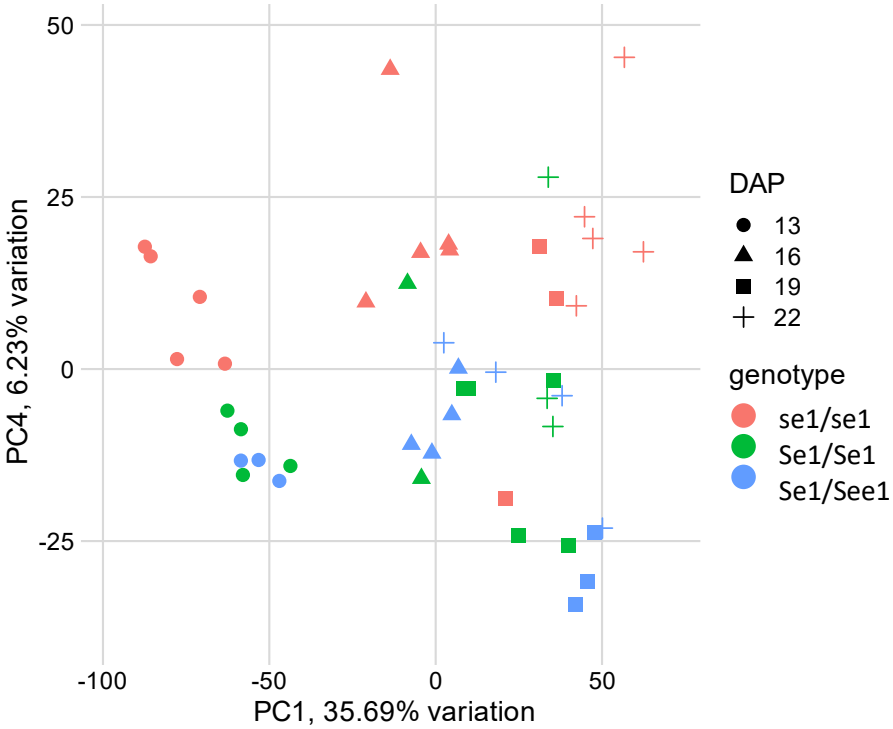

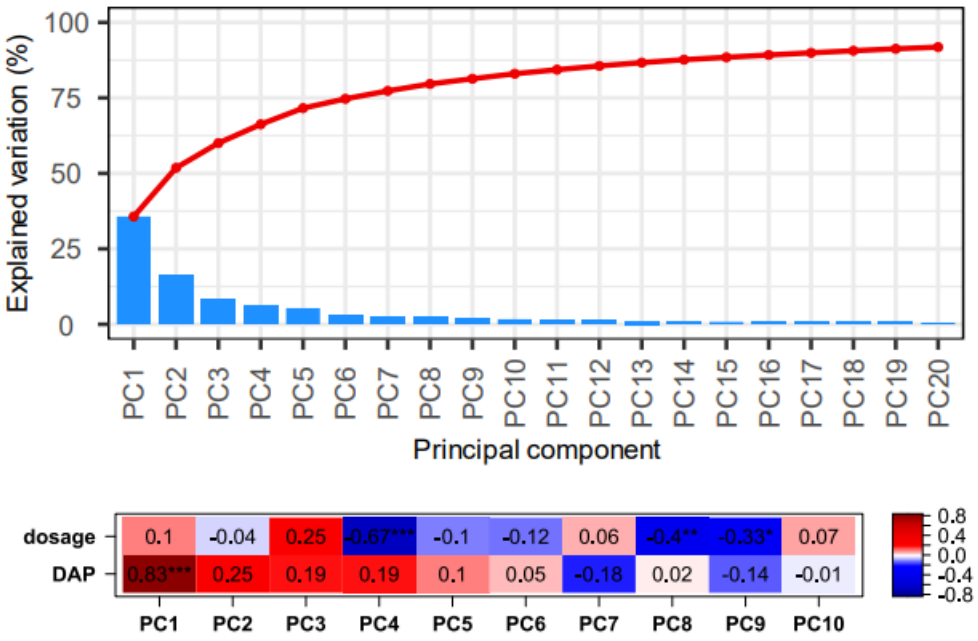

Figure 3.4. Principal components variance and correlation. Scree plot (upper) shows cumulative variance and variance explained by each PC. Pearson correlations (lower) were calculated between each PC and numeric equivalents of either days after pollination (DAP) and dosage of a functional *Se1* allele. *, significant at $p < 0.05$; **, significant at $p < 0.01$, ***, significant at $p < 0.001$.

Significant correlations with genotype, measured as dosage at the *Se1* locus were found with PC4, PC8, and PC9. Variables with the principal component loadings for the highly correlated PCs are genes that drive the difference between genotypes (Table 3.1). A beta-galactosidase (Zm00001eb152540), abscisic stress-ripening protein3 (*aasr5*, Zm00001eb422400), and an alkaline galactosidase (*aga5,* Zm00001eb079430) were all among the top genes that drove variation between genotypes. Gene ontology annotations suggest that the beta-galactosidase is involved in carbohydrate binding and carbohydrate metabolic processes, with additional annotations for cell wall and membrane components (Aleksander et al., 2023). In maize, *aasr3* is a regulator of drought tolerance and ABA sensitivity (Liang et al., 2019; Virlouvet et al., 2011). The alkaline galactosidase, *aga5,* is involved in temperature stress tolerance, seed vigor, and

synthesis of the raffinose-family oligosaccharides (RFOs) raffinose and stachyose (H. Liu, Wang, Liu, Kong, & Fang, 2024; Xu et al., 2023).

Table 3.1. Major Drivers of Variation. Top genes that drive variation along significant principal components are listed. Some genes are significant in more than one PC. Descriptions and gene ontology annotations were sourced from the MaizeMine database (Shamimuzzaman et al., 2020).

Gene	PC	Gene Symbol	Description	Gene Ontology Annotations
Zm00001eb030160	PC1	az19D2	alpha zein 19Kda D2	nutrient reservoir activity
Zm00001eb286170	PC1	esp1	embryo specific protein1	response to ABA, seed dormancy, desication tolerance
Zm00001eb302070	PC1	meg6	maternally expressed gene6	cell wall, plasma membrane
Zm00001eb302150	PC1		thioredoxin-containing protein	
Zm00001eb350070	PC1	rip1	ribosome inactivating protein1 rRNA N-glycosylase	
Zm00001eb413750	PC1	def2	defensin-like protein2	
Zm00001eb413770	PC1	def1	defensin-like protein1	
Zm00001eb355410	PC1,8		dirigent protein	carbohydrate binding, apoplast
Zm00001eb267000	PC1,9		subtilisin-chymotrypsin inhibitor	
Zm00001eb392940	PC1,9		3-beta-hydroxy-delta5-steroid dehydrogenase	steroid biosynthesis
Zm00001eb142290	PC4	betl10	basal endosperm transfer layer	
Zm00001eb168400	PC4		bifunctional inhibitor/plant lipid transfer/seed storage protein	
Zm00001eb172830	PC4	bap2	basal layer antifungal protein2	
Zm00001eb199720	PC4			
Zm00001eb207110	PC4	def6	defensin-like protein6	defense response
Zm00001eb388490	PC4		alpha-carbonic anhydrase	response to CO2
Zm00001eb152540	PC4,8		beta-galactosidase	cell wall, beta galactosidase activity
Zm00001eb411870	PC4,8		secreted protein	
Zm00001eb079430	PC4,9	aga5	alkaline galactosidase/stachyose synthase	galactinol-sucrose galactosyltranferase
Zm00001eb153360	PC4,9		coiled-coil domain	
Zm00001eb005200	PC8	esr2	embryo surrounding region2	
Zm00001eb060460	PC8	glb2	globulin2	
Zm00001eb266150	PC8		transmembrane protein	
Zm00001eb301380	PC8	mmp81	germin-like protein	nutrient reservoir activity
Zm00001eb330460	PC8	csu27	UVB-repressible protein	thylakoid membrane
Zm00001eb353760	PC8	at-S40-3		
Zm00001eb399450	PC8	psk3	phytosulfokine peptide precursor3	
Zm00001eb034220	PC9	TUB8	induced stolon tip	ribosome
Zm00001eb044060	PC9		copper transport protein family	ribosome
Zm00001eb338370	PC9		calcium ion binding	vacuole, transmembrane, salt stress

Zm00001eb391160	PC9		RRM domain-containing protein	
Zm00001eb422400	PC9	aasr5	abscisic acid stress ripening5	
Zm00001eb430890	PC9		cystein-rich transmembrane protein	plasma membrane, kinase activity

3.4.3 Differential Expression Analysis

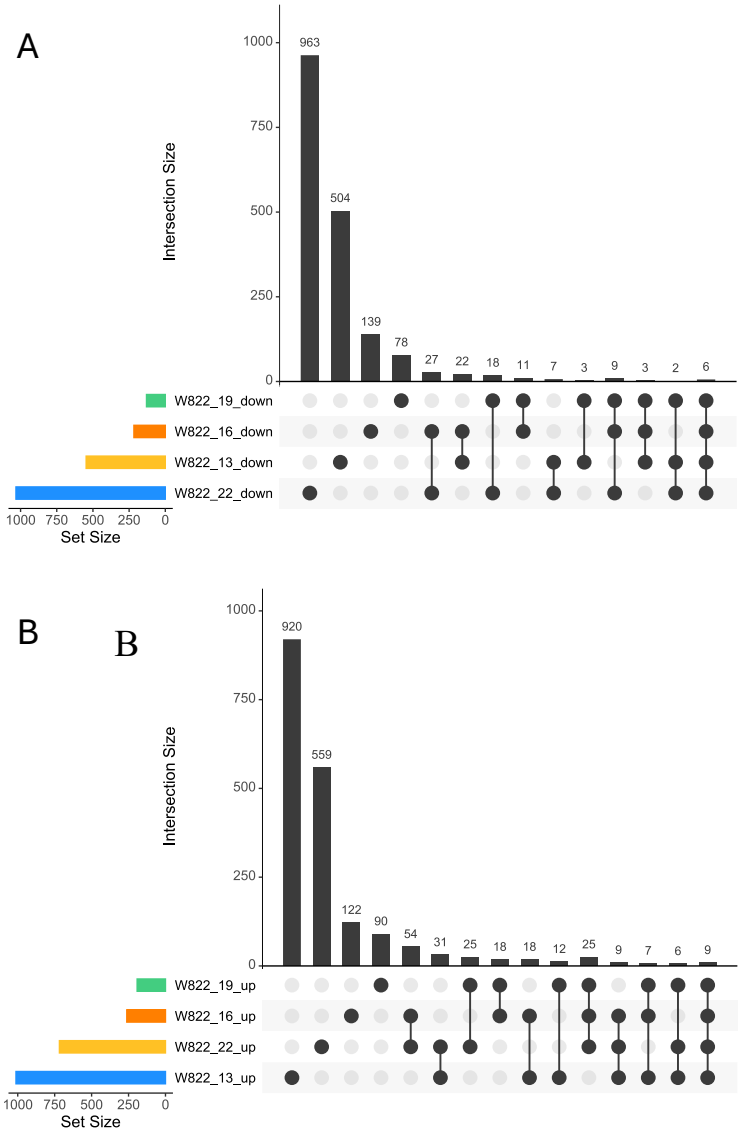

Figure 3.5 Summary of differentially expressed genes between W822 *Se1/Se1* and W822 *se1/se1*. A. DEGs downregulated in W822 *se1/se1*. B. DEGs upregulated in W822 *se1/se1*. Set size is the total number of DEGs up- or downregulated at each timepoint. Intersection size is the number of genes belonging to each category. For each DAP category, points indicate membership in a shared or unique category. DEGs common to all time points are shown at the far right of the plot.

Table 3.2. DEGs up- or downregulated at all DAP. Table of DEGs with significant changes in expression (adjusted p-value < 0.05, log2FoldChange > 1) at all sampled time points. Descriptions and gene ontology annotations were sourced from the MaizeMine database (Shamimuzzaman et al., 2020).

Gene ID	log2FoldChange	Description	GO annotations
Zm00001eb303870	3.03		NA
Zm00001eb411870	2.91	NA	NA
Zm00001eb153360	2.53	Coiled-coil domain-containing protein 25, 27 DAP	NA
Zm00001eb411870	2.49	secreted protein, expressed at 27 DAP, heat treated seedlings, 1 DAP ovaries drought	NA
Zm00001eb307510	2.45	probable serine/threonine-protein kinase PBL23	protein kinase activity, ATP binding, protein phosphorylation, peptidyl-tyrosine modification, microbody
Zm00001eb199720	1.86	NA	NA
Zm00001eb226430	1.61	ABC transporter domain-containing protein	inorganic phosphate transmembrane transporter activity, UDP-glucose transmembrane transporter activity, protein binding, ATP binding, vacuolar membrane, plasma membrane, lipid transport, plastid, response to aluminum ion, vesicle membrane, UDP-glucose transmembrane transport, membrane, lyase activity, phosphate ion transmembrane transport
Zm00001eb244910	1.47	Aldose 1-epimerase	aldose 1-epimerase activity, integral component of membrane, hexose metabolic process, carbohydrate binding, monosaccharide catabolic process
Zm00001eb083840	1.35	Carbonic anhydrase	carbonate dehydratase activity, one-carbon metabolic process, zinc ion binding, chloroplast stroma, integral component of membrane, hydro-lyase activity
Zm00001eb304520	1.34	IAA-amino acid hydrolase ILR1	endoplasmic reticulum, auxin metabolic process, IAA-Ala conjugate hydrolase activity, integral component of membrane, hydrolase activity
Zm00001eb321820	-1.29	MATH domain-containing protein	hydrolase activity
Zm00001eb380430	-1.66	Putative somatic embryogenesis protein kinase 1	protein kinase activity, protein serine/threonine kinase activity, ATP binding, nucleoplasm, cytoplasm, plasma membrane, protein phosphorylation, defense response, immune response, response to virus, integral component of membrane, protein localization to nucleus, negative regulation of multicellular organism growth, identical protein binding
Zm00001eb391160	-1.98	NA	NA
Zm00001eb056900	-2.05	calmodulin-like protein 11	calcium ion binding, integral component of membrane, enzyme regulator activity, regulation of catalytic activity
Zm00001eb166580	-2.43	NA	nutrient reservoir activity

Zm00001eb388490	-4.28	Carbonic anhydrase	carbonate dehydratase activity, one-carbon metabolic process, zinc ion binding, chloroplast stroma, response to carbon dioxide, integral component of membrane

After normalization and filtering with DESeq2, a total of 22,811 genes were expressed in the endosperm tissue. Within each time point, data was screened for differentially expressed genes (DEGs), defined as having a log2 fold-change of greater than 1 or less than -1 and a false discovery rate-adjusted p-value less than 0.05. An interaction effect was observed between genotype and developmental stage, where the number of genes showing an increase or decrease in expression varied between each time point (Figure 3.5, Table 3.2). In the W822 background, more genes were either upregulated or downregulated in the *se1* lines at both 13 DAP and 22 DAP, as compared to 16 and 19 DAP.

3.4.4 Changes in gene expression

To identify changes in patterns of gene expression, gene ontology and KEGG enrichment analysis was done using W822 *se1/se1* and W822 *Se1/Se1* (Figure 3.6). For gene-ontology enrichment, up- and down- regulated DEGs were considered separately. For KEGG enrichment analysis, to identify the strongest changes in gene activity, DEGs with a log2FoldChange with a magnitude greater than one was used. To identify pathways with moderate changes, DEGs with a log2FoldChange with a magnitude greater than 0.5 were used. Over all time points, in the strongly DE pathways, upregulated genes were enriched in terms associated phenylpropanoid biosynthesis, biosynthesis of secondary metabolites, and starch and sucrose metabolism, while downregulated genes were enriched in diterpenoid biosynthesis and glutathione metabolism (Figure 3.6). Interestingly, the KEGG term for “protein processing in the endoplasmic reticulum” was enriched in all three groups with significant KEGG terms. When moderately-expressed

genes were included in the analysis for all time points, tyrosine and phenylalanine metabolism the most highly enriched pathways in downregulated genes; there were no DEG-enriched pathways that were significantly upregulated when moderately-differentially expressed genes were included.

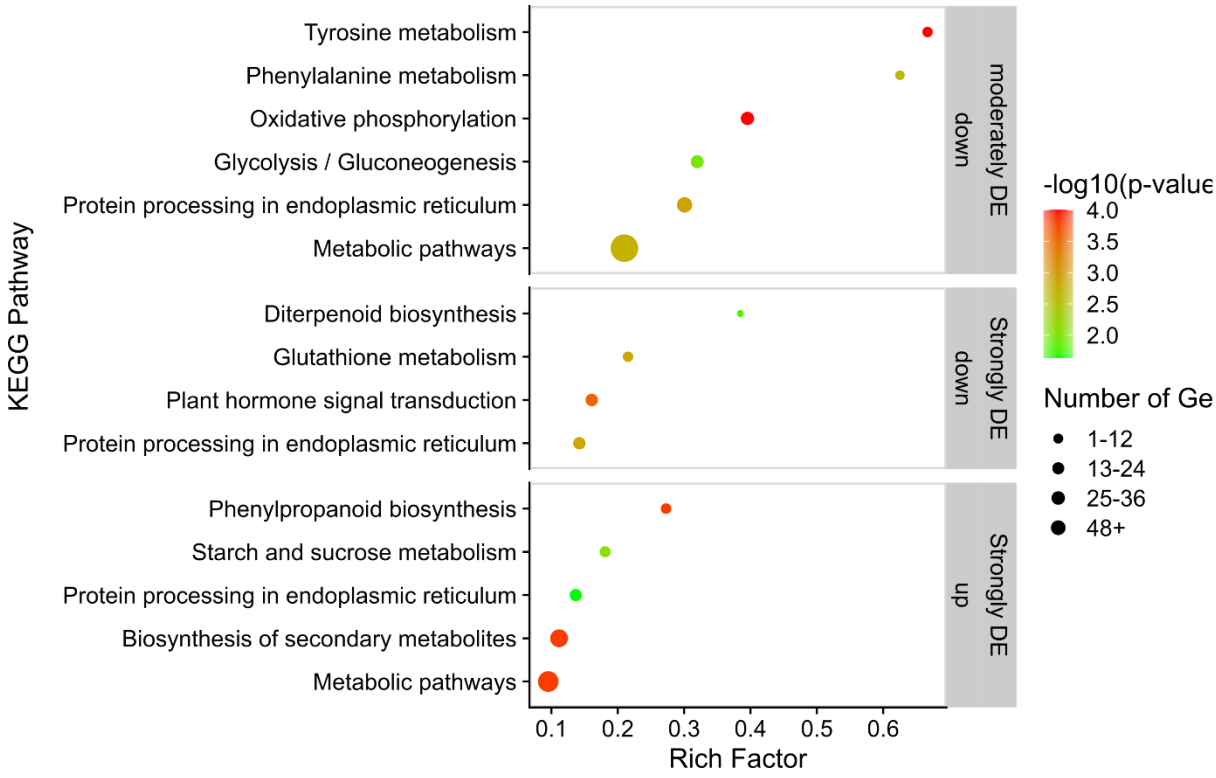

Figure 3.6. KEGG pathway annotations for differentially expressed genes. Pathway enrichment of differentially expressed genes throughout development. Panels are arranged by strength of expression changes and by up- or down-regulation in W822 se1/se1 relative to W822 Se1/Se1.. Moderately DE includes gene with absolute log2FoldChange > 0.5 and strongly DE includes gene with absolute log2FoldChange >1. Rich factor indicates proportion of DE genes detected against the total genes annotated in a pathway.

Differentially expressed genes were further grouped and analyzed via gene ontology enrichment (Aleksander et al., 2023). Early in endosperm development, at 13 DAP, nutrient reservoir activity is the GO term most enriched in downregulated genes. For genes upregulated at 13 DAP, GO terms include abiotic and xenobiotic stress responses, as well as membrane-

associated GO terms. Transmembrane transport functions were the most-enriched terms in both molecular functions and biological processes, and the cell periphery and plasma membrane were the most enriched cellular component terms. At 16 DAP, responses to heat and stress were upregulated, as well as cellular component GO terms for thylakoid and plastid membrane association. At this time point, downregulated genes are enriched in glutathione transferase activity and in 1-deoxy-xylulose-5-phosphate synthase activity. By 19 DAP, the GO term circadian rhythm (plant) was the only term enriched in downregulated in the *se1* NILs. GO terms enriched in upregulated genes at 19 DAP were associated with nucleotide disphosphate activity and carbon and nitrogen metabolism. Hydrolase activity also appears here as an enriched term. At 22 DAP, there were again a large number of DEG-enriched GO terms; this was the first time point with more downregulated terms than upregulated terms. Terms enriched in downregulated DEGs included stress and signaling responses, such as response to abscisic acid, salt stress, and oxidative stress. At 22 DAP GO terms enriched in upregulated DEGs were carbohydrate-centered, including oligo-, di-, and polysaccharide processes, and activity of glucanases, galactosidases, and glycosyl hydrolases. At this point, stress-response terms such as hormone responses and response to heat or salt are enriched in downregulated genes. Here, gene ontology enrichment suggests differing effects of *se1* across developmental timepoints. Early in development, at 13 and 16 DAP, stress responses are upregulated in absence of a functional *se1* allele; GO enrichments suggest that these effects may be localized to cell membranes, including plastid membranes. Later in endosperm development, DEGs are enriched in GO terms for carbohydrate metabolism, while stress response terms, many of which were associated with upregulated genes earlier, becomes downregulated.

3.4.5 Weighted Gene Coexpression Network Analysis

Coexpression networks were used to identify gene expression trends, including those of non-DE genes, within transcriptomic changes between W822 *Se1/Se1* and W822 *se1/se1*. In a network built from 2,2811 endosperm-expressed genes obtained from 14 *Se1/Se1* samples and 18 *se1/se1* samples, 42 coexpression modules were identified using the WGCNA package in R (Langfelder & Horvath, 2008). Module sizes ranged from 33 to 4325 genes. Nine modules with an absolute value of correlation greater than 0.5 were selected for further analysis (Table 3.3).

Table 3.3. Gene Ontology (GO) Enrichments for WGCNA modules. Modules were selected based on significant correlations with the *se1/se1* genotype. *, significant at $p < 0.05$; **, significant at $p < 0.01$, ***, significant at $p < 0.001$. GO terms derived from the Ensembl Plants database via gprofiler2, and selected GO terms were significant at the $p < 0.05$ level.

Module, number of genes	Correlation	GO terms
lightcyan1 n = 33	-0.88***	plant-type cell wall biogenesis, plant-type cell wall organization or biogenesis, cell wall biogenesis, cell wall organization or biogenesis, side of membrane
orangered4 n = 72	-0.57***	RNA binding, mRNA binding, protein import into chloroplast stroma, condensed nuclear chromosome, mitochondrial outer membrane translocase complex, mitochondrial outer membrane, outer mitochondrial membrane protein complex, SAM complex
Purple n = 491	-0.51**	cytoplasm, extracellular region, chloroplast, plastid, photosynthetic membrane, plastid envelope, photosynthesis, photosystem, chloroplast thylakoid membrane, plastid thylakoid membrane, plastid membrane, thylakoid, chloroplast thylakoid, plastid thylakoid, peroxisome, microbody, thylakoid membrane, chloroplast stroma, plastid stroma, outer membrane, organelle outer membrane, photosystem II, chloroplast envelope, photosynthesis, light reaction, photosystem I
Steelblue n = 121	0.53**	single-stranded telomeric DNA binding, sequence-specific single stranded DNA binding, telomere maintenance via telomerase, telomere maintenance via telomere lengthening, RNA-templated DNA biosynthetic process
Yellowgreen n = 81	-0.55***	defense response, indole-containing compound catabolic process, tryptophan catabolic process to kynurenine, tryptophan catabolic process, N-acetylglucosamine metabolic process, beta-1,4-mannosylglycoprotein 4-beta-N-acetylglucosaminyltransferase activity, kynurenine metabolic process, glucosamine-containing compound metabolic process

Zm00001eb115450 was in a module containing 1167 genes. The lightcyan1 module, containing 33 genes, was enriched in GO terms for plant cell wall functions. This module contained the hub gene Zm00001eb421200 , an acetylglucosaminyltransferase and Zm00001eb115470, which is just downstream from *Se1*. MAX2 F-box proteins encoded by Zm00001eb3766660 and

Zm00001eb270950 were also included in this module. MAX2 is part of the strigolactone signaling pathway and has stress response functions (Conn & Nelson, 2016; Struk, 2018). Module lightcyan1, which was strongly associated with the *se1/se1* genotype, also included genes encoding alpha-amylase and a tryptophan aminotransferase involved in auxin biosynthesis (Glawischnig et al., 2000; Leclere, Schmelz, & Chourey, 2010).

3.4.6 Metabolomic Analysis

Untargeted metabolomics was performed on samples collected from the *Se1/Se1* and se1/se1 genotypes at 22 days after pollination in order to identify differential metabolites at a developmental stage comparable to harvest-maturity in commercial sweet corn. 1,803 metabolites were detected using UPLC-MS/MS, with 138 metabolites upregulated in the *se1/se1* NILs compared to the *Se1/Se1* NILs, and 159 metabolites downregulated. Discriminant analysis by orthogonal partial least squares was used to identify which variables contributed the most to differentiation between groups, ranked by variable importance in projection (VIP), with VIP values greater than 1 suggesting differentiation between *Se1/Se1* and *se1/se1*. Here, methyl gallate, a phenylpropanoid, was identified as having the highest VIP with a value of 1.626. Compounds involved in starch and sucrose metabolism are show in Table 3.4.

Table 3.4. Saccharide compounds differing between *Se1/Se1* and *se1/se1* samples. VIP, variable importance in projection from orthogonal partial least-squares. Log2FC, log2 fold change of *se1/se1* over *Se1/Se1* samples. Significant compounds had VIP values greater than 1 and $p < 0.05$.

Compounds	VIP	P-value	Log2FC
Raffinose	1.60	0.00	0.56
D-Panose	1.60	0.00	0.44
Dihydroxyoctanoic acid glucoside	1.60	0.00	-1.15
Stachyose	1.59	0.00	0.92
D-Arabinose	1.57	0.00	-0.53
N-Acetyl-D-glucosamine	1.56	0.00	-1.02
Verbascose	1.56	0.01	1.77

D-Maltotetraose	1.54	0.02	1.24
Manninotriose	1.54	0.01	1.10
4-(3-Methylbutanoyl)Sucrose	1.53	0.01	-1.96
D-Galactaric acid	1.52	0.01	-0.52
DL-Xylose	1.51	0.01	-0.95
D-Saccharic acid	1.47	0.02	-0.59
Glucopyranose 6-Hydroxydecanoate	1.46	0.01	-1.04
Sedoheptulose	1.46	0.02	-0.45
DMelezitose O-rhamnoside	1.46	0.02	0.88

45 upregulated metabolites had current functional annotations from the KEGG database, as did 72 downregulated metabolites; KEGG annotations were used in a pathway enrichment analysis. Only compounds associated with amino sugar/nucleotide sugar metabolism were down represented. Biosynthesis pathways for sphingolipids, stilbenoids, and phenylpropanoids were contra-regulated, with these pathways enriched for both higher- and lower-accumulating metabolites. However, even within contra-regulated pathways, there were greater numbers of pathways overrepresented in W822 *se1/se1* than those underrepresented. KEGG pathways for ABC transporters and nucleotide metabolism were most enriched in higher-abundance metabolites.

3.5 Discussion

3.5.1 Altered expression of starch and sucrose metabolism genes in W822 se1/se1

In terms of sweet corn breeding for commercial markets, the *se1* gene is associated with higher eating quality when combined with *su1*, relative to *su1* alone (Tracy et al., 2019). Sugars and other carbohydrate compounds are of particular interest in sweet corn metabolomics, given the potential quality implications. At the fresh-eating stage, *se1/se1* inbreds have higher sucrose, similar starch content, and fewer water-soluble polysaccharides (La Bonte & Juvik, 1990; X.

Zhang et al., 2019). The increased abundance of maltose and other products of starch degradation in mature se1/se1 inbreds is the strongest piece of evidence that *se1* is involved in starch and sucrose metabolism (La Bonte & Juvik, 1990; X. Zhang et al., 2019). In this experiment, two important starch degradation products were enriched in W822 *se1/se1*; maltotetraose, which is a product of amylase activity on starch, and a trisaccharide identified as panose, which is a product of pullulanase activity on starch (Hii, Tan, Ling, & Ariff, 2012; Naik et al., 2023). The combination of both high VIP values and strong fold-changes on the aforementioned metabolites indicates that carbohydrate metabolism is a primary effect of *se1*. Enzymes in the starch synthesis pathway, including genes used in sweet corn breeding, were also highly differentially expressed in the endosperm at the time points in this study (Figure 3.7, Supplementary figure 3.1).

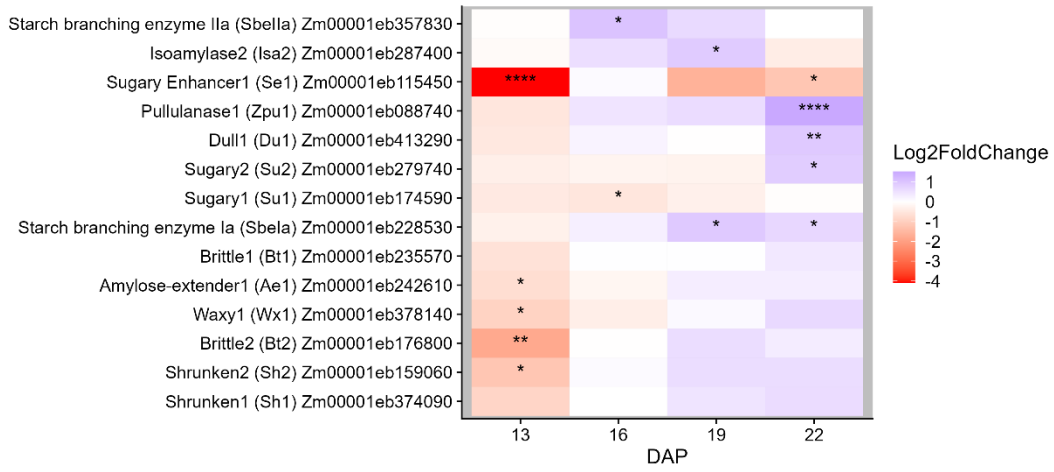

Figure 3.7. Differential expression of genes uses in sweet corn breeding. Starch synthesis genes shown are either currently used or have been experimented with in sweet corn breeding programs. Genes with higher expression are lower on the heatmap. Genes are up- (blue) or downregulated (red) in W822 se1/se1 compared to W822 Se1/Se1. *, significant at $p < 0.05$; **, significant at $p < 0.01$, ***, significant at $p < 0.001$, **** significant at $p < 0.0001$. Expression changes for additional genes involved in the starch synthesis pathway are shown in Supplementary Figure S3.1.

ADP-glucose pyrophosphorylase, including the large subunit *Sh2* and small subunit *Bt2,* were the most abundant transcripts in the endosperm starch synthesis pathway. *Bt2* and *Sh2* were downregulated in *se1/se1* endosperm at 13 DAP. Also at 13 DAP, starch synthases (Zm00001eb353810, Zm00001eb191890, Zm00001eb376100) and *amylose extender1 (ae1,* Zm00001eb242610*)* were downregulated in W822 *se1/se1* relative *Se1/Se1*. Later in endosperm development, genes for starch degradation enzymes are upregulated. At 19 and at 22 DAP, there was an upregulation of the pullulanase *Zpu1* (Zm00001eb088740), and at 22 DAP, the starch degradation enzymes Zm00001eb273940, a glycosyl-hydrolase, Zm00001eb307700, a beta-amylase, and Zm00001eb390820, an alpha-glucosidase, are all upregulated. The upregulation of starch-degrading enzymes in W822 *se1/se1* explains the increased abundance of panose and maltooligosaccharides.

Other key carbohydrate metabolites that were enriched in W822 *se1/se1* relative to W822 *Se1* were the raffinose-family oligosaccharides (RFOs) raffinose, stachyose, and verbascose. These compounds had a log2 fold change of 0.92, 0.56, and 1.77, respectively. Supporting the changes in RFO levels is the differential expression of genes in the RFO biosynthesis pathway (Supplementary Table S3.4). The same alkaline galactosidase *aga5* (Zm00001eb079430) contributing significant variation for principal component separation between W822 *se1/se1* and W822 *Se1/Se1* is strongly downregulated; the genes *aga4* (Zm00001eb061880) and *aga2* (Zm00001eb281720), genes for two other enzymes with RFO synthetic activity, are significantly upregulated at 22 DAP. According to the maize Qteller database, all three raffinose-synthase genes show a response to salt or temperature stress (Woodhouse et al., 2022). Other literature points to RFOs as critical compounds in abiotic stress tolerance and desiccation tolerance in

developing seeds (H. Liu et al., 2024). Zm00001eb079430 is also annotated as a seed imbibition protein involved in seed vigor (T. Li et al., 2017).

3.5.2 Altered expression of carotenoid and tocotrienol synthesis genes in W822 se1/se1

Genome-wide association studies, in both sweet corn and field corn, have identified genes that contribute to variation in kernel carotenoid levels, including important genes in the carotenoid biosynthesis pathway (Baseggio et al., 2020; Diepenbrock et al., 2021; Finegan et al., 2022). Similar studies have done the same with regards to tocochromanols (Baseggio et al., 2019; Diepenbrock et al., 2017; Hershberger et al., 2022). Carotenoid beta-ring hydroxylases (*crtRB1* and *crtRB3*), lycopene epsilon cyclase (*lcyE)*, phytoene synthase *(PSY1),* deoxyxylulose synthase (*DXS2),* and plastid terminal oxidase (*PTOX*) control kernel carotenoid levels in maize; homogentisate geranylgeranyltranferase (*hggt1*), gamma-tocopherol methyltransferase (*vte4*), and tocopherol cyclase (*vte1*) control significant variation for tocochromanols. *crtRB1*, *lcyE* , *vte4*, and *hggt1* were again identified in a sweet corn-only panel. As part of previous work on the genetic associations of vitamin levels in sweet corn, W822 *se1/se1* has been shown to have lower levels of certain carotenoids and tocotrienols compared to W822 *Se1/Se1* (Branch, Baseggio, Resende, & Tracy, 2024). Exploring the combined transcriptomics and metabolomics in this study provides a way to further explore those pathways in the context of the *Se1* gene. Differentially-expressed genes were found between W822 *Se1/Se1* and W822 *se1/se1* in both the carotenoid and tocochromanol pathways.

In the primary carotenoid synthesis pathway (Supplementary figure S3.2), the phytoene synthase (*Y1*, Zm00001eb271860) was downregulated at 13 DAP and upregulated at 22 DAP, change in expression of this gene would affect the movement entering the main carotenoid synthetic pathway. This could at least partially explain the pale endosperm color of *se1* inbreds;

kernels with defective *y1* alleles have no carotenoids and are white in color. Early in development, at 13 and 16 DAP, a carotene beta-ring hydroxylase (*lut5,* Zm00001eb258960), that converts zeinoxanthin to lutein, was also downregulated. This is particularly notable; zeinoxanthin was the only carotenoid to be more abundant in *se1/se1* inbreds compared to *Se1/Se1* inbreds, and a downward shift in *lut5* expression would explain that change. Other changes in the carotenoid synthesis pathway included a decrease in expression of another carotenoid beta-ring hydroxylase (*crtRB5,* Zm00001eb403700) in W822 *se1/se1* at 19 and 22 DAP. Violaxanthin de-epoxidase (*vde1*, Zm00001eb085840), which converts violaxanthin to antheraxanthin and then antheraxanthin to zeaxanthin was upregulated at 16 and 22 DAP. Also in the xanthophyll cycle, a zeaxanthin epoxidase/temperature induced lipocalin *(zep1,* Zm00001eb247000) was upregulated at 13 DAP.

Carotenoid levels can also be influenced by the rates of carotenoid degradation and conversion to other substances. Carotenoid-derived compounds are also a large part of the metabolic interactions within the developing endosperm. Abscisic acid, ABA, is produced from zeaxanthin through the action of nine'-carotenoid-cleavage dioxygenases (NCEDs); downregulation of NCEDs is another potential avenue in producing stable high-carotenoid levels in maize and other crops (Cuttriss, Cazzonelli, Wurtzel, & Pogson, 2011; Perrin et al., 2017; Song et al., 2022). However, there were no significant changes in NCED gene expression in this experiment.

Se1 is also associated with changes in tocochromanols, specifically the abundances of the tocotrienols; unlike tocopherols, tocotrienols are plastid-synthesized in the endosperm (Sen, Khanna, & Roy, 2006). Genes in the tocotrienol biosynthesis pathway showed fewer changes in expression than genes in the carotenoid pathway (Supplementary Table S3.3). The only gene

with significance at the 0.05 level was a plastid homogentisate geranylgeranyltransferase (Zm00001eb382300) which was downregulated at 13 DAP. While other genes in the tocochromanol pathway showed slight downregulation at 22 DAP, none were statistically significant.

Geranylgeranyl diphosphate (GGPP) is a common substrate in synthesis of both carotenoids, where lycopene is formed from two units of GGPP, and tocotrienols, where initial synthesis requires join?? GGPP with homogentisate. The methylerythritol pathway (MEP) contributes to GGPP production; genes in the MEP pathway have also been associated with carotenoid and tocochromanol variation. In W822 *se1/se1, dxs1* and *dxs2* (Zm00001eb287860 and Zm00001eb302370, respectively) were downregulated at 16 and 22 DAP; these enzymes catalzye a rate limiting step in GGPP synthesis, and reduced expression could lower metabolic flux through the MEP pathway and indirectly reduce abundance of MEP-derived compounds. GGPP is a link between carbon metabolism and a number of secondary metabolites; through the MEP pathway, glyceraldehde-3-phosphate and pyruvate can be turned into GGPP, which is a precursor to not only carotenoids and tocochromanols, but gibberellins as well, making it an indirect factor in the abundance of both ABA and GA in the developing kernel (Cordoba, Salmi, & León, 2009; Kasahara et al., 2002).

3.5.3 Gene expression in se1/se1 endosperm is enriched in stress response and germination pathways

Gene ontology and KEGG pathway enrichment analysis, using both transcriptomic and metabolomic data, suggests that *Se1* has a role in modulating stress responses in the developing kernel; this also hints at a function for the FAF domain present in the *Se1* exon and a connection between *Se1* and hormonal regulation of a variety of plant metabolic processes. FAF and FAF-

like genes are implicated in stress and phytohormone responses (Lim et al., 2022). This experiment suggests parallels between the effects of the loss of *Se1* in maize endosperm and role of *C. annuum* FAF genes in drought and salt stress. At 13, 16, and 22 DAP time points, GO terms for salt and osmotic stress were over-represented among DEGs upregulated in W822 *se1/se1*. Furthermore, specific genes in with roles in stress response are differentially expressed, with roles in carbohydrate metabolism and in antioxidant activity. The salt-responsive transcription factor Zm00001eb184100 and a glyceraldehyde-3-phosphate dehydrogenase, Zm00001eb246370, which converts between glyceraldehyde-3-phosphate and 3-phospho-glyceroyl phosphate in glycolysis and gluconeogenesis, were each strongly downregulated in W822 *se1/se1.* Superoxide dismutases (Zm00001eb016940, Zm00001eb394700, Zm00001eb285090, and Zm00001eb347200), which have antioxidant activity associated with an increase in stress tolerance, were also downregulated. These superoxide dismutatase, or SOD, genes participate in ROS degradation by catalyzing the production of hydrogen peroxide from superoxide (Ali, Sami, Haider, Ashfaq, & Javed, 2024; L. Guan & Scandalios, 1998). SOD proteins are also less abundant in ABA-deficient *vp5* mutants, which lack a phytoene desaturase and have decreased levels of both carotenoids and ABA. In this case, in W822 *se1/se1,* several distinct and highly expressed SOD genes were downregulated. Two heat shock proteins with salt stress, heat stress, and H2O2 response GO terms, Zm00001eb011900 and Zm00001eb121900, were downregulated. In the *C. annuum* FAF study, both the accumulation of proline and the expression of genes involved in proline synthesis were used as markers for tolerance to salt and osmotic stress (Lim et al., 2022). W822 *se1/se1* shows altered proline metabolism; metabolomics data indicates that proline is less abundant than in W822 *Se1/Se1,* and a delta-pyrroline carboxylase (*pcs1*, Zm00001eb289900) was upregulated at 16, 19, and 22 DAP. Increased *pcs1*

activity could favor proline degradation to glutamate, reducing the ability of cells to use proline for osmotic stability (Ghosh, Islam, Siddiqui, Cao, & Khan, 2022).

In addition to changes in salt-stress associated responses, W822 *se1/se1* shows transcriptomic and metabolic changes indicative of drought response; drought and salt stress responses are phenotypically similar and rely on many of the same regulators and reaction. ABA is a key regulator of both of these pathways, along with other types of abiotic stress (North et al., 2007; J. Zhang, Jia, Yang, & Ismail, 2006). Both drought and salt stress affect water dynamics. In leaves, drought stress will result in ABA-mediated stomatal closure to prevent water loss and salt stress can further reduce a plant's ability to take in water. In a greenhouse study evaluating drought stress in maize plants, seedlings four weeks after emergence showed a reduction in caffeoylshikimate and coumaroylquinate (Tugizimana et al., 2022). These compounds, known as chlorogenic acids, are secondary metabolites that participate in abiotic stress responses (Surówka et al., 2021; Tugizimana et al., 2022). Here, in W822 *se1/se1,* multiple isomers of caffeoylshikimic acid and coumaroylquinic acid were less abundant than in W822 *Se1/Se1*, mirroring an expected drought response.

The mobilization of storage reserves, including carbohydrates, is a hallmark of seed germination; this process is tightly controlled by hormonal regulation, primarily abscisic acid, which promotes seed dormancy, and gibberellin, which promotes germination (Hoecker, Vasil, & McCarty, 1995; Xue et al., 2021). During early stages of germination, amylase, glucosidase, and galactosidase activity increases to break down starch into its component sugars (Han et al., 2020; Hoecker et al., 1995). In W822 *se1/se1* compared to W822 *Se1/Se1*, differentially expressed genes are associated with seed germination, including an upregulation in W822 *se1/*se1 of alpha-amylase Zm00001eb25580 and the alpha galactosidases Zm00001eb330650 and

Zm00001eb044860. Together with the accumulation of starch degradation products, including malto-oligosaccharides and panose, the transcriptional changes in W822 *se1*/*se1* suggest a metabolism more similar to seed germination than seed dormancy. Changes in expression of genes in several major plant hormone pathways, including altered metabolism and function of abscisic acid, gibberellin, brassinosteroids, cytokinin, and auxin are also observed. These changes could result in a shift towards germination-like processes, but not to the extent required to develop the vivipary seen in mutants that completely lack steps in hormonal pathways.

This experiment confirms the effects of *se1* on carbohydrate metabolism, characterized by an increase in starch-degradation products. However, a close association between presence of se1 and decreased levels of carotenoids and tocotrienols suggests that the Se1 gene has a broader regulatory function in the developing endosperm. This broad role is further hinted at by changes in the biosynthesis and signaling pathways of several phytohormones; not only do shifts in hormonal balance between W822 *Se1/Se1* and W822 *se1/se1* offer a connection to the function of *Se1* as a regulatory component, but the effects of phytohormone rebalancing suggests mechanisms for the observed effects on kernel carbohydrate phenotypes.

3.5.4 Phytohormone synthesis and signaling pathways are differentially regulated in W822 se1/se1

3.5.4.1 Auxin

The auxin indole-acetic acid (IAA) has a role in almost all plant growth processes, including endosperm development, seed maturation, and germination. In maize, IAA is primarily synthesized through tryptophan via indole pyruvate, with tryptophan-pyruvate aminotransferases and indole-3-pyruvate monooxygenases catalyzing the reactions (Glawischnig et al., 2000; Jones & Setter, 2000; Yue, Lingling, Xie, Coulter, & Luo, 2021). In W822 *se1/se1,* tryptophan

aminotransferase (Zm00001eb336530) and indole-3-pyruvate monooxygenases (Zm00001eb409250 and Zm00001eb332870) are upregulated at 13 DAP, possibly leading to greater auxin levels in *se1* endosperm.

In addition to direct biosynthesis from precursor amino acids, IAA levels can also be regulated through the conjugation or hydrolysis of IAA from different amino acids (Leclere et al., 2010). The IAA-amino acid hydrolase (ILR1, Zm00001eb304520), which releases active IAA, is upregulated at all time points in W822 *se1/se1*, most strongly at 13 DAP. At the same time as this IAA activation is a shift in expression of auxin amido synthetases (Zm00001eb020510, Zm00001eb108330, and Zm00001eb326420); these are all downregulated at 22 DAP, which would reduce the rate that IAA is stored as amino acid conjugates, further increasing the free IAA levels.

Transcriptional changes in W822 correspond to changes in compounds detected in the widely-targeted metabolomics analysis. Levels of IAA-amino acid conjugates indole-3-acetyl-L-aspartic acid and indole-3-acetyl-L-alanine are decreased, reflecting both the increased gene expression in the IAA activation pathway and the decreased expression in the IAA deactivation pathway. Free IAA was also detected as a metabolite driving differences between W822 *se1/se1* and W822 *Se1/Se1* and was the most strongly upregulated metabolite in the plumerane class, with a log2-fold change of 1.80.

Several defective kernel mutants, such as *dek18*, are auxin deficient, while other defective kernel mutants have abnormally high auxin levels; a change in either direction has the potential to disrupt normal endosperm development (Bernardi et al., 2016). Interestingly, auxin can also contribute to seed dormancy through the interactions of the auxin-responsive transcription factor *iaa8* (Zm00001eb122410) and the ABA receptor *abscisic acid insensitive3*

(X. Liu et al., 2013). If an increase in auxin levels suggest a dormancy response in developing endosperm, any germination-like activity would require a change in that particular auxin interaction, and that is observed here. In W822 *se1/se1*, *iaa8* was upregulated at 13 DAP but downregulated at 22 DAP.

3.5.4.2 Abscisic acid

In maize, abscisic acid (ABA) is a cleavage product of higher carotenoids; ABA synthesis requires 9'-carotenoid cleavage dioxygenases (NCEDs) to produce xanthoxin, which is then converted to abscisic aldehyde via xanthoxin dehydrogenase and then oxidized into abscisic acid via ABA aldehyde oxidase (Vallabhaneni & Wurtzel, 2010; Yue et al., 2021). Here, the xanthoxin dehydrogenase *SCA1* (Zm00001eb212270) was upregulated at 13 DAP. Zeaxanthin epoxidase (*til1,* Zm00001eb247000), which produces ABA-precursor xanthophylls from zeaxanthin, was also upregulated. These changes would lead to an increase in ABA availability at early time points. Inactivation of ABA, through hydroxylation to phaseic acid, is catalyzed by ABA 8'-hydroxylases. One such such enzyme, *abh3,* (Zm00001eb176720) was strongly upregulated in W822 *se1/se1* at 22 DAP*,* which would hasten the degradation and reduce the pool of available ABA. However, the metabolic analysis did not detect any differences in ABA levels between W822 *se1/se1* and W822 *Se1/Se1. ZmPTF1* (Zm00001eb374120), is a transcription factor that upregulates NCED genes; this was upregulated in W822 *se1/se1* at 22 DAP.

In addition to transcriptional changes relating to synthesis and degradation, modulating sensitivity is another way that a plant can regulate a hormone pathway; upregulation of a receptor gene will increase sensitivity, and downregulation of a receptor will decrease sensitivity (X. Liu et al., 2013; K. Wang et al., 2018). A central regulator of the ABA response pathway is *abscisic acid insensitive5* (ABI5), which is a transcription factor that will promote germination

inhibition, fatty acid synthesis, stress adaptation, chlorophyll production, and inhibit leaf senescence (Skubacz, Daszkowska-Golec, & Szarejko, 2016).

At 13 DAP in W822 *se1/se1*, there was significant differential expression of ABA-insensitive 5-like (ABI5) transcription factors. ABI5-like 5 proteins (Zm00001eb176680, Zm00001eb038010, Zm00001eb314860, Zm00001eb100750) are upregulated at 13 DAP; ABI5-like protein 2 factors are downregulated at 13 DAP. Accordingly, genes and pathways that are upregulated by ABI5 were in turn upregulated at 13 DAP. Overexpression studies with ABI5 have observed enhanced effects of ABA, including an increase in raffinose production (Zinsmeister et al., 2016). At 22 DAP, ABI5 expression is reversed, with ABI5-5 transcription factors being downregulated in W822 *se1/se1.* One gene known to downregulate ABI5 is MFT (MOTHER OF FT AND TFL1, Zm00001eb126300), which is also a positive regulator of germination, and could contribute to the transcriptional changes in W822 *se1/se1* (Xi, Liu, Hou, & Yu, 2010). Here, MFT was upregulated at 22 DAP, but not earlier. By suppressing ABI5, MFT would reduce ABA sensitivity, further shifting the hormone balance towards germination.

3.5.4.3 Gibberellin

Based on a coexpression network analysis, Finegan et. al. 2021 suggested that *se1* has a role in allowing for starch degradation through gibberellin signaling (Finegan et al., 2022). Gibberellin synthesis, like carotenoid and tocotrienol synthesis starts with the production of geranylgeranyl diphosphate (GGPP); in the case of gibberellins, GGPP is then converted into ent-kaurene via ent-copalyl diphosphate synthase and ent-kaurene synthase. GA_{12} is then produced from ent-kaurene via a series of oxidation reactions. Bioactive forms of GA are GA_1, GA3, and GA4, which are all produced from GA12 via gibberellin-3-oxidases (Hedden, 2020; White & Rivin, 2000). The transcriptional effects of the *se1* deletion on gibberellin metabolism

are opposite of the effects on the metabolism of IAA. The expression of genes encoding enzymes for early steps towards GA production, GGPP synthesis, is largely unchanged at earlier time points. However, at 22 DAP in W822 *se1/se1*, GGPP synthesis genes, especially those in the mevalonate pathway, trend toward downregulation. A 3-hydroxy-3-methylglutaryl coenzyme A synthase (Zm00001eb403920), a isopentenyl diphosphate isomerase (Zm00001eb349410), a diphosphomevalonate decarboxylase (Zm00001eb257840), and a phosphomevalonate kinase (Zm00001eb010900), are downregulated; these enzymes function to convert acetyl-CoA to prenyl diphosphate, the major GGPP precursor (Cordoba et al., 2009). The synthesis of bioactive GAs from GA12, including enzymes for gibberellin oxidases (Zm00001eb303030, Zm00001eb219040, and Zm00001eb095390), is also downregulated at 22 DAP. These transcriptomic changes indicate a shift towards higher GA levels in W822 *se1/se1*. Gibberellin 2-beta-dioxygenases, which turn active forms of GA into inactive forms, are strongly downregulated at 13 DAP, but are slightly upregulated at 22 DAP. Together, these transcriptional changes show a trend toward higher GA synthesis early in development, but a reduction in GA precursor-generating enzymes at 22 DAP. High GA production, especially early in development, could play a role in initiating some of the germination-like processes seen in W822 *se1/se1*.

3.5.4.4 Brassinosteroids

With the exception of Zm00001eb196530, which encodes a cytochrome P450 monooxygenase, brassinosteroid synthesis is largely unchanged. However, in the pathway for inactivation and catabolism of brassinosteroids, the P450 enzyme *brc2 (*Zm00001eb385730) is strongly upregulated at 13 DAP in W822 *se1/se1*, which would reduce the level of brassinosteroid activity. The brassinosteroid signaling pathway was also modified in W822 *se1/se1.* Genes for brassinosteroid-insensitive1-associated receptor kinase-like (*bak1*) proteins, in

particular, were affected. As a whole, genes with bak1-like annotations were contra-regulated in the absence of *Se1*; some, including Zm00001eb369250 and Zm00001eb112380, were upregulated at 13 DAP but not at later time points. Interestingly, another *bak1* gene, Zm00001eb380430, was downregulated at all time points. At 22 DAP, brassinosteroid signaling kinases are downregulated. Overall, this would lead to a subdued brassinosteroid signaling pathway in W822 *se1/se1*.

As growth regulators, brassinosteroids are implicated in affecting grain filling and starch synthesis in monocots; overexpression of brassinosteroid synthesis leads to increased seed size and starch content (Kour et al., 2021; Sun et al., 2021; Xiong et al., 2022). *Drg10* (Zm00001eb080110), when overexpressed, led to an increase brassinosteroid levels as well as an increase in total starch, but a decrease in amylose content (Sun et al., 2021). In addition, brassinosteroids also contribute to abiotic stress tolerance, including promoting resistance to drought and salt stress (S. Li, Zheng, Lin, Wang, & Sui, 2021). An overexpression of brassinosteroid signaling kinase *bsk1* increased responses to salt stress by promoting ROS scavenging and proline synthesis. In the presence of other hormones, brassinosteroids can work antagonistically with abscisic acid by downregulating PP2C proteins and reducing ABA signaling (Kour et al., 2021; Skubacz et al., 2016).

3.5.4.5 Cytokinins

Cytokinins are plant hormones that generally complement auxins as plant growth regulators. In maize tissues, including maize endosperm, the prominent cytokinin is *trans*-zeatin (Jones & Setter, 2000). Like the GGPP leading to GA synthesis, zeatin synthesis begins with prenyl diphosphate, a product of the mevalonate or MEP pathways. Zeatin is then created by the activities of dimethylallyltransferases and zeatin riboside phosphoribohydrolases (Hluska et al.,

2016). Two of the Cytokinin riboside 5'-monophosphate phosphoribohydrolases, Zm00001eb294370 and Zm00001eb15520, either of which catalyze the final step in trans-zeatin production, are downregulated in W822 *se1/se1* at 22 DAP.

Here, the widely-targeted metabolomics assay was able to detect several forms of zeatin or zeatin-adjacent metabolites. The abundances of zeatin, in both the *cis*- and *trans*- form, were significantly increased in W822 *se1/se1* based on VIP score, with log2 fold-changes of 2.5 and 2.18, respectively. *Cis*-zeatin riboside, an intermediate in the zeatin synthetic process, was also moderately more abundant.

3.5.4.6 Strigolactone

Closely correlated to the synthesis of ABA is the metabolism of another phytohormone, strigolactone. Like ABA, strigolactone starts out as carotenoids precursors (Yoda et al., 2021). Beta-carotene, instead of proceeding towards zeaxanthin and ABA synthesis, is, in the case of strigolactone, instead converted to carlactone and then to 5-deoxystrigol, the bioactive strigolactone (J. C. Guan et al., 2023; Struk, 2018). In this pathway, the beta-carotene isomerase Zm00001eb417120 is downregulated at 16 and 19 DAP; the beta-carotene isomerase Zm00001eb260820 is slightly upregulated at 22 DAP.

Perception of strigolactones involves KAI2-like esterases, which then bind to MAX2/More Axillary Growth; the KAI2/MAX2 complex is involved in ubiquination and degradation of SMAX1/Suppressor of MAX1, and the strigolactones responses, including helping to induce germination, occur (Conn & Nelson, 2016; Zheng et al., 2020). In W822 *se1/se1*, KAI2 esterases Zm00001eb393500 and Zm00001eb020660 are upregulated at 13 DAP, and the former is also downregulated at 22 DAP. Genes encoding MAX2 proteins, Zm00001eb376660 and Zm00001eb270950, are upregulated at 13 and 16 DAP. Strigolactone

signaling has been shown to have played a role in maize domestication. Koch et. al. (2022) identified strigolactone as contributing to the *tga1* domestication phenotypes, including kernel size and kernel biomass, and strigolactone deficiency led to decreased seed size (J. C. Guan et al., 2023).

3.6 Conclusion

Modern sweet corn breeding has shifted away from the use of *se1* in most commercial germplasm; this decision has been based less on an understanding of the function of *Se1* in sugar and starch metabolism than on the greater impact of other endosperm mutations. However, interest in other quality traits in sweet corn, including levels of carotenoids and tocochromanols, has revealed connections to the *Se1* gene in these compounds as well. In this study, further evidence is provided that *Se1* is a regulatory gene, with effects beyond in the starch synthesis pathway. The transcriptomic and metabolomic profiles of *se1/se1* kernels show patterns relating to germination and abiotic stress response. An investigation into the corresponding phytohormone pathways shows changes the metabolism of several different hormones, but most notably an increase in IAA in W822 *se1/se1*. Not only would it explain the role of the gene's FAF domain, loss of *Se1* and the induced change in phytohormone regulation would be a global link between starch synthesis, carotenoid and tocochromanol production, and the germination and stress-response pathways in developing kernels.

3.7 Chapter 3 References

Aleksander, S. A., Balhoff, J., Carbon, S., Cherry, J. M., Drabkin, H. J., Ebert, D., … Westerfield, M. (2023). The Gene Ontology knowledgebase in 2023. *Genetics*, *224*(1), 1–14. https://doi.org/10.1093/genetics/iyad031

Ali, Q., Sami, A., Haider, M. Z., Ashfaq, M., & Javed, M. A. (2024). Antioxidant production promotes defense mechanism and different gene expression level in Zeamays under abiotic stress. *Scientific Reports*, *14*(1), 1–14. https://doi.org/10.1038/s41598-024-57939-6

Azanza, F., Tadmor, Y., Klein, B. P., Rocheford, T. R., & Juvik, J. A. (1996). Quantitative trait loci influencing chemical and sensory characteristics of eating quality in sweet corn. *Genome*, *39*(1), 40–50. https://doi.org/10.1139/g96-006

Baseggio, M., Murray, M., Magallanes-Lundback, M., Kaczmar, N., Chamness, J., Buckler, E. S., … Gore, M. A. (2020). Natural variation for carotenoids in fresh kernels is controlled by uncommon variants in sweet corn. *Plant Genome*, *13*(1), 1–19. https://doi.org/10.1002/tpg2.20008

Baseggio, M., Murray, M., Magallanes-Lundback, M., Kaczmar, N., Chamness, J., Buckler, E. S., … Gore, M. A. (2019). Genome-Wide Association and Genomic Prediction Models of Tocochromanols in Fresh Sweet Corn Kernels. *The Plant Genome*, *12*(1), 180038. https://doi.org/10.3835/plantgenome2018.06.0038

Bernardi, J., Li, Q. B., Gao, Y., Zhao, Y., Battaglia, R., Marocco, A., & Chourey, P. S. (2016). The Auxin-Deficient Defective Kernel18 (dek18) Mutation Alters the Expression of Seed-Specific Biosynthetic Genes in Maize. *Journal of Plant Growth Regulation*, *35*(3), 770–777. https://doi.org/10.1007/s00344-016-9581-6

Blighe, K., & Lun, A. (2021). *PCAtools: Everything Principal Components Analysis*. Retrieved from https://github.com/kevinblighe/PCAtools

Bolger, A. M., Lohse, M., & Usadel, B. (2014). Trimmomatic: A flexible trimmer for Illumina sequence data. *Bioinformatics*, *30*(15), 2114–2120. https://doi.org/10.1093/bioinformatics/btu170

Branch, C. A., Baseggio, M., Resende, M. F. R., & Tracy, W. F. (2024). The Sugary enhancer1 (se1) Allele is Associated with Significant Decreases in Carotenoids and Tocotrienols in Yellow (Y1) sugary1 (su1) Sweet Corn. *Journal of the American Society for Horticultural Science*. Submitted for publication

Chong, J., & Xia, J. (2018). MetaboAnalystR: An R package for flexible and reproducible analysis of metabolomics data. *Bioinformatics*, *34*(24), 4313–4314. https://doi.org/10.1093/bioinformatics/bty528

Conn, C. E., & Nelson, D. C. (2016). Evidence that KARRIKIN-INSENSITIVE2 (KAI2) receptors may perceive an unknown signal that is not karrikin or strigolactone. *Frontiers in Plant Science*, *6*(JAN2016), 1–7. https://doi.org/10.3389/fpls.2015.01219

Cordoba, E., Salmi, M., & León, P. (2009). Unravelling the regulatory mechanisms that modulate the MEP pathway in higher plants. *Journal of Experimental Botany*, *60*(10), 2933–2943. https://doi.org/10.1093/jxb/erp190

Creech, R. G., & McArdle, F. J. (1966). Gene Interaction for Quantitative Changes in Carbohydrates in Maize Kernels. *Crop Science*, *6*(2), 192–194. https://doi.org/10.2135/cropsci1966.0011183x000600020026x

Creech, Roy G. (1965). GENETIC CONTROL OF CARBOHYDRATE SYNTHESIS IN MAIZE ENDOSPERM'. *Genetics*, *52*, 1175–1186. Retrieved from https://academic.oup.com/genetics/article/52/6/1175/5988171

Cuttriss, A. J., Cazzonelli, C. I., Wurtzel, E. T., & Pogson, B. J. (2011). Carotenoids. In *Advances in Botanical Research* (Vol. 58, pp. 1–36). https://doi.org/10.1016/B978-0-12-386479-6.00005-6

Diepenbrock, C. H., Ilut, D. C., Magallanes-Lundback, M., Kandianis, C. B., Lipka, A. E., Bradbury, P. J., … DellaPenna, D. (2021). Eleven biosynthetic genes explain the majority of natural variation in carotenoid levels in maize grain. *Plant Cell*, *33*(4), 882–900. https://doi.org/10.1093/plcell/koab032

Diepenbrock, C. H., Kandianis, C. B., Lipka, A. E., Magallanes-Lundback, M., Vaillancourt, B., Góngora-Castillo, E., … DellaPenna, D. (2017). Novel loci underlie natural variation in vitamin E levels in maize grain. *Plant Cell*, *29*(10), 2374–2392. https://doi.org/10.1105/tpc.17.00475

Dobin, A., Davis, C. A., Schlesinger, F., Drenkow, J., Zaleski, C., Jha, S., … Gingeras, T. R. (2013). STAR: Ultrafast universal RNA-seq aligner. *Bioinformatics*, *29*(1), 15–21. https://doi.org/10.1093/bioinformatics/bts635

Finegan, C., Boehlein, S. K., Leach, K. A., Madrid, G., Hannah, L. C., Koch, K. E., … Resende, M. F. R. (2022). Genetic Perturbation of the Starch Biosynthesis in Maize Endosperm Reveals Sugar-Responsive Gene Networks. *Frontiers in Plant Science*, *12*(February), 1–16. https://doi.org/10.3389/fpls.2021.800326

Gao, M., Wanat, J., Stinard, P. S., James, M. G., & Myers, A. M. (1998). Characterization of dull1, a maize gene coding for a novel starch synthase. *Plant Cell*, *10*(3), 399–412. https://doi.org/10.1105/tpc.10.3.399

Ghosh, U. K., Islam, M. N., Siddiqui, M. N., Cao, X., & Khan, M. A. R. (2022). Proline, a multifaceted signalling molecule in plant responses to abiotic stress: understanding the physiological mechanisms. *Plant Biology*, *24*(2), 227–239. https://doi.org/10.1111/plb.13363

Glawischnig, E., Tomas, A., Eisenreich, W., Spiteller, P., Bacher, A., & Gierl, A. (2000). Auxin biosynthesis in maize kernels. *Plant Physiology*, *123*(3), 1109–1119. https://doi.org/10.1104/pp.123.3.1109

Guan, J. C., Li, C., Flint-Garcia, S., Suzuki, M., Wu, S., Saunders, J. W., … Koch, K. E. (2023). Maize domestication phenotypes reveal strigolactone networks coordinating grain size evolution with kernel-bearing cupule architecture. *Plant Cell*, *35*(3), 1013–1037. https://doi.org/10.1093/plcell/koac370

Guan, L., & Scandalios, J. G. (1998). Two structurally similar maize cytosolic superoxide dismutase genes, Sod4 and Sod4A, respond differentially to abscisic acid and high osmoticum. *Plant Physiology*, *117*(1), 217–224. https://doi.org/10.1104/pp.117.1.217

Han, Z., Wang, B., Tian, L., Wang, S., Zhang, J., Guo, S. L., … Chen, Y. (2020). Comprehensive dynamic transcriptome analysis at two seed germination stages in maize (Zea mays L.). *Physiologia Plantarum*, *168*(1), 205–217. https://doi.org/10.1111/ppl.12944

Hannah, L. C., & Nelson, O. E. (1976). Characterization of ADP-glucose pyrophosphorylase from shrunken-2 and brittle-2 mutants of maize. *Biochemical Genetics*, *14*(7–8), 547–560. https://doi.org/10.1007/BF00485834

Hedden, P. (2020). The current status of research on gibberellin biosynthesis. *Plant and Cell Physiology*, *61*(11), 1832–1849. https://doi.org/10.1093/pcp/pcaa092

Hershberger, J., Tanaka, R., Wood, J. C., Kaczmar, N., Wu, D., Hamilton, J. P., … Gore, M. A. (2022). Transcriptome-wide association and prediction for carotenoids and tocochromanols in fresh sweet corn kernels. *Plant Genome*, *15*(2), 1–16. https://doi.org/10.1002/tpg2.20197

Hii, S. L., Tan, J. S., Ling, T. C., & Ariff, A. Bin. (2012). Pullulanase: Role in starch hydrolysis and potential industrial applications. *Enzyme Research*, *2012*. https://doi.org/10.1155/2012/921362

Hluska, T., Dobrev, P. I., Tarkowská, D., Frébortová, J., Zalabák, D., Kopečný, D., … Galuszka, P. (2016). Cytokinin metabolism in maize: Novel evidence of cytokinin abundance, interconversions and formation of a new trans-zeatin metabolic product with a weak anticytokinin activity. *Plant Science*, *247*, 127–137. https://doi.org/10.1016/j.plantsci.2016.03.014

Hoecker, U., Vasil, I. K., & McCarty, D. R. (1995). Integrated control of seed maturation and germination programs by activator and repressor functions of viviparous-1 of maize. *Genes and Development*, *9*(20), 2459–2469. https://doi.org/10.1101/gad.9.20.2459

Hu, Y., Colantonio, V., Müller, B. S. F., Leach, K. A., Nanni, A., Finegan, C., … Resende, M. F. R. (2021). Genome assembly and population genomic analysis provide insights into the evolution of modern sweet corn. *Nature Communications*, *12*(1), 1227. https://doi.org/10.1038/s41467-021-21380-4

Hufford, M. B., Seetharam, A. S., Woodhouse, M. R., Chougule, K. M., Ou, S., Liu, J., … Dawe, R. K. (2021). De novo assembly, annotation, and comparative analysis of 26 diverse maize genomes. *Science*, *373*(6555), 655–662. https://doi.org/10.1126/science.abg5289

Ibrahim, K. E., & Juvik, J. A. (2009). Feasibility for improving phytonutrient content in vegetable crops using conventional breeding strategies; case study with carotenoids and tocopherols in sweet corn and broccoli. *Journal of Agricultural and Food Chemistry*, *57*(11), 4636–4644. https://doi.org/10.1021/jf900260d

Jones, R. J., & Setter, T. L. (2000). Hormonal regulation of early kernel development. *Physiology and Modeling Kernel Set in Maize*, (29), 25–42. https://doi.org/10.2135/cssaspecpub29.c3

Kasahara, H., Hanada, A., Kuzuyama, T., Takagi, M., Kamiya, Y., & Yamaguchi, S. (2002). Contribution of the mevalonate and methylerythritol phosphate pathways to the biosynthesis of Gibberellins in Arabidopsis. *Journal of Biological Chemistry*, *277*(47), 45188–45194. https://doi.org/10.1074/jbc.M208659200

Kinsella, R. J., Kähäri, A., Haider, S., Zamora, J., Proctor, G., Spudich, G., … Flicek, P. (2011). Ensembl BioMarts: A hub for data retrieval across taxonomic space. *Database*, *2011*, 1–9. https://doi.org/10.1093/database/bar030

Kour, J., Kohli, S. K., Khanna, K., Bakshi, P., Sharma, P., Singh, A. D., … Sharma, A. (2021). Brassinosteroid Signaling, Crosstalk and, Physiological Functions in Plants Under Heavy Metal Stress. *Frontiers in Plant Science*, *12*(March). https://doi.org/10.3389/fpls.2021.608061

La Bonte, D. R., & Juvik, J. A. (1990). Characterization of sugary-1 (su-1) sugary enhancer (se) Kernels in Segregating Sweet Corn Populations. *Journal of the American Society for Horticultural Science*, *115*(1), 153–157. https://doi.org/10.21273/jashs.115.1.153

Langfelder, P., & Horvath, S. (2008). WGCNA: An R package for weighted correlation network analysis. *BMC Bioinformatics*, *9*. https://doi.org/10.1186/1471-2105-9-559

Leclere, S., Schmelz, E. A., & Chourey, P. S. (2010). Sugar levels regulate tryptophan-dependent auxin biosynthesis in developing maize kernels. *Plant Physiology*, *153*(1), 306–318. https://doi.org/10.1104/pp.110.155226

Li, S., Zheng, H., Lin, L., Wang, F., & Sui, N. (2021). Roles of brassinosteroids in plant growth and abiotic stress response. *Plant Growth Regulation*, *93*(1), 29–38. https://doi.org/10.1007/s10725-020-00672-7

Li, T., Zhang, Y., Wang, D., Liu, Y., Dirk, L. M. A., Goodman, J., … Zhao, T. (2017). Regulation of Seed Vigor by Manipulation of Raffinose Family Oligosaccharides in Maize and Arabidopsis thaliana. *Molecular Plant*, *10*(12), 1540–1555. https://doi.org/10.1016/j.molp.2017.10.014

Liang, Y., Jiang, Y., Du, M., Li, B., Chen, L., Chen, M., … Wu, J. (2019). ZmASR3 from the maize ASR gene family positively regulates drought tolerance in transgenic arabidopsis. *International Journal of Molecular Sciences*, *20*(9), 1–20. https://doi.org/10.3390/ijms20092278

Lim, C. W., Bae, Y., & Lee, S. C. (2022). Differential role of Capsicum annuum FANTASTIC FOUR-like gene CaFAF1 on drought and salt stress responses. *Environmental and Experimental Botany*, *199*(April), 104887. https://doi.org/10.1016/j.envexpbot.2022.104887

Liu, H., Wang, F., Liu, B., Kong, F., & Fang, C. (2024). Significance of Raffinose Family Oligosaccharides (RFOs) metabolism in plants. *Advanced Biotechnology*, *2*(13). https://doi.org/10.1007/s44307-024-00022-y

Liu, X., Zhang, H., Zhao, Y., Feng, Z., Li, Q., Yang, H. Q., … He, Z. H. (2013). Auxin controls seed dormancy through stimulation of abscisic acid signaling by inducing ARF-mediated ABI3 activation in Arabidopsis. *Proceedings of the National Academy of Sciences of the United States of America*, *110*(38), 15485–15490. https://doi.org/10.1073/pnas.1304651110

Love, M. I., Huber, W., & Anders, S. (2014). Moderated estimation of fold change and dispersion for RNA-seq data with DESeq2. *Genome Biology*, *15*(12), 1–21. https://doi.org/10.1186/s13059-014-0550-8

Naik, B., Kumar, V., Goyal, S. K., Dutt Tripathi, A., Mishra, S., Joakim Saris, P. E., … Rustagi, S. (2023). Pullulanase: unleashing the power of enzyme with a promising future in the food industry. *Frontiers in Bioengineering and Biotechnology*, *11*(June), 1–16. https://doi.org/10.3389/fbioe.2023.1139611

North, H. M., Almeida, A. De, Boutin, J. P., Frey, A., To, A., Botran, L., … Marion-Poll, A. (2007). The Arabidopsis ABA-deficient mutant aba4 demonstrates that the major route for stress-induced ABA accumulation is via neoxanthin isomers. *Plant Journal*, *50*(5), 810–824. https://doi.org/10.1111/j.1365-313X.2007.03094.x

Perrin, F., Hartmann, L., Dubois-Laurent, C., Welsch, R., Huet, S., Hamama, L., … Geoffriau, E. (2017). Carotenoid gene expression explains the difference of carotenoid accumulation in carrot root tissues. *Planta*, *245*(4), 737–747. https://doi.org/10.1007/s00425-016-2637-9

Picart-Armada, S., Fernández-Albert, F., Vinaixa, M., Yanes, O., & Perera-Lluna, A. (2018). FELLA: An R package to enrich metabolomics data. *BMC Bioinformatics*, *19*(1), 1–9. https://doi.org/10.1186/s12859-018-2487-5

Raudvere, U., Kolberg, L., Kuzmin, I., Arak, T., Adler, P., Peterson, H., & Vilo, J. (2019). G:Profiler: A web server for functional enrichment analysis and conversions of gene lists (2019 update). *Nucleic Acids Research*, *47*(W1), W191–W198. https://doi.org/10.1093/nar/gkz369

Revilla, P., Anibas, C. M., & Tracy, W. F. (2021). Sweet corn research around the world 2015–2020. *Agronomy*, *11*(3), 1–49. https://doi.org/10.3390/agronomy11030534

Sen, C. K., Khanna, S., & Roy, S. (2006). Tocotrienols: Vitamin E Beyond Tocopherols. *Life Sciences*, *78*(18), 2088–2098.

Shamimuzzaman, M., Gardiner, J. M., Walsh, A. T., Triant, D. A., Le Tourneau, J. J., Tayal, A., … Elsik, C. G. (2020). MaizeMine: A Data Mining Warehouse for the Maize Genetics and Genomics Database. Frontiers in Plant Science, 11(October), 1–15. https://doi.org/10.3389/fpls.2020.592730

Shang, L., Tao, J., Song, J., Wang, Y., Zhang, X., Ge, P., … Zhang, Y. (2024). CRISPR/Cas9-mediated mutations of FANTASTIC FOUR gene family for creating early flowering mutants in tomato. *Plant Biotechnology Journal*, *22*(3), 774–784. https://doi.org/10.1111/pbi.14223

Skubacz, A., Daszkowska-Golec, A., & Szarejko, I. (2016). The role and regulation of ABI5 (ABA-insensitive 5) in plant development, abiotic stress responses and phytohormone crosstalk. *Frontiers in Plant Science*, *7*(DECEMBER2016), 1–17. https://doi.org/10.3389/fpls.2016.01884

Soberalske, R. M., & Andrew, R. H. (1978). Gene Effects on Kernel Moisture and Sugars of Near-Isogenic Lines of Sweet Corn 1 . *Crop Science*, *18*(5), 743–746. https://doi.org/10.2135/cropsci1978.0011183x001800050012x

Soberalske, R. M., & Andrew, R. H. (1980). Gene Effects on Water Soluble Polysaccharides and Starch of Near-Isogenic Lines of Sweet Corn 1 . *Crop Science*, *20*(2), 201–204. https://doi.org/10.2135/cropsci1980.0011183x002000020013x

Song, H., Liu, J., Chen, C., Zhang, Y., Tang, W., Yang, W., … Chen, D. (2022). Down-regulation of NCED leads to the accumulation of carotenoids in the flesh of F1 generation of peach hybrid. *Frontiers in Plant Science*, *13*(November), 1–14. https://doi.org/10.3389/fpls.2022.1055779

Struk, S. (2018). *Elucidation of the protein-protein interaction network at play during strigolactone and karrikin signaling*. Retrieved from https://biblio.ugent.be/publication/8584183/file/8584184.pdf

Sun, H., Xu, H., Li, B., Shang, Y., Wei, M., Zhang, S., … Wu, Y. (2021). The brassinosteroid biosynthesis gene, ZmD11, increases seed size and quality in rice and maize. *Plant Physiology and Biochemistry*, *160*(January), 281–293. https://doi.org/10.1016/j.plaphy.2021.01.031

Surówka, E., Latowski, D., Dziurka, M., Rys, M., Maksymowicz, A., Żur, I., … Miszalski, Z. (2021). Ros-scavengers, osmoprotectants and violaxanthin de-epoxidation in salt-stressed arabidopsis thaliana with different tocopherol composition. *International Journal of Molecular Sciences*, *22*(21), 1–23. https://doi.org/10.3390/ijms222111370

Tracy, W. F., & Galinat, W. C. (1987). Thickness and Cell Layer Number of the Pericarp of Sweet Corn and Some of Its Relatives. *HortScience*, *22*(4), 645–647. https://doi.org/10.21273/hortsci.22.4.645

Tracy, William F., Shuler, S. L., & Dodson-Swenson, H. (2019). The use of endosperm genes for sweet corn improvement: A review of developments in endosperm genes in sweet corn since the seminal publication in plant breeding reviews, volume 1, by Charles Boyer and Jack Shannon (1984). *Plant Breeding Reviews*, *43*, 215–241. https://doi.org/10.1002/9781119616801.ch6

Tracy, William F., Whitt, S. R., & Buckler, E. S. (2006). Recurrent mutation and genome evolution: Example of Sugary 1 and the origin of sweet maize. *Crop Science*. https://doi.org/10.2135/cropsci2006-03-0149tpg

Tugizimana, F., Nephali, L., Lephatsi, M., Chele, K., Steenkamp, P., Buthelezi, N., … Huyser, J. (2022). Decoding the metabolic landscape of maize responses to experimentally controlled drought stress: A greenhouse case study. In *Applied Environmental Metabolomics: Community Insights and Guidance from the Field*. https://doi.org/10.1016/B978-0-12-816460-0.00009-5

USDA-NASS. (2023). US Department of Agriculture–National Agricultural Statistics Service. Retrieved from https://quickstats.nass.usda.gov/

Vallabhaneni, R., & Wurtzel, E. T. (2010). From epoxycarotenoids to ABA: The role of ABA 8′-hydroxylases in drought-stressed maize roots. *Archives of Biochemistry and Biophysics*, *504*(1), 112–117. https://doi.org/10.1016/j.abb.2010.07.005

Vennapusa, A. R., Somayanda, I. M., Doherty, C. J., & Jagadish, S. V. K. (2020). A universal method for high-quality RNA extraction from plant tissues rich in starch, proteins and fiber. *Scientific Reports*, *10*(1), 1–13. https://doi.org/10.1038/s41598-020-73958-5

Virlouvet, L., Jacquemot, M. P., Gerentes, D., Corti, H., Bouton, S., Gilard, F., … Coursol, S. (2011). The ZmASR1 protein influences branched-chain amino acid biosynthesis and maintains kernel yield in maize under water-limited conditions. *Plant Physiology*, *157*(2), 917–936. https://doi.org/10.1104/pp.111.176818

Wahl, V., Brand, L. H., Guo, Y. L., & Schmid, M. (2010). The FANTASTIC FOUR proteins influence shoot meristem size in Arabidopsis thaliana. *BMC Plant Biology*, *10*. https://doi.org/10.1186/1471-2229-10-285

Wang, K., He, J., Zhao, Y., Wu, T., Zhou, X., Ding, Y., … Gong, Z. (2018). EAR1 negatively regulates ABA signaling by enhancing 2C protein phosphatase activity. *Plant Cell*, *30*(4), 815–834. https://doi.org/10.1105/tpc.17.00875

Wang, T., Wang, M., Hu, S., Xiao, Y., Tong, H., Pan, Q., … Yang, X. (2015). Genetic basis of maize kernel starch content revealed by high-density single nucleotide polymorphism markers in a recombinant inbred line population. *BMC Plant Biology*, *15*(1), 1–12. https://doi.org/10.1186/s12870-015-0675-2

White, C. N., & Rivin, C. J. (2000). Gibberellins and seed development in maize. II. Gibberellin synthesis inhibition enhances abscisic acid signaling in cultured embryos. *Plant Physiology*, *122*(4), 1089–1097. https://doi.org/10.1104/pp.122.4.1089

Woodhouse, M. R., Sen, S., Schott, D., Portwood, J. L., Freeling, M., Walley, J. W., … Schnable, J. C. (2022). qTeller: A tool for comparative multi-genomic gene expression analysis. *Bioinformatics*, *38*(1), 236–242. https://doi.org/10.1093/bioinformatics/btab604

Xi, W., Liu, C., Hou, X., & Yu, H. (2010). MOTHER OF FT and TFL1 regulates seed germination through a negative feedback loop modulating ABA signaling in Arabidopsis. *Plant Cell*, *22*(6), 1733–1748. https://doi.org/10.1105/tpc.109.073072

Xiong, M., Yu, J., Wang, J., Gao, Q., Huang, L., Chen, C., … Li, Q. F. (2022). Brassinosteroids regulate rice seed germination through the BZR1-RAmy3D transcriptional module. *Plant Physiology*, *189*(1), 402–418. https://doi.org/10.1093/plphys/kiac043

Xu, J., You, X., Leng, Y., Li, Y., Lu, Z., Huang, Y., … Liu, T. (2023). Identification and Alternative Splicing Profile of the Raffinose synthase Gene in Grass Species. *International Journal of Molecular Sciences*, *24*(13). https://doi.org/10.3390/ijms241311120

Xue, X., Du, S., Jiao, F., Xi, M., Wang, A., Xu, H., … Wang, M. (2021). The regulatory network behind maize seed germination: Effects of temperature, water, phytohormones, and nutrients. *Crop Journal*, *9*(4), 718–724. https://doi.org/10.1016/j.cj.2020.11.005

Yoda, A., Mori, N., Akiyama, K., Kikuchi, M., Xie, X., Miura, K., … Nomura, T. (2021). Strigolactone biosynthesis catalyzed by cytochrome P450 and sulfotransferase in sorghum. *New Phytologist*, *232*(5), 1999–2010. https://doi.org/10.1111/nph.17737

Yue, K., Lingling, L., Xie, J., Coulter, J. A., & Luo, Z. (2021). Synthesis and regulation of auxin and abscisic acid in maize. *Plant Signaling and Behavior*, *16*(7). https://doi.org/10.1080/15592324.2021.1891756

Zhang, D., Ai, G., Ji, K., Huang, R., Chen, C., Yang, Z., … Zhang, J. (2024). EARLY FLOWERING is a dominant gain-of-function allele of FANTASTIC FOUR 1/2c that

promotes early flowering in tomato. *Plant Biotechnology Journal*, *22*(3), 698–711. https://doi.org/10.1111/pbi.14217

Zhang, J., Jia, W., Yang, J., & Ismail, A. M. (2006). Role of ABA in integrating plant responses to drought and salt stresses. *Field Crops Research*, *97*(1 SPEC. ISS.), 111–119. https://doi.org/10.1016/j.fcr.2005.08.018

Zhang, X., Haro von Mogel, K. J., Lor, V. S., Hirsch, C. N., de Vries, B., Kaeppler, H. F., … Kaeppler, S. M. (2019). Maize sugary enhancer1 (se1) is a gene affecting endosperm starch metabolism. *Proceedings of the National Academy of Sciences of the United States of America*, *116*(41), 20776–20785. https://doi.org/10.1073/pnas.1902747116

Zheng, J., Hong, K., Zeng, L., Wang, L., Kang, S., Qu, M., … Xiong, G. (2020). Karrikin signaling acts parallel to and additively with strigolactone signaling to regulate rice mesocotyl elongation in darkness. *Plant Cell*, *32*(9), 2780–2805. https://doi.org/10.1105/TPC.20.00123

Zinsmeister, J., Lalanne, D., Terrasson, E., Chatelain, E., Vandecasteele, C., Ly Vu, B., … Leprince, O. (2016). ABI5 is a regulator of seed maturation and longevity in legumes. *Plant Cell*, *28*(11), 2735–2754. https://doi.org/10.1105/tpc.16.00470

3.8 Chapter Three Appendix

3.8.1 Chapter Three Supplementary Figures

Supplementary Figure S3.1. Gene expression in the starch synthesis pathway at four time points. Genes with higher expression are lower on the heatmap. Genes are up- (blue) or downregulated (red) in W822 *se1/se1* compared to *W822* Se1/Se1. •, 0.05 < p < 0.01; *, significant at p < 0.05; **, significant at p < 0.01, ***, significant at p < 0.001, ****

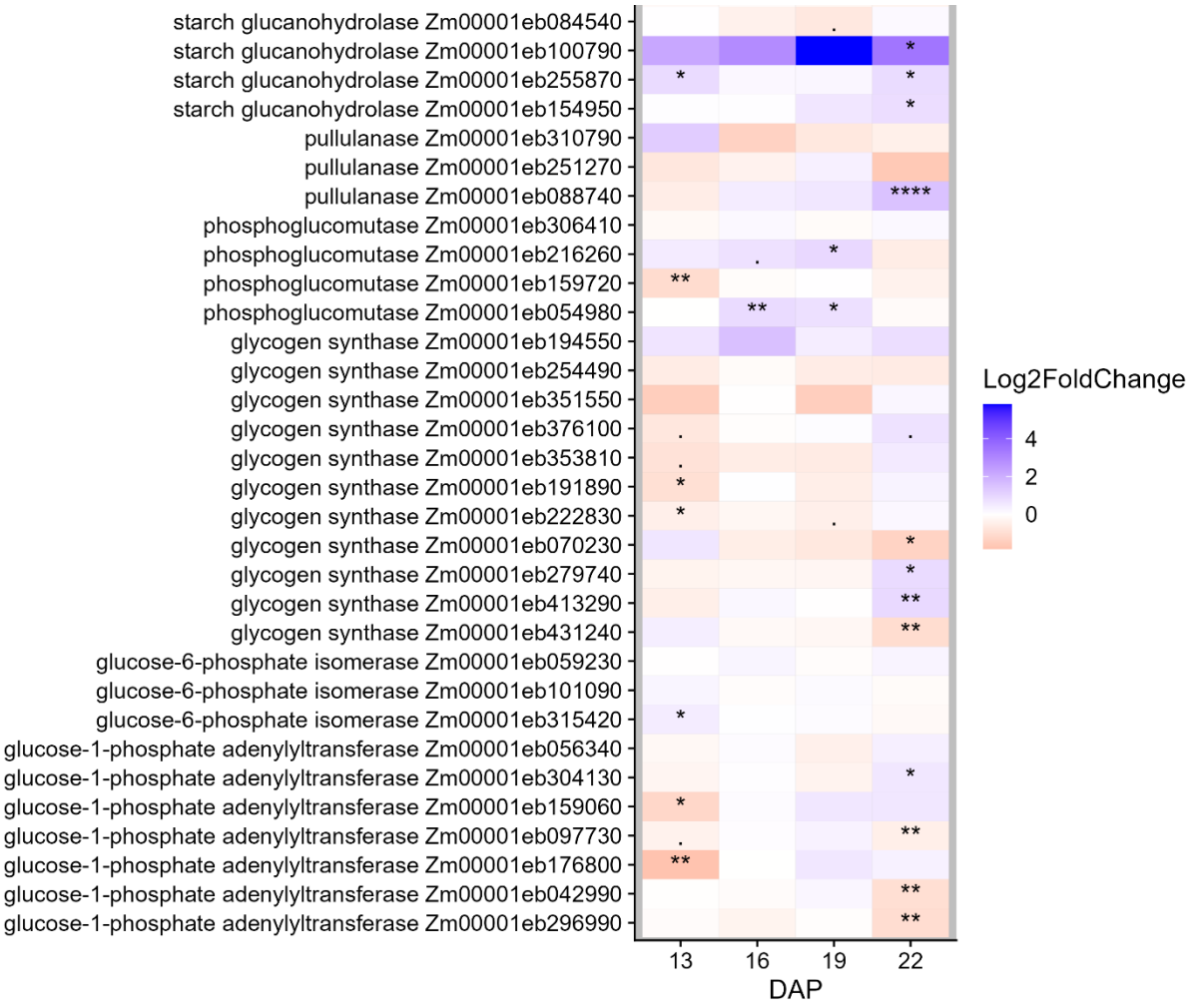

Supplementary Figure S3.2. Gene expression in the carotenoid synthesis pathway at four time points. Genes are up- (blue) or downregulated (red) in W822 se1/se1 compared to W822 Se1/Se1. •, 0.05 < p < 0.01; *, significant at p < 0.05; **, significant at p < 0.01, ***, significant at p < 0.001.

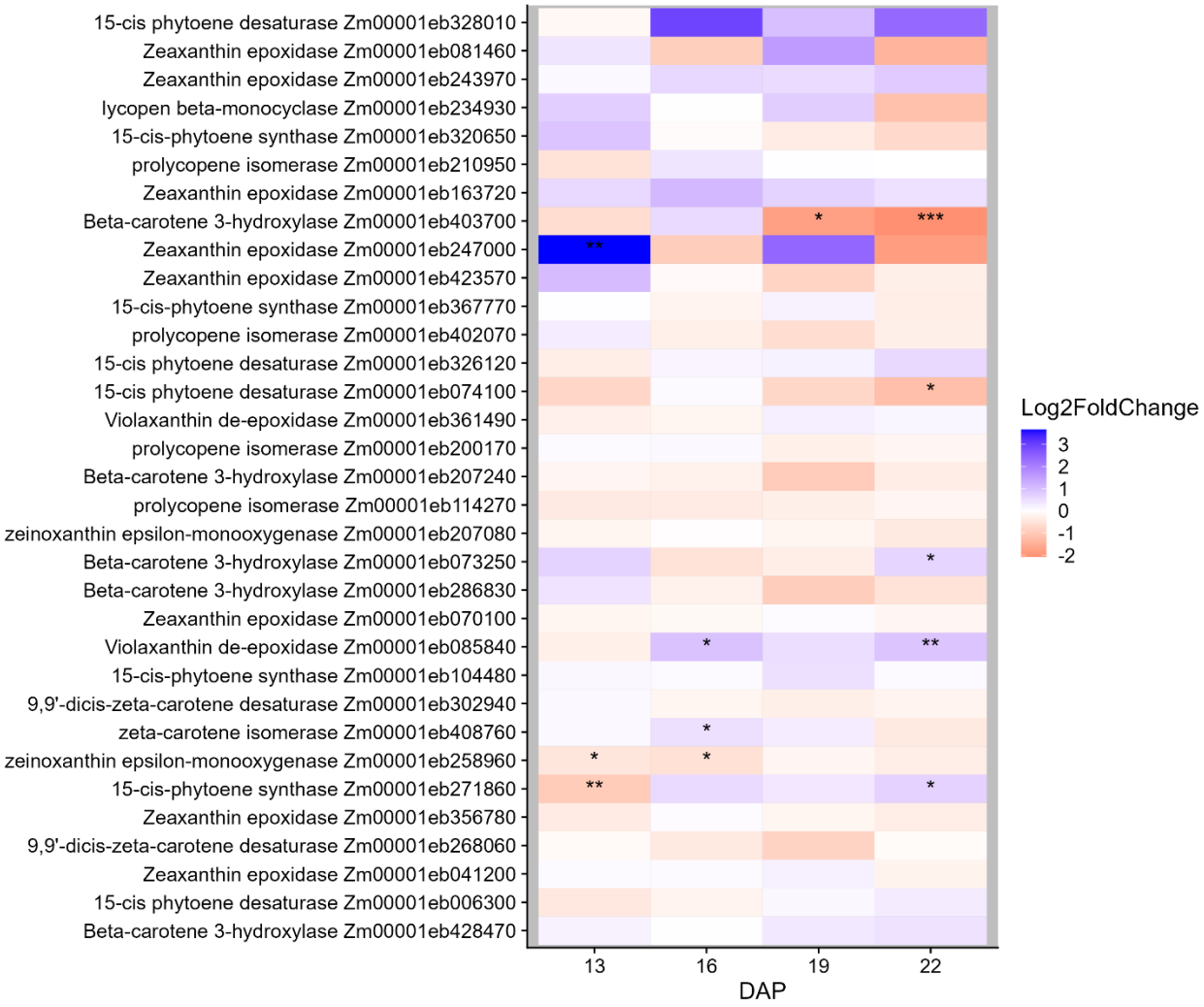

Supplementary Figure S3.3. Gene expression in the tocotrienol synthesis pathway at four time points. Genes are up- (blue) or downregulated (red) in W822 *se1/se1* compared to *W822* Se1/Se1. •, 0.05 < p < 0.01; •, 0.05 < p < 0.01; *, significant at p < 0.05; **, significant at p < 0.01, ***, significant at p < 0.001, **** significant at p < 0.0001

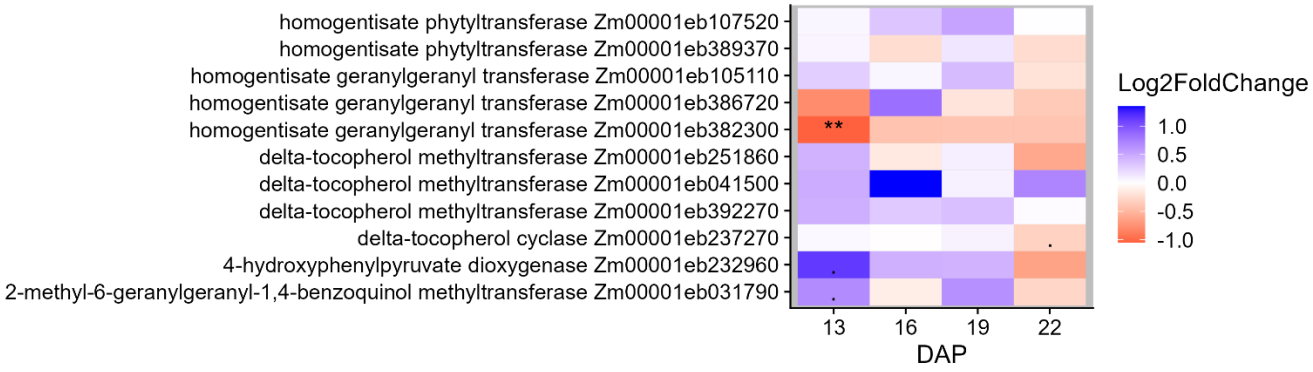

Supplementary Figure S3.4. Gene expression in the raffinose-family oligosaccharide synthesis pathway at four time points. Genes with higher expression are placed lower on the heatmap. Genes are up- (blue) or downregulated (red) in W822 *se1/se1* compared to *W822* Se1/Se1. •, 0.05 < p < 0.01; *, significant at p < 0.05; **, significant at p < 0.01, ***, significant at p < 0.001, **** significant at p < 0.0001

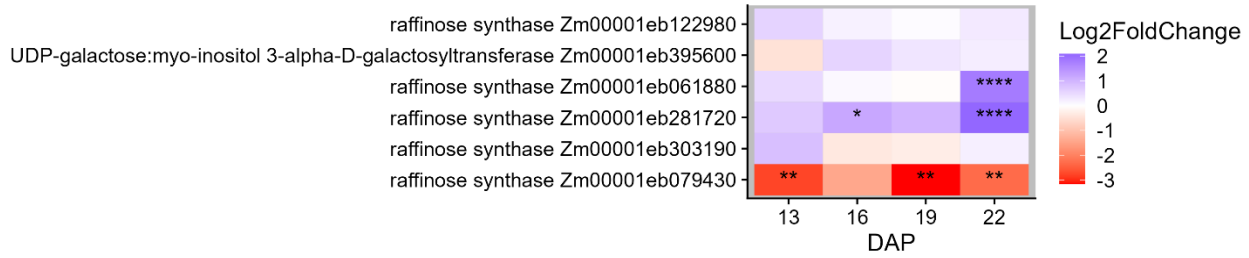

3.8.2 Supplementary material describing widely-targeted metabolomics sample processing and UPLC-MS/MS analysis

3.8.2.1 Dry sample extraction

Lyophilized samples were ground in a ball mill grinder (30 Hz, 1.5 min) (MM 400, Retsch). 50 mg of the ground sample was mixed with 1200 µL of -20°C pre-cooled 70% methanol with internal standards. The mixture was mixed by vortex for 30 sec every 30 min for a total of 6 times, followed by centrifugation (12000 rpm, 3 min, 4°C). The supernatant was collected and filtered through a 0.22um filter membrane and kept for UPLC-MS/MS analysis.

3.8.2.2 Chromatography-mass spectrometry acquisition conditions

The data acquisition instruments consisted of Ultra Performance Liquid Chromatography (UPLC) (ExionLC™ AD, https://sciex.com/) and tandem mass spectrometry (MS/MS) (Applied Biosystems QTRAP 6500, https://sciex.com/).

Liquid phase conditions were as follows:

（1）Chromatographic column: Agilent SB-C18 1.8 μm, 2.1 mm * 100 mm;

（2）Mobile phase: A phase was ultrapure water (0.1% formic acid added), B phase was acetonitrile (0.1% formic acid added);

（3）Elution gradient: 0.00 min, the proportion of B phase was 5%, within 9.00 min, the proportion of B phase increased linearly to 95%, and remained at 95% for 1 min, 10.00-11.10 min, the proportion of B phase decreased to 5%, and balanced at 5% upto 14 min;

（4）Flow rate: 0.35 mL/min;

（5）Column temperature: 40 °C;

（6）Injection volume 2 μL.

The mass spectrum conditions were as follows:

LIT and Triple Quadrupole (QQQ) scans were obtained on a triple quadrupole Linear Ion TRAP Mass Spectrometer (Q TRAP) (AB6500 Q TRAP UPLC/MS/MS system). Operating parameters of ESI source were as follows: ion source, turbine spray; Source temperature 550°C; Ion spray voltage (IS) 5500 V (positive ion mode) /-4500 V (negative ion mode); The ion source gas I (GSI), gas II (GSII) and curtain gas (CUR) were set to 50, 60 and 25.0 psi respectively, and the

collision-induced ionization parameter was set to high. QQQ scan used MRM mode and collision gas (nitrogen) was set to medium. DP and CE of each MRM ion pair were completed by further DP and CE optimization. A specific set of MRM ion pairs was monitored at each period based on the eluted metabolites in each period.

3.8.2.3 qualitative and quantitative analysis of metabolites

Analyst 1.6.3 was used to process mass spectrum data. The characteristic ions of each compound were selected by triple quadrupole and measured for their signal intensity (CPS). The mass spectrometry data was analyzed using MultiQuant software and the chromatographic peaks were integrated and corrected. The peak area of each chromatographic peak represents the relative abundance of the corresponding compound. Mass spectrum peak of each metabolite in different samples was corrected based on retention time and peak distribution information to ensure the accuracy of qualitative and quantitative analysis. A quality control (QC) sample was prepared from a mixture of all sample extracts to examine the reproducibility of the entire metabolomics process. During data collection, one quality control sample was inserted for every 10 test samples.

4 Chapter Four: Divergent Selection for Timing of Vegetative Phase Change

Carl A. Branch, William F. Tracy

Dep. of Agronomy, University of Wisconsin, 1575 Linden Drive, Madison, WI 53706, USA. Corresponding author (cbranch2@wisc.edu)

Received for publication November 25, 2022. Accepted for publication May 5, 2023. Version of record published online in Crop Science June 13, 2023. Volume 146, Issue 3.
https://doi.org/10.1002/csc2.21016

4.1 Preface

As discussed in previous chapters, sweet corn breeding is unusual in that it relies on the disruption of the starch synthesis pathway during endosperm development. While newer technologies increasingly support exploration and exploitation of these key starch synthesis genes and their regulators as way to increase quality, no plant breeding education is complete without gaining a respect for the power of selection as what really results in crop improvement over time. Maintaining variation is equally important for allowing continued genetic gain in a population. This chapter describes work that takes advantage of a divergently selected sweet corn population, unique in that the timing of certain stages of plant development was pushed in opposite directions in each of two subpopulations. The results indicate, first and foremost, that selection works. This is an idea that plant breeders must not forget among the temptations to get lost in various metabolomic pathways for a trait of interest—when in doubt, make selections. Where variation exists, selection can lead to great phenotypic change and start to push biological limits, as shown in this research, without requiring any knowledge of specific genes or proteins. Using methods described by S.A. Eberhart in 1964, this work illustrates the continued relevance of classical plant breeding for improving quantitative traits and demonstrates that the maize

genome provides extensive and continued variation to fuel improvement, even over long-term selection.

With the exception of this preface, the chapter is presented as published.

4.2 Abstract

Vegetative phase change is a key trait in plant development and marks the transition from juvenile to adult growth phases. In maize (*Zea mays* L.), juvenile plants and plants with a late phase change can be identified by the increased production of tillers, aerial roots, and distinctive epicuticular wax. Resistance to agronomically significant pathogens can also differ between juvenile and adult plants. Using last leaf with juvenile wax as the target of selection, the maize population Minnesota 11 underwent 16 cycles of divergent selection. The objectives of this research were to identify emergent trends for each trait and to determine the magnitude and direction of phenotypic changes over long-term selection compared to the source population. Phenotypic data on plant architecture traits, ear traits, and common rust resistance were collected in 2020 and 2021 by concurrently growing plants from selection cycles representing both directions of selection. Last leaf with juvenile wax, the direct target of selection increased to leaf 17.8 in the late phase change population and decreased to leaf 5 in the early phase change population from leaf 9 in the source population. Late vegetative phase change was positively correlated with increased common rust infection and plant height, and negatively correlated with ear size traits. This study shows that the observed phenotypic changes follow patterns of genetic variation consistent with divergent selection, but with possible effects of inbreeding.

4.3 Introduction

Normal plant development is marked by a series of distinct growth phases, juvenile vegetative, adult vegetative, and reproductive (R. S. Poethig, 2010). Plants move through both vegetative growth phases before floral initiation and seed development, thus the timing of these growth phases and the regulation of the transition is an area of agronomic importance in maize (*Zea mays L.*), with implications for yield, plant architecture, and pathogen interactions (Basso, Hurkman, Riedeman, & Tracy, 2008; Lawrence, Springer, Helliker, & Poethig, 2021; Riedeman, Chandler, & Tracy, 2008).

In maize, the juvenile and adult vegetative phases are marked by distinct tissue types. Juvenile leaf tissue is identified by a thick blue gray epicuticular leaf wax, lack of trichomes, and rounded epidermal cells. In contrast, adult vegetative growth produces trichome-covered leaves, 3 μm cuticles, transparent leaf wax, and a plant able to initiate reproductive growth. Reduced apical dominance in juvenile plants also increases the number of basal lateral branches (tillers) and aerial root production compared to the adult phase (R. S. Poethig, 2010). The first leaves are fully juvenile tissue, followed by a transition zone composed of leaves with both juvenile and adult traits (Figure 1).

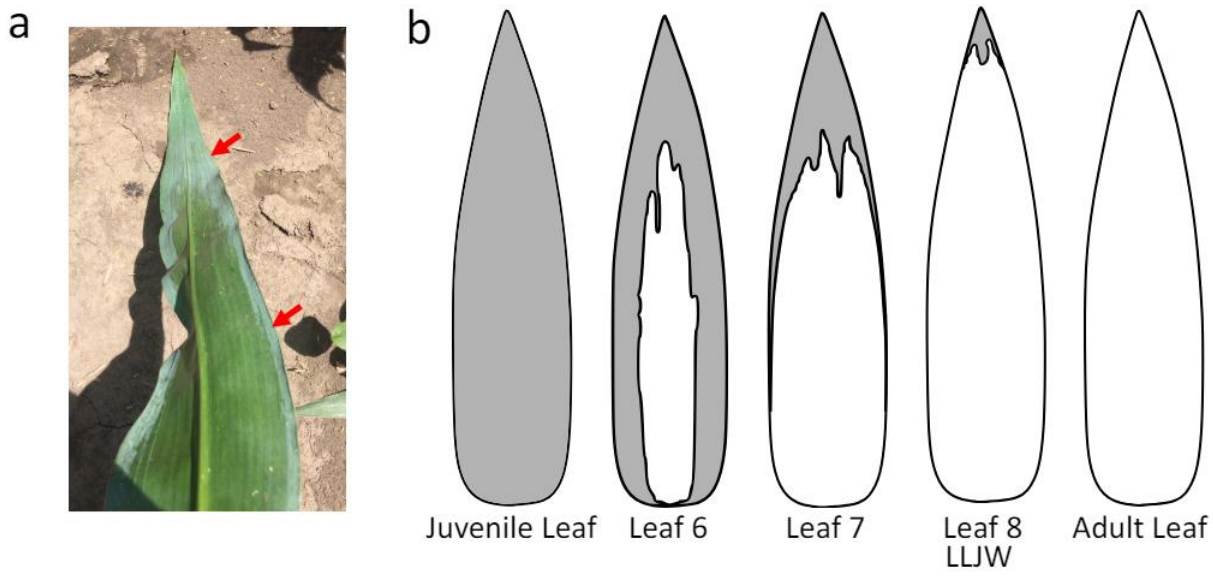

Figure 4.1. The transition from juvenile vegetative phase to adult vegetative phase as indicated by epicuticular juvenile leaf wax. (a) transition leaves have blue-grey epicuticular wax at leaf margins (red arrows); (b) shaded areas indicate distribution of juvenile leaf wax on consecutive leaves during vegetative phase change.

The uppermost leaf of the transition zone will have only a small region of juvenile tissue, marked by juvenile leaf wax at the leaf tip. The appearance of the last leaf with juvenile wax (LLJW) indicates that vegetative phase change has fully occurred. After the transition zone comes the adult phase in which the leaves are fully adult tissue (Revilla et al., 2002). Vegetative phase change, or the transition between the juvenile and adult vegetative growth phases, is regulated in part by light intensity but is largely under genetic control (Xu, Hu, & Poethig, 2021). In a panel of historically significant open-pollinated sweet corn cultivars, phase change traits were found to be both variable and highly heritable (Abedon, Revilla, & Tracy, 1996). Early research into regulators of vegetative phase change identified a number of single-gene mutations with significant effects; the teopod genes *Tp1*, *Tp2*, and *Tp3* are a group of dominant mutations that prolong the juvenile growth phase (Poethig, 1988). *Corngrass1 (Cg1)* is another dominant allele that confers a highly juvenile phenotype—highly expressed *Cg1* mutants present the classic juvenile leaf traits described above, but also have staminate reproductive structures replaced with

vegetative growth and small ears often with enlarged glumes (B. G. Abedon & Tracy, 1996). Large-effect quantitative trait loci (QTL), including *Glossy15*, were identified as being significant in the control of phase change related traits; more recently, systemic signaling pathways have been shown to be intimately involved in the control of the juvenile to adult vegetative transition (Foerster, Beissinger, de Leon, & Kaeppler, 2015). MicroRNAs (miRNAs) have emerged as one of the most significant regulators controlling the timing of vegetative phase change, in particular the ratio of the juvenility-inducing miR156 and the flowering-promoting miR172 (Fouracre, He, Chen, Sidoli, & Poethig, 2021; Poethig, 2009). *Cg1* encodes two versions of miR156; the overexpression of which causes the extreme corngrass phenotypes (Chuck, Cigan, Saeteurn, & Hake, 2007). These small RNAs are produced in and accumulate at the shoot apex, where there they interact with transcription factors to control shoot and tissue development, resulting in differential gene expression between juvenile and adult tissue (Nogueira et al., 2009; Strable et al., 2008). Application of jasmonic acid, which is coexpressed with miR156, will prolong the juvenile growth phase (Beydler et al., 2016).

Among the agronomic traits that are affected by the timing of vegetative phase change in maize, biotic stress tolerances, in the form of interactions with pathogens and insect predators, is the most economically significant in maize. Common rust, *Puccinia sorghi,* can result in substantial yield losses in both sweet corn and field corn (Shah & Dillard, 2006). Juvenile- and adult-phase plants have been shown to differ in susceptibility to common rust and there are associations between growth phase and European corn borer predation (Riedeman et al., 2008). Both of these interactions are hypothesized to be related to the differences between juvenile and adult tissue, including the higher lignin content and thicker cuticle of adult leaves and the epicuticular leaf wax on juvenile leaves (Abedon, Hatfield, & Tracy, 2006). Plant architecture

traits resulting from the lateral shoot development from nodes in juvenile plants, adventitious aerial roots and the production of tillers are also both strongly associated with juvenility in maize and have the potential to affect the favorability of canopy conditions for disease progression.

Vegetative phase change typically occurs between the fifth and eighth leaf in most maize genotypes (Foerster et al., 2015; Riedeman & Tracy, 2010). In order to take advantage of the genetic variation for the timing of vegetative phase change and investigate the effects of phase change on traits of agronomic importance, divergently selected populations from a single source population can be used to quantitatively assess phenotypic traits of interest. Divergent recurrent selection studies are a way to observe the intersection of selection, inbreeding, pleiotropy, and genetic linkage; the combination of these factors will determine the trends in genetic gain over time. Eberhart (1964) suggests that as genetic variance in a population is affected by a combination of inbreeding and the effects of selection, a quantitative trait will exhibit quadratic and then cubic trends as variance increases and then finally decreases as the frequency of desired alleles approaches 1 (Eberhart, 1964). If this is the case for the timing of vegetative phase change, then the expectation would be for a reduction and leveling-off in genetic gain in later cycles. Conversely, Crow uses the Illinois Long Term Selection Experiment as evidence that genetic variance (and then genetic gain) can be maintained over many cycles of recurrent selection. Mid to high frequency alleles in their respective directions of selection increase in frequency, reducing overall variance, but low frequency favorable alleles also increase in frequency, maintaining genetic variance (Crow, 2008). This has the overall effect of allowing gains from selection in a quantitative trait to continue over time, as demonstrated by changes in oil content in the Illinois Long Term Selection Experiment, and would contribute to genetic gain in a constant, linear trend for the timing of vegetative phase change. Here, divergent selection for

the timing of vegetative phase change can be done efficiently by selecting for LLJW, the direct target of selection. By selecting only on LLJW, researchers have altered a suite of phase change-related traits, including architecture traits, ear size, lodging, flowering time, and resistance to common rust (Revilla et al., 2002; Riedeman et al., 2008). Previous studies have demonstrated that timing of vegetative phase change is a highly polygenic trait with substantial variation within populations, providing an opportunity to investigate the effects of selection for altered timing of the vegetative phase change transition.

The University of Wisconsin-Madison sweet corn breeding and genetics program has continued to divergently select an open-pollinated maize population for both early and late phase change; these populations present an opportunity to quantitatively study the effects of altered timing of phase change in maize (Basso et al., 2008; Riedeman et al., 2008; Riedeman & Tracy, 2010). These previous studies have determined that selection for timing of the vegetative phase transition using LLJW affected other traits. The objectives of this research were to identify emergent trends for each trait to evaluate flux in the levels of genetic variation and inbreeding over long-term selection compared to the source population. If divergent selection is driving any phenotypic changes, then hypotheses on the magnitude and direction of direct and indirect selection can be tested through a comparison with selection for the LLJW. If factors other than divergent selection are present, such as inbreeding, then phenotypic changes may have a lower correlation with the LLJW.

4.4 Materials and Methods

4.4.1 Population Development

Minnesota 11 (Minn11) is a *sugary1* open-pollinated sweet corn population from the University of Minnesota breeding program, and has been the base of divergent selection work at the UW-Madison (Basso et al., 2008; De Vries, Shuler, & Tracy, 2016). To initiate the vegetative phase change divergent selection study, seed from 100 Minn11 ears were planted ear-to-row as half-sib families. The timing of vegetative phase change was assessed using LLJW. Leaves above the LLJW have no juvenile leaf wax and signal that vegetative phase change has fully occurred. LLJW was visually determined for five plants in each family, and the average leaf number was calculated for each row. The twenty families with the smallest average last leaf values were selected as the parents of the cycle 1 early phase change population (C1E) and twenty families with the largest average values were selected as the parents of the cycle 1 late phase change population (C1L). Within each of the early and late populations, five plants from each selected family were used as males, pollen from those plants was bulked over rows and then used to pollinate as many plants as possible in the selected families. Balanced seed bulks of the bulk pollinated ears were C1E and C1L. Individual seed samples from each of the ears were also saved. Plants from these individual ears were then grown in an ear to row fashion for selection in each direction the following season. For each subsequent cycle of selection, ear-rows from the previous cycle's selections were planted and a selection intensity of 20% was targeted for both early and late cycles. This has been repeated for eighteen cycles of selection in each direction. Sixteen cycles were completed when this study was initiated.

4.4.2 Trait Evaluation

Seed of nine cycles were planted in a randomized complete-block design, Minn11 starting population (C0), and cycles from both early and late directions including cycles four, eight, twelve, and sixteen (C4E, C8E, C12E, C16E and C4L, C8L, C12L, and C16L). Each entry was grown in four row plots with four replicates per environment in a total of four environments. All trials were grown in Madison, WI in a Plano silt loam, with planting dates of May 22, 2020, June 5, 2020, May 18, 2021, and June 3, 2021. Rows were 3.5 meters long and 0.76 meters apart. Each plot was thinned to twelve plants per row for a final density of 46,970 plants per hectare. In order to keep accurate track of leaf numbers for LLJW and total leaf count data, the fifth, eighth, twelfth, and sixteenth leaves were marked using a paper punch.

Twelve traits were evaluated for each of the nine evaluated cycles, including numbers of leaves, number of tillers, number of nodes with aerial roots, rust infection, plant height, ear height, days after planting to midpollen, days after planting to midsilk, ear length, ear width, tip fill, and row count. Phenotypic data were taken on the interior plants from the center rows of each plot. Juvenile wax data on seven plants per row were taken after the appearance of LLJW. Data on tiller number, total leaf number, plant and ear height, and number of nodes with aboveground aerial roots were collected for ten plants per row. Flowering time was recorded as a whole-plot average for days after planting until 50% silk and 50% pollen shed. Rust infection was assessed as percentage of leaf area infected with common rust within a plot. Plots were not inoculated with common rust spores, because the pathogen is endemic and highly mobile. In this study 100% of the plants were infected. Row count and ear dimensions were taken as a five-ear average.

4.4.3 Statistical Analysis

In order to test whether or not there were differences among cycles of selections, all data was compiled into plot means for each entry and each replicate within each environment, and an analysis of variance (ANOVA) was performed for each trait in order to determine the significance of cycle effects at the $\alpha = .05$ level. Here, cycle of selection was treated as a fixed effect for each trait, with all other effects being random. Pearson correlation coefficients were also calculated between traits. If significant cycle effects showed that means were different among cycles of selection, then the data were fit to four models of orthogonal polynomial contrasts with a single intercept as described in Eberhart (1964) and as used by Riedeman et al. (2008). Selection for early vegetative phase change and selection for late vegetative phase change were each considered a separate method of selection for the purposes of comparison. For each trait, a single linear model was fit to determine effects and statistical significance averaged between directions of selection. Next, this average model was expanded to two linear models, representing early and late vegetative phase change populations. Traits with significant linear trends were similarly fit with an average quadratic trend and then quadratic trends split by direction. Slopes or derivatives of these models represent genetic gain per cycle. Due to the nature of the experimental design, with orthogonal treatments in a balanced design, these models could be analyzed as contrasts between directions of selection, or the difference between slopes, and contrasts among directions of selection, or the average slope. Using these methods, the magnitude, symmetry, and direction of response to selection can be quantified. Wright's inbreeding coefficient was calculated from the equation $F = 1/(2N) + [1 - 1/(2N)]F'$, with N being the effective population size and F' being the inbreeding coefficient from the previous generation (Hallauer, Carena, & Filho, 2012). Statistical analysis was done using R 4.1.2 with

the *lme4* and *emmeans* packages with FDR-adjusted p-values (Bates, Mächler, Bolker, & Walker, 2015; Lenth, 2022; R Core Team, 2021).

4.5 Results

Significant environmental effects were found for a subset of phenotypic traits, with only LLJW, plant height, row count, and tip fill having non-significant environmental effects. Genotype by environment interactions were significant for flowering time, plant height, ear width, and tip fill. Block effects were significant only for common rust infection, number of tillers, ear length, and plant height (Table 1). The main effect of cycle of selection was significant for all traits except tip fill, which was not further analyzed. The inbreeding coefficients after 16 cycles of selection were 0.259 and 0.251 in the early and late directions, respectively.

Table 4.1. Mean Squares from the ANOVA for Divergently Selected Minnesota 11 grown in four environments over the 2020 and 2021 growing seasons.

Source of Variation	Mean Squares					
	LLJW†	Total leaves‡	Tiller number†	Total nodes with aerial roots†	Rust infection†	Plant height†
Environment	1.79	32.37***	6.78***	1.12***	2287.45***	560.89***
Block/environment	0.38	1.01	0.33	0.08	472.71*	158.50**
Cycle	399.39***	32.09***	0.49**	1.43***	3550.00***	1414.80***
Two linear regressions	3048.53***	232.11***	2.72***	9.18***	22041.67***	10241.07***
Avg. linear regression	80.11	20.49	0.12	1.48**	4180.18**	39.99
Among linear regressions	6016.95***	443.77***	5.32***	16.61***	42551.93***	20442.15***
Two quadratic regressions	25.94***	1.31	0.12	0.12	668.05*	190.03*
Avg. quadratic regression	0.88	nc	nc	nc	429.69	60.90
Among quadratic regressions	51.57	nc	nc	nc	906.48*	319.26*
cycle x environment	1.29	0.47	0.06	0.04	35.80	393.67***
error	0.62	0.94	0.10	0.07	130.13	109.45

Source of Variation	Mean Squares						
	Ear height†	Days to midpollen†	Days to midsilk†	Ear length†	Ear width†	Kernel row count†	Tip fill†
Environment	1677.74***	460.08***	425.72***	29.06***	1.22***	33.56	2.57

Block/environment	47.88	2.89	1.92	8.19*	0.03	82.66	1.49
Cycle	3618.63***	129.60***	153.69***	20.70***	1.19***	711.818***	1.08
Two linear regressions	26113.32***	698.70***	733.51***	109.35***	2.69***	5087.60***	nc
Avg. linear regression	2068.845**	284.03*	486.88***	32.06*	1.28	61.11	nc
Among linear regressions	50157.85***	1113.86***	979.61***	186.64***	4.09***	10114.09***	nc
Two quadratic regressions	22.51	0.26	0.091	0.91	0.19*	2.68	nc
Avg. quadratic regression	nc	nc	nc	nc	0.04	nc	nc
Among quadratic regressions	nc	nc	nc	nc	0.33	nc	nc
cycle x environment	105.06	14.55***	9.14*	3084	0.20*	173.5	4.91*
error	81.89	2.09	1.78	3.16	0.06	87.05	1.14

*Significant at the 0.05 probability level;
**Significant at the 0.01 probability level;
***Significant at the 0.001 probability level.
†Evaluated in four environments
‡Evaluated in two environments
nc: not calculated

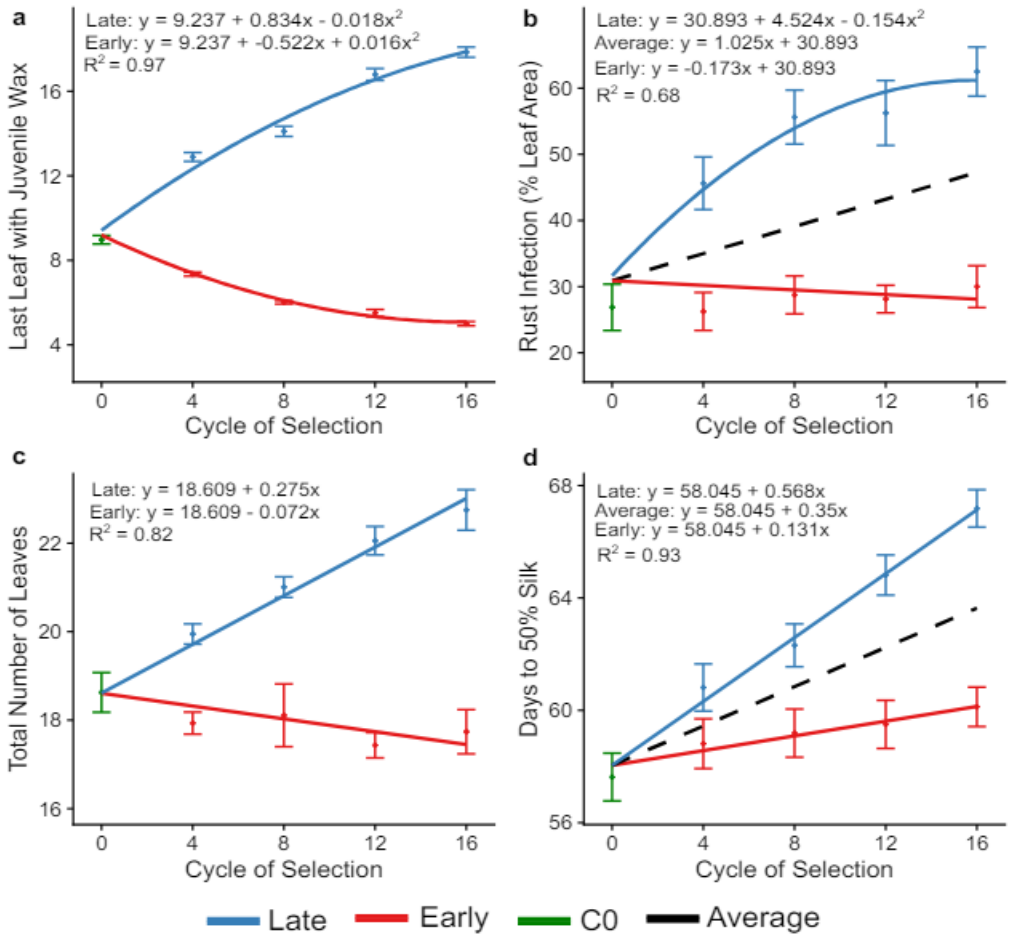

Figure 4.2. Direct and indirect responses to divergent recurrent selection for last leaf with juvenile wax (LLJW). (a) LLJW; (b) *P. sorghi* infection; (c) total leaf number; (d) days to midsilk. Statistically significant linear or quadratic trends are shown; significant average linear trends are shown in black. Red lines indicate early direction of selection, blue lines indicate late direction of selection. Population means are shown with standard errors. In the presence of a significant quadratic trend, first-order linear trends are not shown for the given trait or direction.

The direct target of selection LLJW (Figure 4.2, Table 4.1, and Supplemental Table S4.1) changed significantly in both directions and has continued to respond for 16 cycles. The linear model for LLJW split into two linear models was significant, with contrast among linear models also significant ($p < 0.001$). The regression trend for LLJW had a negative slope in the early direction and a positive slope for late direction. The average trend for LLJW was not significant, indicating that the response to selection was not only different between early and late

populations, but that there is an equal and opposite response for each direction of selection. LLJW was fit with a quadratic trend for both directions of selection; indicating that quadratic models explained significant variation that was not included in the linear models ($p < 0.01$). As with the LLJW linear trend, the average quadratic trend was not significant. Phase change traits directly associated with juvenile plant phenotypes were all significantly correlated with LLJW and with each other (Table 4.2).

Table 4.2 Phenotypic correlation coefficients between cycle means in Minn11 divergently selected for timing of vegetative phase change.

Trait	Total leaves‡	Tiller number†	Total nodes with aerial roots†	Rust infection†	Plant height†	Ear height†	Days to midpollen†	Days to midsilk†	Ear length†	Ear width†	Kernel row count†
LLJW	0.86***	0.27	0.62***	0.64***	0.56***	0.82***	0.57***	0.59***	-0.37***	-0.39***	-0.52***
Total leaves‡		0.33	0.57***	0.62***	0.34	0.71***	0.69***	0.72***	-0.38	-0.5***	-0.49**
Tiller number			0.42***	0.12	0.26	0.41***	-0.03	0.28	0.13	-0.0059	-0.14
Total nodes with aerial roots†				0.48***	-0.34**	0.6***	0.23	0.32***	-0.045	-0.43***	-0.36***
Rust infection					0.31**	0.59***	0.36***	0.41***	-0.33**	-0.43***	-0.28
Plant height						0.52***	0.45***	0.43***	-0.17	-0.029	-0.34**
Ear height							0.46***	0.51***	-0.27	-0.33**	-0.4***
Days to midpollen								0.95***	-0.2	-0.12	-0.32*
Days to midsilk†									-0.14	-0.2	-0.31*
Ear length										0.17	0.18
Ear width											0.42***
Kernel row count											

*Significant at the 0.05 probability level.
**Significant at the 0.01 probability level.
***Significant at the 0.001 probability level.

Leaf count ($R^2 = 0.82$), number of tillers ($R^2 = 0.65$), and number of nodes with aerial roots ($R^2 = 0.61$) were each fit by two linear models ($p < 0.001$, Supplementary Figure S1). Contrasts among the two linear models for leaf count and tiller number were significant, but the average trend was not, showing that the response to selection was different for each direction of selection, and was roughly equal in magnitude. However, for nodes with aerial roots, the average

linear trend was significant. Quadratic models and their respective contrasts were not significant any of the associated phase change traits. For this set of traits, values increased with cycle of selection in the late direction and decreased with selection in the early direction.

Common rust infection was also highly correlated with the timing of vegetative phase change; two-linear and among-linear model contrasts were significant, with late vegetative phase change populations becoming more susceptible to infection ($R^2 = 0.68$, $p < 0.001$). The linear regression in the early phase did not have a significant slope; the regression for the late phase change had a significant and positive slope as well as a significant quadratic trend. Here, the average linear trend was significant and positive, showing that the strong effect in the late direction were much greater in magnitude than any effects of selection in the early direction.

Plant growth traits, including plant and ear height and days to flowering showed significant cycle effects and significant two-linear model fits, and plant height showed a significant quadratic trend in the late direction of selection. Ear height ($R^2 = 0.87$) showed a linear increase in the late phase change populations ($p < 0.05$). However, flowering traits—days to midpollen ($R^2 = 0.88$) and days to midsilk ($R^2 = 0.86$) showed different trends. Distinct linear trends were observed in each flowering trait, and a significant positive average trend ($p < 0.01$) was also seen, indicating that selection for both early and late phase change resulted in delayed flowering. The two flowering traits were also the pair of traits with the highest phenotypic correlation.

Ear and yield traits were also affected by phase change selection. The two-linear model was significant for ear length ($R^2 = 0.44$), ear width ($R^2 = 0.62$), and kernel row count ($R^2 = 0.40$) with a significant contrasts among linear models for each trait indicating that there was distinct response in both directions due to cycles of selection; significant average trends were

observed in ear dimensions but not kernel row count. Ear length is slowly increasing in the early phase change populations and ear width is decreasing in the late phase change populations.

4.6 Discussion

After sixteen cycles of selection for early or late vegetative phase change, there are indications that selection is either depleting the genetic variation in the population or that limits to selection are being reached. While the strong linear trend for each direction of selection illustrates that genetic gain, as measured by LLJW, is predominately both constant and consistent, the significant quadratic trends suggest a decline in genetic variation after long-term selection. It remains to be seen if magnitude of quadratic trends increases with further selection; the majority of current variation is still explained by purely linear trends. Average LLJW went from 8.9 in the source population to 4.9 in the early population and 18.3 in the late population. There is a biological limit to selection in the early direction compared to the late direction; here, the early direction (where the rate of gain has been lower) exhibits the strongest quadratic trends as the limit is approached. Previous work has shown that using seven cycles of selection, the only trait that exhibited a quadratic trend was ear length; quadratic trends emerged for LLJW, plant height, rust infection, and ear width after sixteen cycles (Riedeman et al., 2008). While statistical inferences cannot be made, LLJW means in the newest populations, C17 and C18 exhibit smaller changes than were observed in the randomized trials including cycles up to C16. If balanced and randomized trials are repeated with additional cycles of selection, it's possible that stronger quadratic or cubic trends will emerge as genetic variance continues to change over time with long-term selection as suggested in Eberhart (1964). Further genetic studies would shed light on the primary mechanisms that allow for the demonstrated shifts in genetic variance. Genetic gain in both directions could be due to selection on targets of the miRNAs that regulate

vegetative phase change, selection on heritable epigenetic variation, selection of gene groups that regulate the production and accumulation of the miRNAs themselves, or a combination thereof.

Common rust was the only disease considered in this study. We clearly show that while selection for early vegetative phase change does not increase resistance and is in fact neutral in terms of changes in overall infection, increasing the timing of late vegetative phase change greatly increases susceptibility to common rust. Given that environmental conditions have a large role in most plant pathogen interactions, abundant vegetative growth, including production of tillers, in the C12L and C16L populations may have contributed to higher rust infection by better maintaining a higher humidity environment compared the early phase change populations, in addition to increasing amounts of juvenile vegetation. The juvenile wax itself remains a likely cause of increased susceptibility; compositional differences between juvenile and adult leaf wax and the effects on the physical properties of leaf surfaces have been implicated in rust resistance and susceptibility. Interestingly, absence of leaf wax has been shown to prevent differentiation and development of rust spore germ tubes, and in wheat and barley, non-waxy traits are linked to multiple rust-resistance genes (Uppalapati et al., 2012; Vaz Patto & Niks, 2001). A more closely controlled experiment would be required to determine specific mechanisms that control resistance in response to changes in divergent Minnesota 11 populations.

While many traits evaluated here showed response to selection in opposite directions, with the response in each direction positively correlated with LLJW, flowering time was positively correlated with LLJW in late populations, and negatively correlated in early populations. In both directions of selection, later generations had delayed flowering for both silk and tassels, contrary to the expectation that early phase change populations would have an earlier flowering time. When evaluated after only seven cycles of selection, the delay in flowering time

was only observed in the late direction of selection (Riedeman et al., 2008). Later flowering time occurs with inbreeding in maize and the later flowering time in both directions indicates that our population sizes may have been too small. However, the calculated inbreeding coefficients of 0.251 in the late direction and 0.259 in the early direction were low enough that inbreeding, while likely a factor, is far from being the main driver of the observed phenotypic changes in this population. Additionally, the anthesis-silk interval increased with later cycles of selection in both early and late populations. As this interval increases, it becomes more difficult to ensure good quality pollination and seed production, which may become a limiting factor for genetic gain if selection is continued for many cycles.

Here, the timing of vegetative phase change is shown to have heritable variation that provides a base for divergent recurrent selection. Considerable phenotypic changes differentiate early phase change populations and late phase change populations; despite a marked increases in disease susceptibility and flowering time after selecting for LLJW, distinct linear trends illustrate that the limits of selection have not yet been reached, but genetic gain is slowing. The divergent Minnesota 11 populations used in this study will serve as a platform for future studies on the genetic control of the vegetative phase change transition.

4.7 Acknowledgements

This research was supported by USDA-NIFA-SCRI 2018-51181-28419, USDA-NIFA-OREI 2018-51300-28430, and the University of Wisconsin-Madison College of Agricultural and Life Sciences. We thank Patrick Flannery for managing the divergent recurrent selection program for this study, Cécile Ané from the Statistics Consulting Lab at UW-Madison, and current and former graduate students and undergraduate interns for assistance in data collection.

4.8 Conflict of Interest

The authors declare no conflict of interest.

4.9 Chapter Four References

Abedon, B. G., Revilla, P., & Tracy, W. F. (1996). Vegetative phase change in sweet corn populations: Genetics and relationship with agronomic traits (vegetative phase change in open- pollinated sweet corn). *Maydica*, Vol. 41, pp. 77–82.

Abedon, B. G., & Tracy, W. F. (1996). Corngrass1 of maize (Zea mays l.) delays development of adult plant resistance to common rust (Puccinia sorghi Schw.) and European corn borer (Ostrinia nubilalis Hubner). *Journal of Heredity*, *87*(3), 219–223. https://doi.org/10.1093/oxfordjournals.jhered.a022988

Abedon, Bruce G., Hatfield, R. D., & Tracy, W. F. (2006). Cell wall composition in juvenile and adult leaves of maize (Zea mays L.). *Journal of Agricultural and Food Chemistry*, *54*(11), 3896–3900. https://doi.org/10.1021/jf052872w

Basso, C. F., Hurkman, M. M., Riedeman, E. S., & Tracy, W. F. (2008). Divergent selection for vegetative phase change in maize and indirect effects on response to Puccinia sorghi. *Crop Science*, *48*(3), 992–999. https://doi.org/10.2135/cropsci2007.08.0476

Bates, D., Mächler, M., Bolker, B., & Walker, S. (2015). *"Fitting Linear Mixed-Effects Models Using lme4."* (pp. 1–48). pp. 1–48.

Beydler, B., Osadchuk, K., Cheng, C., Manak, J. R., Irish, E. E., Beydler, B., … Irish, E. E. (2016). *The Juvenile Phase of Maize Sees Upregulation of Stress-Response Genes and Is Extended by Exogenous Jasmonic Acid 1*. *171*(4), 2648–2658. https://doi.org/10.1104/pp.15.01707

Chuck, G., Cigan, A. M., Saeteurn, K., & Hake, S. (2007). The heterochronic maize mutant Corngrass1 results from overexpression of a tandem microRNA. *Nature Genetics*, *39*(4), 544–549. https://doi.org/10.1038/ng2001

Crow, J. F. (2008). Maintaining evolvability. *Journal of Genetics*, *87*(4), 349–353. https://doi.org/10.1007/s12041-008-0057-8

De Vries, B. D., Shuler, S. L., & Tracy, W. F. (2016). Endosperm carbohydrates in pseudostarchy and extreme-sugary maize inbreds during kernel development. *Crop Science*, Vol. 56, pp. 2448–2456. https://doi.org/10.2135/cropsci2015.11.0723

Eberhart, S. A. (1964). Least Squares Method For Comparing Progress Among Recurrent Selection Methods. *Crop Science*, (1335), 230–231.

Foerster, J. M., Beissinger, T., de Leon, N., & Kaeppler, S. (2015). Large effect QTL explain natural phenotypic variation for the developmental timing of vegetative phase change in maize (Zea mays L.). *Theoretical and Applied Genetics*, *128*(3), 529–538. https://doi.org/10.1007/s00122-014-2451-3

Fouracre, J. P., He, J., Chen, V. J., Sidoli, S., & Poethig, R. S. (2021). VAL genes regulate vegetative phase change via miR156-dependent and independent mechanisms. *PLoS Genetics*, *17*(6), 1–25. https://doi.org/10.1371/journal.pgen.1009626

Hallauer, A. R., Carena, M. J., & Filho, J. B. M. (2012). *Quantitative Genetics in Maize Breeding*. Retrieved from https://books.google.com/books?id=PrNDNAEACAAJ

Lawrence, E. H., Springer, C. J., Helliker, B. R., & Poethig, R. S. (2021). MicroRNA156-mediated changes in leaf composition lead to altered photosynthetic traits during vegetative phase change. *New Phytologist*, *231*(3), 1008–1022. https://doi.org/10.1111/nph.17007

Lenth, R. V. (2022). *emmeans: Estimated Marginal Means, aka Least-Squares Means*. Retrieved from https://cran.r-project.org/package=emmeans

Nogueira, F. T. S., Chitwood, D. H., Madi, S., Ohtsu, K., Schnable, P. S., Scanlon, M. J., & Timmermans, M. C. P. (2009). Regulation of small RNA accumulation in the maize shoot apex. *PLoS Genetics*, *5*(1). https://doi.org/10.1371/journal.pgen.1000320

Poethig, R. S. (1988). Heterochronic mutations affecting shoot development in maize. *Genetics*, *119*(4), 959–973. https://doi.org/10.1093/genetics/119.4.959

Poethig, R. S. (2009). Small RNAs and developmental timing in plants. *Current Opinion in Genetics and Development*, *19*(4), 374–378. https://doi.org/10.1016/j.gde.2009.06.001

Poethig, R. S. (2010). The past, present, and future of vegetative phase change. *Plant Physiology*, *154*(2), 541–544. https://doi.org/10.1104/pp.110.161620

R Core Team. (2021). *R: A language and environment for statistical computing*. Retrieved from https://www.r-project.org/

Revilla, P., Malvar, R. A., Butrón, A., Tracy, W. F., Abedon, B. G., & Ordás, A. (2002). Response to selection for the timing of vegetative phase transition in a maize population. *Crop Science*, *42*(5), 1471–1474. https://doi.org/10.2135/cropsci2002.1471

Riedeman, E. S., Chandler, M. A., & Tracy, W. F. (2008). Divergent recurrent selection for vegetative phase change and effects on agronomic traits and corn borer resistance. *Crop Science*, *48*(5), 1723–1731. https://doi.org/10.2135/cropsci2007.09.0511

Riedeman, E. S., & Tracy, W. F. (2010). Vegetative phase change characteristics and resistance to common rust of corn cultivars developed in different eras. *Crop Science*, *50*(1), 87–92. https://doi.org/10.2135/cropsci2008.11.0656

Shah, D. A., & Dillard, H. R. (2006). Yield loss in sweet corn caused by Puccinia sorghi: A meta-analysis. *Plant Disease*, *90*(11), 1413–1418. https://doi.org/10.1094/PD-90-1413

Strable, J., Borsuk, L., Nettleton, D., Schnable, P. S., Irish, E. E., & City, I. (2008). *Microarray analysis of vegetative phase change in maize*. 1045–1057. https://doi.org/10.1111/j.1365-313X.2008.03661.x

Uppalapati, S. R., Ishiga, Y., Doraiswamy, V., Bedair, M., Mittal, S., Chen, J., … Mysore, K. S. (2012). Loss of abaxial leaf epicuticular wax in Medicago truncatula irg1/palm Mutants

results in reduced spore differentiation of anthracnose and nonhost rust pathogens. *Plant Cell*, *24*(1), 353–370. https://doi.org/10.1105/tpc.111.093104

Vaz Patto, M. C., & Niks, R. E. (2001). Leaf wax layer may prevent appressorium differentiation but does not influence orientation of the leaf rust fungus Puccinia hordei on Hordeum chilense leaves. *European Journal of Plant Pathology*, *107*(8), 795–803. https://doi.org/10.1023/A:1012410330287

Xu, M., Hu, T., & Poethig, R. S. (2021). Low light intensity delays vegetative phase change. *Plant Physiology*, *187*(3), 1177–1188. https://doi.org/10.1093/plphys/kiab243

4.10 Chapter Four Supplemental Material

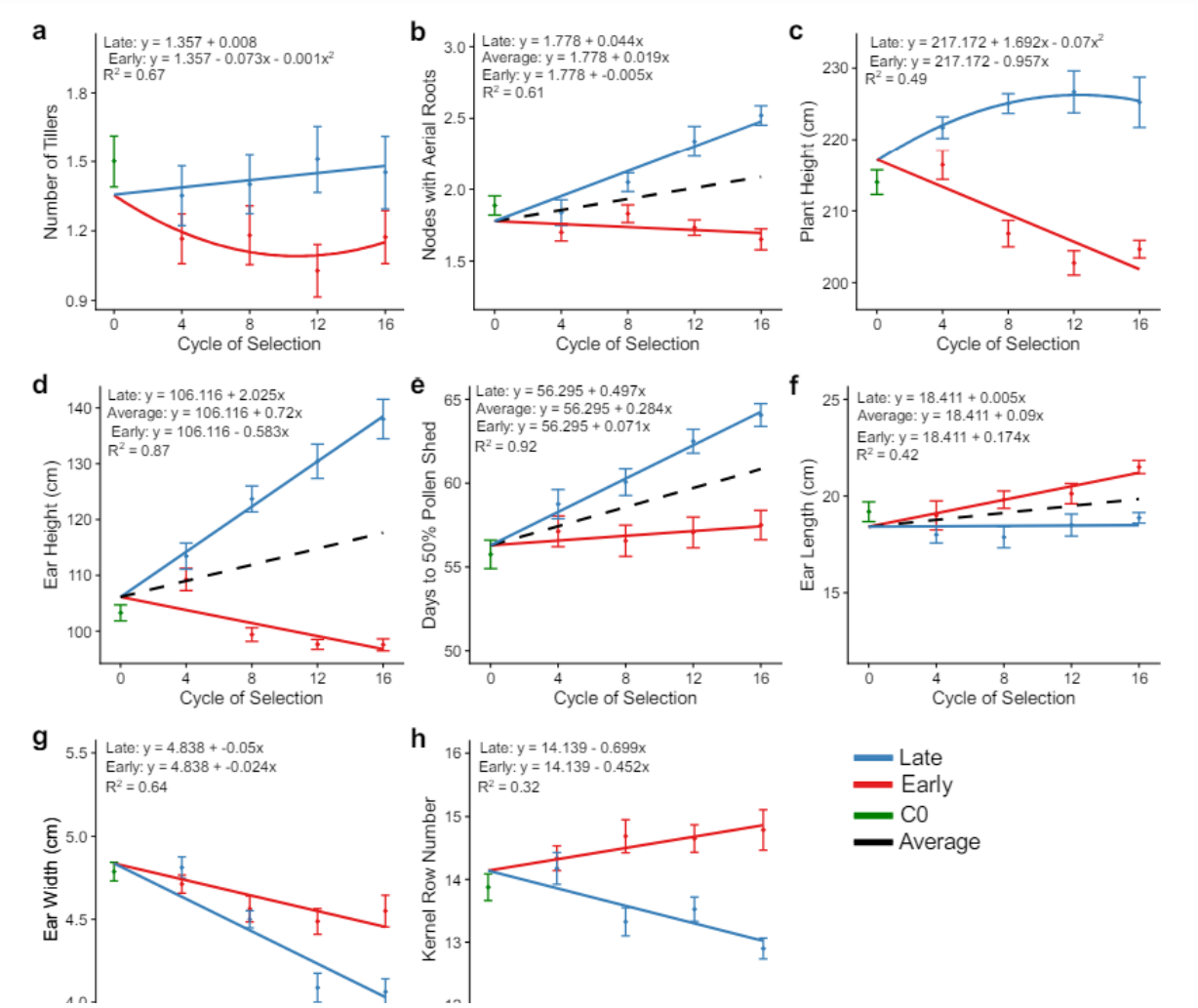

Supplemental Figure 1. Response to selection for traits affected by timing of vegetative phase change. Number of tillers (a); total nodes with aerial roots (b), plant height (c); ear height (d); days to midpollen (e); ear length (f); ear width (g); and row count (h). Means and standard errors for each cycle are shown along with significant trends; Early direction (red), late direction (blue), source population (green), average linear trend (black).

Supplementary Table S4.1 Phenotypic means and least-squares estimates for divergently selected Minnesota 11 sweet corn populations grown in four environments.

Cycle[†]	LLJW	Total leaves	Tiller number	Total nodes with aerial roots	Rust infection	Plant height	Ear height	Days to midpollen	Days to midsilk	Ear length	Ear width	Kernel row count
	Leaf no.				% leaf area	cm	cm	d	d	cm	cm	
16E	5.00	17.74	1.17	1.65	31.25	204.65	97.56	57.50	60.13	21.50	4.55	14.79
12E	5.51	17.43	1.03	1.73	28.75	202.73	97.63	57.06	59.50	20.13	4.49	14.65
8E	6.02	18.11	1.18	1.83	25.00	206.82	99.39	56.56	59.19	19.81	4.56	14.69
4E	7.35	17.93	1.17	1.70	26.25	216.42	109.27	57.13	58.81	19.00	4.71	14.34
C0	8.97	18.63	1.50	1.89	25.00	213.99	103.28	55.75	57.63	19.19	4.79	13.88
4L	12.89	19.95	1.35	1.84	42.50	221.70	113.44	58.75	60.81	18.00	4.81	14.18
8L	14.10	21.01	1.40	2.05	52.50	225.07	123.69	60.06	62.31	17.88	4.50	13.33
12L	16.79	22.06	1.51	2.34	50.00	226.69	130.44	62.50	64.81	18.50	4.09	13.53
16L	17.85	22.75	1.45	2.52	60.00	225.24	138.00	64.06	67.19	18.88	4.06	12.90
LSD	0.42	0.96	0.22	0.163	7.75	6.65	5.79	1.02	0.91	1.24	0.16	0.652
$\mathbf{b_0}$	9.24***	18.61**	1.35*	1.78***	30.89**	217.17***	106.11***	56.30***	58.05***	18.41***	4.83**	14.13***
$\mathbf{b_x^L}$	0.83***	0.28*	0.008	0.044**	4.52*	1.692*	2.025***	0.50**	0.57**	0.005	-0.05**	-0.69***
$\mathbf{b_q^L}$	-0.018**				-0.15*	-0.07*						
$\mathbf{b_x^E}$	-0.52***	-0.072*	-.073*	-0.005	-0.17	-0.96*	-0.58*	0.071	0.131*	0.17***	-0.02	0.045*
$\mathbf{b_q^E}$	-0.016**		0.003*									
$\mathbf{b_x^{avg}}$	0.14	0.11	0.005	0.02***	1.025***	-0.14	.72**	0.269*	0.35***	0.09***	-0.04	-0.12
$\mathbf{b_q^{avg}}$	-0.89											
$\mathbf{R^2}$	0.97	0.82	0.67	0.61	0.68	0.49	0.87	0.92	0.93	0.42	0.64	0.32

[†]Cycle of selection (16x,12x, …), early direction of selection (E), late direction of selection (L), least significant different at 0.05 level (LSD), intercept (b_0), linear (b_x), quadratic (b_q), response in the late direction of selection (b^L), response in the early direction of selection (b^E), average linear (b_x^{avg}), average quadratic (b_q^{avg})

*Significant at the 0.05 probability level.

**Significant at the 0.01 probability level.

***Significant at the 0.001 probability level.